T.C.

TOKAT GAZİOSMANPAŞA UNIVERSITY

GRADUATE EDUCATION INSTITUTE

DEPARTMENT OF BIOLOGY

MASTER DEGREE PROGRAM

INVESTIGATION OF THE REGULATION OF LKB1 AND STING GENES IN GYNECOLOGIC CANCERS

YÜKSEK LİSANS TEZİ

Bahra Naji HamaSalih

Danışman: Doç. Dr. Ercan ÇAÇAN

İkinci Danışman: Prof. Dr. Tahir Abdulla HAWRAMY

TOKAT- 2024

This thesis study was supported by Tokat Gaziosmanpaşa University Scientific Research Projects Coordination with project number 2022/70.

ETHICS CONTRACT

According to the thesis writing guide of Tokat Gaziosmanpaşa University Graduate Education Institute, the Master's thesis titled " Investigation of The Regulation of LKB1 and STING Genes in Gynecologic Cancers", which I prepared under the supervision of Assoc. Prof. Dr Ercan CACAN and Prof. Dr Tahir Abdulla HAWRAMY is an original study following scientific, ethical values and rules. I declare that it is and will accept all legal sanctions if the contrary is determined.

22/02/2024

Bahra Naji HamaSalih

JÜRİ KABUL VE ONAY

BAHRA NAJI HAMASALIH tarafından hazırlanan "**Investigation of The Regulation of LKB1 and STING Genes in Gynecologic Cancer**" adlı tez çalışmasının savunma sınavı 22.01.2024 tarihinde yapılmış olup aşağıda verilen Jüri tarafından Oy Birliği ile Tokat Gaziosmanpaşa Üniversitesi Lisansüstü Eğitim Enstitüsü Biyoloji Anabilim Dalı'nda Yüksek Lisans Tezi olarak kabul edilmiştir.

Jüri Üyeleri (Unvanı, Adı Soyadı) **İmzası**

Üye (Danışman): Doç. Dr. Ercan ÇAÇAN

Üye (Başkan): Dr. Öğr. Üyesi Hatice Sevim NALKIRAN

Üye : Dr. Öğr. Üyesi Nilgün YERSAL

ONAY

../../2024

Lisansüstü Eğitim Enstitüsü Müdürü

PREFACE

My valuable advisor, who enlightened my path in my graduate education, believed in and supported me more than I did and from whose academic knowledge and experience I could benefit unconditionally. I want to express my endless respect and gratitude to Prof. Dr Ercan ÇAÇAN.

I also would like to thank valuable Prof. Dr Tahir Abdulla HAWRAMI for his help in collecting the samples and for his full cooperation in the work.

I thank the distinguished thesis committee for accepting my thesis defence and their wealth of experience and insight.

I am eternally grateful to everyone who helped me with my research and gave me knowledge, encouragement, and support especially Dr. Çağlar BERKEL, Burak KÜÇÜK, Dr. Feyzanur ÇALDIRAN. For their constant support and assistance during my thesis work, I would like to thank my lab mates Çağla SEVİNÇ, Aysun KESKIN, Soumaya MENADI, Esra YILMAZ, Burcu BAL, F. Nihan ÇELİK and Gökçe ULUSOY for their support through out my research work.

I want to express my gratitude to my family since they have inspired me throughout my life with their love and support, have supported me in every way with their tolerance and belief in me, and have been instrumental in helping me get to this point in my life especially my sister Dr Shaista Naji. I am grateful to my beloved husband, Hazheer Hazhar, who has always shown me the utmost love and support whenever I have faltered.

I dedicate this thesis to my dear family.

Bahra NAJI
22 /02/2024

ÖZET

JİNEKOLOJİK KANSERLERDE LKB1 VE STING GENLERİNİN DÜZENLENMESİNİN ARAŞTIRILMASI

Bahra NAJI
Yüksek Lisans, Biyoloji Anabilim Dalı
Moleküler Biyoloji Bilim Dalı
Tez Danışmanı: Doç. Dr. Ercan ÇAÇAN
İkinci Danışman: Prof. Dr. Tahir Abdulla HAWRAMY
Şubat 2024, vii + 89 sayfa

Kadınlık, doğurganlık ve cinsel yaşamla ilgili organları etkileyen jinekolojik maligniteler daha az tedavi edilebilir ve dünya çapındaki tüm vakaların yaklaşık %17'sini oluşturmaktadır. Jinekolojik kanesrler içerisinde rahim, yumurtalık ve servikal en yaygın türlerdir. Jinekolojik kanserin tanısı ve tedavisi kadınlar ve aileleri için stres, kaygı, umutsuzluk ve ölüm korkusu yaratarak üzücü olabililmektedir. Onkogenler ve tümör baskılayıcı genler kanser gelişimi ve ilerlemesinde iki önemli gen gurubu olup çeşitli kanserlerde düzensiz bir şekilde ifade edilirler. Çeşitli fonksiyonlara sahip bir serin/treonin kinaz olan LKB1, hücre polaritesini, proliferasyonunu, apoptozu ve enerji tüketimini etkilemektedir. Bu gen aynı zamanda bir tümör baskılayıcı gen olarak da görev yapmaktadır. STING, cGAMP üreterek dsDNA aracılı gen indüksiyonunu destekleyen kritik bir doğal immün sinyal proteinidir. Bu protein, antitümör bağışıklık tepkilerini artırarak kanserin ilerlemesini önler. IFI16, transkripsiyon, apoptoz, otoimmünite ve hücre döngüsü düzenlemesinde rol oynayan bir DNA bağlayıcı proteindir. IFI16 ekspresyonu, kemoterapi direnciyle bağlantılı çeşitli malignitelerde görev almaktadır. Bir hücrenin transkripsiyonel olasılıklarındaki değişiklik, DNA nükleotid dizisinde kodlanmayan epigenetiktir. LKB1 düzenlemesi, epigenetik veya translasyon sonrası süreçler yoluyla birçok organdaki malign transformasyonla ilişkilendirilmiştir. STING gen ekspresyonu ve metilasyonu ters ilişkilidir; metilasyon, birçok tümör tipinde STING ekspresyonunu potansiyel olarak azaltır. Deasetilasyonun neden olduğu IFI16 susturulması, doğuştan gelen bağışıklık tepkisini azaltarak kanser hücresi çoğalmasını ve hayatta kalmasını artırabilir. Bu tez çalışmasında, 17β-Estradiol, vorinostat ve desitabin'in yumurtalık ve endometriyal kanser hücre hatlarında çeşitli hedef genler üzerinde nasıl bir etki ortaya koyduğu araştırıldı. Ayrıca, sağlıklı ve jinekolojik kanserli hastalardan alınan kan ve doku örneklerinde LKB1, STING ve IFI16 gibi hedef genlerin ekspresyon düzeylerindeki değişimler ortaya konuldu.

Anahtar Kelimeler: Jinekolojik Kanserler, Epigenetik, LKB1, STING, IFI16, 17β-Estradiol

ABSTRACT

INVESTIGATION OF THE REGULATION OF LKB1 AND STING GENES IN GYNECOLOGIC CANCERS

Bahra NAJI
Master's Degree, Department of Biology
Subdivision of Molecular Biology
Thesis Advisor: Assoc. Prof. Dr. Ercan CACAN
Second Advisor: Prof. Dr. Tahir Abdulla HAWRAMY
February, 2024, vii + 89 pages

Gynecological malignancies affecting organs related to femininity, fertility and sexual life are less treatable and account for approximately 17% of all cases worldwide. Among gynecological cancers, uterine, ovarian and cervical are the most common types. Diagnosis and treatment of gynecological cancer can be distressing for women and their families, creating stress, anxiety, hopelessness and fear of death. Oncogenes and tumor suppressor genes are two important gene groups in cancer development and progression and are expressed irregularly in various cancers. LKB1, a serine/threonine kinase with various functions, affects cell polarity, proliferation, apoptosis and energy consumption. This gene also acts as a tumor suppressor gene. STING is a critical innate immune signalling protein that promotes dsDNA-mediated gene induction by producing cGAMP. This protein prevents cancer progression by enhancing antitumor immune responses. IFI16 is a DNA-binding protein involved in transcription, apoptosis, autoimmunity, and cell cycle regulation. IFI16 expression is involved in various malignancies associated with chemotherapy resistance. The change in a cell's transcriptional probabilities is epigenetic, which is not encoded in the DNA nucleotide sequence. LKB1 regulation has been associated with malignant transformation in many organs through epigenetic or post-translational processes. STING gene expression and methylation are inversely related; methylation potentially reduces STING expression in many tumor types. IFI16 silencing caused by deacetylation may increase cancer cell proliferation and survival by reducing the innate immune response. In this thesis study, it was investigated what effect 17β-Estradiol, vorinostat and decitabine exert on various target genes in ovarian and endometrial cancer cell lines. In addition, changes in the expression levels of target genes such as LKB1, STING and IFI16 were revealed in blood and tissue samples taken from healthy and gynecological cancer patients.

Keywords: Gynecologic Cancers, Epigenetics, LKB1, STING, IFI16, 17β-Estradiol

CONTENTS

List of Abbreviations and Symbols

TSGs: Tumour suppressor genes
CPGs: cancer-promoting genes
AMPK: adenosine monophosphate (AMP)-dependent kinase
LKB1: liver kinase B1
STING: stimulator of interferon genes
cGAS: Cyclic GMP-AMP synthase
IFI16: Interferon Gamma Inducible Protein 16
HDACs: Histone deacetylases
HATs: histone acetyltransferases
SAHA: Vorinostat
5-Aza: Decitabine
E2: Estrogen
SEER: Surveillance, Epidemiology and End Results Program
IGF-1: insulin-like growth factor-1
AUB: abnormal uterine bleeding
LH: Laparoscopic hysterectomy
VH: vaginal hysterectomy
AH: Abdominal hysterectomy
EIN: endometrial intraepithelial neoplasia
UPSC: uterine papillary serous carcinoma
EmGD: Endometrial glandular dysplasia
ERT: estrogen replacement therapy
FIGO: International Federation of Gynecology and Obstetrics Committee
TNM: Tumour Node Metastasis
UICC: International Organization for Cancer Control
MOC: mucinous ovarian cancer
ENOC: endometrioid ovarian carcinoma
CCOC: clear cell ovarian carcinomas
STRAD: sterile-20-related adaptor
MO25: mouse protein 25
EREs: estrogen response elements
TBK1: TANK-binding kinase 1
ISGs: IFN-stimulated genes
APCs: antigen-presenting cells
IRF3: interferon regulatory factor 3
DNMT: DNA methyltransferase
HIN: Hematopoietic interferon-inducible nuclear

LIST OF FIGURES

Figure Page Number

LIST OF TABLES

Table Page Number

1. INTRODUCTION

Annually, 10 million people are diagnosed with cancer worldwide, and about 60% of diagnosed people are losing their lives at some point (Akyuz et al., 2007). Among cancer types, gynecologic malignancies are known as less curable, and the estimated worldwide incidence of gynecologic malignancies is around 17% (Jemal et al., 2011). Uterine (53 %), ovarian (25 %), and cervical (14 %) cancers are the most frequent types of gynecologic cancers, while vaginal and vulvar cancers are less common (Siegel et al., 2012). Endometrial and ovarian cancers typically strike women after menopause, but cervical cancer strikes women younger (Likes et al., 2007). Gynecologic cancers are unique in that they affect organs associated with femininity, fertility, and sexual life, and the diagnosis and treatment of gynecologic cancer can be distressing for women and their families (Costanzo et al., 2006; Ekwall et al., 2003). In addition to psychological symptoms, including stress, anxiety, sadness, and fear of dying, patients receiving treatment for gynecologic cancer can endure physical symptoms such as pain, nausea, vomiting, insomnia, and lethargy. A woman's daily routine, social relationships, work position, and quality of life are all altered by cancer therapy (De Groot et al., 2005; Ekwall et al., 2003; Holzner et al., 2003).

Tumour suppressor genes (TSGs) and oncogenes, also known as cancer-promoting genes (CPGs), are two broad categories into which many genes can be classified (Lee et al., 2010; Oren., 1992). TSGs and oncogenes are both abnormally expressed in distinct malignancies via different processes, and each gene serves a specific purpose according to the characteristics of the malignancy (Sadikovic et al., 2008). Through the phosphorylation and activation of adenosine monophosphate (AMP)-dependent kinase (AMPK) and other substrates, liver kinase B1 (LKB1) is a multifunctional serine/threonine kinase that regulates cell polarity, proliferation, apoptosis, cell cycle progression, and energy metabolism. It also plays a broad tumour suppressor role. Peutz-Jeghers syndrome, which is characterised by hamartomatous polyps and an elevated prevalence of numerous malignancies, including gynecologic cancers, is caused by germline mutations of the LKB1 gene, also known as serine/threonine kinase 11 [STK11] (Van Lier et al., 2010; Hearle et al., 2006).

STING (stimulator of interferon genes; also known as TMEM173, MPYS, ERIS and MITA) is an endoplasmic reticulum (ER)-associated multi-transmembrane protein that operates as an essential innate immunity signalling molecule required for activating dsDNA-mediated gene induction (Ishikawa et al., 2008; Ishikawa et al., 2009). Cyclic GMP-AMP synthase (cGAS) detects abnormal cytoplasmic dsDNA and creates the second messenger cGAMP, which activates STING and promotes its cellular relocalisation (Kitajima et al., 2016). While

STING signalling developed as an innate immune response to protect against viral and other infections, it has become increasingly clear that STING is commonly triggered as a result of a variety of different abnormalities that cause cytoplasmic dsDNA build-up (Barber., 2015). STING signalling has been critical for protecting cells from infections and preventing cancer growth by increasing antitumor immune responses (Woo et al., 2015).

Interferon Gamma Inducible Protein 16 IFI16 is a multifunctional DNA-binding protein with several biological processes, including controlling transcription, apoptosis, autoimmunity, and the cell cycle (Jakobsen et al., 2014). IFNs (α, β, or γ) may induce the expression of IFI16 protein in various cells; the type of IFN and the type of cell will determine the degree of IFN-induced IFI16 expression (Johnstone et al., 1999; Der et al., 1998). IFI16 expression has been examined in several cancers. In breast and prostate cancer, the disease develops due to the epithelial cells' loss of IFI16 expression (Xin et al., 2003; Alimirah et al., 2007). In ovarian cancer, on the other hand, patients' higher IFI16 expression was linked to chemotherapy resistance (Ju et al., 2009).

The gene expression sequences that distinguish differentiated cells are formed during development and are upheld during mitosis. Therefore, cells inherit genetic information, and information not encoded in DNA's nucleotide sequence is known as epigenetic information (Waterland., 2006). The word "epigenetics" describes two variations in a cell's transcriptional possibilities: long-term, stable changes that are not necessarily heritable and heritable variations in gene activity and expression in the offspring of cells or individuals (Gibney et al., 2010). LKB1 regulation by various epigenetic or posttranslational mechanisms has been strongly linked to the malignant transformation of many organs, including the breast, colon, lung, skin, and cervix (Esteller et al., 2000; Trojan et al., 2000). LKB1 phosphorylation in the regulatory domains can occur at different sites, and upstream kinases phosphorylate them and influence LKB1 cytoplasmic translocation as well as LKB1-dependent growth suppression (Zhu et al., 2013; Sapkota et al., 2002). The LKB1 gene has previously been studied for hypermethylation in cervical, lung, colon, head and neck, pancreatic, and breast cancers. Methylation silencing of the LKB1 gene does not appear to be the primary cause of LKB1 loss in these tumour types (Co et al., 2014). Deacetylation can be used to modify LKB1 after it has been translated. SIRT1, which is a conserved NAD+-dependent deacetylase, can deacetylate LKB1. SIRT1 promotes deacetylation, ubiquitination, and proteasome-mediated degradation of LKB1 in primary endothelium cells, acting as a regulator of LKB1/AMPK signalling (Lan et al., 2008).

The amount of methylation and STING gene expression were negatively correlated; methylation may significantly reduce STING expression in many tumour types (Konno et al., 2018). Histones surrounding the STING gene promoter region may be acetylated, which would improve accessibility and ease transcription. Histone deacetylases (HDACs) and histone acetyltransferases (HATs) can impact the expression of the STING gene. Thus, elevated HAT activity or decreased HDAC activity may result in elevated STING expression (Dai et al., 2019).

Certain malignancies have been shown to have DNA hypermethylation of the IFI16 promoter region, which results in the downregulation of IFI16 expression. This implies that by inhibiting IFI16's anti-tumour properties, abnormal DNA methylation patterns may aid in the development of tumours. IFI16 suppression can encourage cell migration, invasion, and proliferation, all of which can aid in the growth of tumours (Khan et al., 2022; Kerur et al., 2011). Deacetylation-induced IFI16 silencing may contribute to tumour development. The innate immune response is being weakened. IFI16 is essential for recognising viral infections and triggering the innate immune response. Its silencing may help cancer cells to avoid immune monitoring and proliferate uncontrollably. It has also been linked to enhanced cancer cell growth and survival. This could be because it regulates critical biological processes involved in cell growth and survival (Li et al., 2012).

This thesis study investigates the epigenetic effects of different concentrations of 17β-Estradiol, Vorinostat (SAHA) and Decitabine (5-Aza) on ovarian and endometrium cancer cell lines. For this purpose, the viability of the cell lines, the effects on the expression levels of genes (LKB1, STING and IFI16) that inhibit tumours and the effects on the protein expression were examined. It has been observed that 17β-Estradiol, Vorinostat and Decitabine can affect the viability, gene expression and protein expression in ovarian and endometrium cancer cell lines. It also analyses gene expressions in gynecologic cancer blood and tissue samples and protein expression in gynecologic cancer serum and tissue samples, with distinct gene and protein expressions observed according to the healthy groups.

2. Literature Review

2.1. Gynecologic Cancers, Uterine Cancer

2.1.1. Uterine Cancer and Epidemiology

The uterus is a hollow, muscular structure in the female pelvis located posterior to the bladder and anterior to the rectum. The uterus has three layers: perimetrium, myometrium, and endometrium from the outside to the inside (Gasner, 2020). An embryo and fetus develop in the uterus, a reproductive organ, throughout pregnancy. Menstruation, in which the uterine lining multiplies in anticipation of an ovum that has been fertilised and then sheds if fertilisation is unsuccessful, occurs in the uterus (Critchley et al., 2020).

The incidence of uterine cancer is lowest in Southern and Eastern Asia and most of Africa, intermediate in Southern Europe and temperate South America, and most significant in North America and Northern Europe (Ferlay et al., 2013). With an estimated 319,600 cases worldwide in 2012, uterine cancer was the sixth most frequent malignancy overall. Before 45, the disease is not common, but the risk increases significantly among women of all races in their late 40s to mid-60s (Torre et al., 2017). Between 2010 and 2014, the Surveillance, Epidemiology and End Results Program (SEER) reported an average yearly age-adjusted incidence of uterine cancer of 25.7 per 100,000 women (Siegel et al., 2018). 95% of uterine malignancies are carcinomas, which develop from the endometrium, the epithelial layer of the uterus (Ratner et al., 2010). Adenocarcinoma is the most common pathological subtype in this tissue, accounting for 89% of cases, followed by uterine papillary serous carcinomas (6%) and clear cell tumours (5%) (Christopherson et al., 1982; Christopherson et al., 1983). Sarcomas and carcinosarcomas make up the remaining 5% of uterine malignancies (Ratner et al., 2010). GLOBOCAN data shows the incidence rate estimation in ovarian and endometrial cancer, as shown in Figure 2.1.

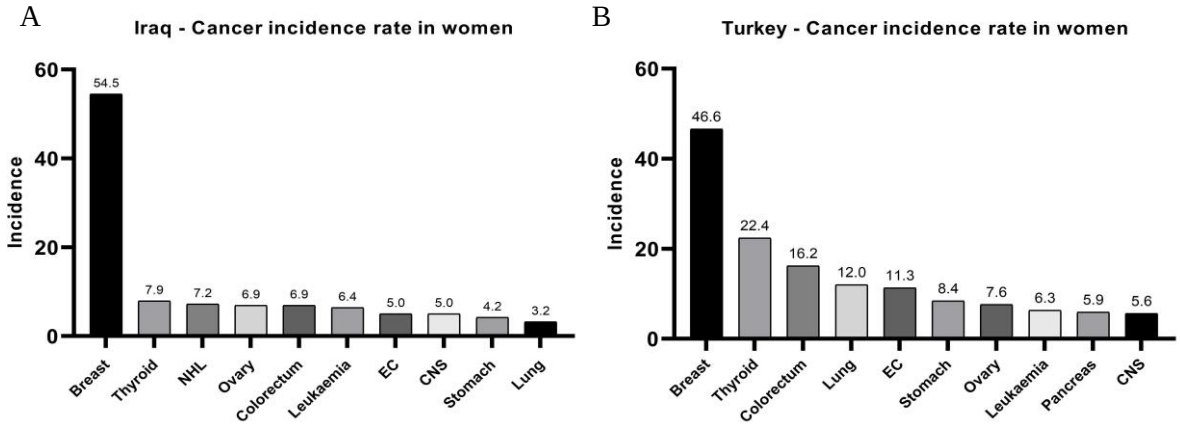

Figure 2. 1. Top ten types of cancer that are most frequently diagnosed in women in A) Iraq and B) Turkiye percentages (GLOBOCAN, 2020)

2.1.2. Uterine Cancer Etiology and Risk Factors

Endometrial cancer, which is the most common type of uterine cancer, is another name for uterine cancer. The majority of endometrial carcinomas develop from a condition of simple to complex endometrial hyperplasia (EH), which is characterised by unchecked endometrial growth that is hormonally promoted by endogenous or exogenous estrogen without progesterone or progestin resistance. In this environment, histologically detectable atypical premalignant lesions, known as endometrial intraepithelial neoplasia (EIN), can develop into endometrioid carcinoma, which is typified by the invasion of the stroma and myometrium (Lax, 2017). Furthermore, various factors may also be associated with the development of uterine cancer.

2.1.2.1. Age

Endometrial cancer is more common after menopause, and its risk rises with age. When compared to younger women, endometrial malignancies identified in older women typically have higher grades and stages (Amant et al., 2005; Yap et al., 2006).

2.1.2.2. Obesity

One of the most significant risk factors for the development of endometrial cancer is obesity. It is widely believed that the rising incidence of endometrial cancer worldwide, especially in industrialised nations, is partly caused by the rising prevalence of obesity (Fader et al., 2009). nearly all investigations found a statistically significant positive correlation between BMI and the risk of endometrial cancer (La Vecchia et al., 1984). Free Estradiol has been linked to an increased risk of endometrial cancer in postmenopausal women. Consequently, elevated plasma levels of bioavailable estrogen due to increases in endogenous estrogen production by adipose tissue raise the risk of endometrial cancer in obese postmenopausal women (Kaaks et al., 2002). Chronically elevated insulin levels and insulin-like growth factor-1 (IGF-1) activity are linked to obesity. Insulin stimulates the formation of tumours in premenopausal and postmenopausal women by binding to IGF-1 and insulin receptors in the endometrium (Roy et al., 1999).

2.1.2.3. Fertility and breastfeeding

Infertility and endometrial cancer are substantially correlated in the majority of published research to date. Infertile patients with normal estrogen levels and progesterone insufficiency

had a much higher risk of endometrial cancer by nine times than the general population (Modan et al., 1998; Cetin et al., 2008).

There was a correlation found between not breastfeeding and a higher prevalence of endometrial cancer. When endogenous estrogen is "unopposed" by progesterone, the risk of endometrial cancer rises with exposure to this hormone. Nevertheless, compared to typical postpartum cycles, nursing reduces endogenous estrogen and progesterone exposure levels (Sugawara et al., 2013; Xue et al., 2008).

2.1.2.4. Smoking

A few lifestyle choices may potentially have an impact on endometrial cancer risk. It has been proposed that cigarette smoking has an antiestrogenic effect by causing weight loss, earlier menopause, or changes in hormone metabolism. Factors linked to low levels of circulating estrogen may lower the risk of endometrial cancer because these hormones have a role in the development of this malignant condition. Consequently, smoking cigarettes may influence the risk of endometrial cancer (Michnovicz et al., 1986).

2.1.3. Diagnosis and Treatment of Uterine Cancer

The primary symptom that should raise the possibility of endometrial cancer is abnormal uterine bleeding (AUB). The majority of endometrial cancer diagnoses occur during AUB investigations. The age at the time of bleeding is correlated with the risk of cancer, not the volume of bleeding. Consequently, it is critical to identify the age range at which a haemorrhagic pattern necessitates an endometrial biopsy (Fraser et al., 2007; Seebacher et al., 2009). For women between the ages of 20 and 34, the chance of endometrial cancer is 1.6%. The prevalence rises to 6.2% among women between the ages of 35 and 44. Consequently, endometrial examination should be considered for women in this age group who do not react to pharmacological therapy or who experience prolonged periods of unopposed estrogen stimulation. Endometrial biopsies should be performed on all women over 44 who exhibit AUB symptoms, such as intermenstrual bleeding, frequent menstruation (with a 21-day interval between bleeding episodes), heavy menstrual bleeding (with a total volume of >80 mL), or prolonged menstrual bleeding (lasting longer than seven days) (Hauk; 2014). Younger women have a lower rate of advanced-stage disease, a higher degree of tumour differentiation, and a better prognosis than women older than 44 (Pellerin et al., 2005).

Because transvaginal ultrasonography is readily available, reasonably priced, and highly sensitive, it is frequently the first diagnostic test chosen when assessing for endometrial

cancer. Endometrial thickness can be determined with transvaginal ultrasonography. A tissue sample should be used for evaluation in postmenopausal patients whose endometrial thickness is more significant than 5 mm, mainly when bleeding is evident. There is no established cut-off point for assessing premenopausal women (Podrasky et al., 2013). In every patient, a tissue biopsy is necessary if bleeding continues despite a typical transvaginal ultrasonography result (Sorosky et al., 2012). An endometrial tissue sample is necessary for a conclusive diagnosis of endometrial cancer. Endometrial assessment through biopsy or endometrial cell sampling is less invasive than hysteroscopy, dilatation, and curettage (D&C). The curettage method has historically been the method of acquiring a tissue sample. Although the more recent Pipelle approach provides an option, patients who have more than 4 mm of endometrial thickness with postmenopausal bleeding may not require an endometrial biopsy or hysteroscopy. A referral for dilation and curettage should be considered if a sufficient sample cannot be collected. Further assessment is required if the biopsy results are benign but the symptoms still exist (Elsandabesee et al., 2005; Saso et al., 2011). The endometrial cavity can also be assessed with saline infusion sonohysterography. In order to better visualise structural alterations, this study technique involves infusing saline into the endometrial cavity and then performing ultrasonography. This is especially useful in cases where patients have localised anomalies such as polyps, submucosal fibroids, or endometrial hyperplasia. Although infrequently used, saline infusion sonohysterography may be an option for insufficient transvaginal ultrasonography or endometrial biopsies (Podrasky et al., 2013). Hysteroscopy provides a direct vision of the endometrial cavity and is frequently performed to assess abnormal uterine bleeding. Hysteroscopy may be carried out in conjunction with curettage or a targeted biopsy. According to a comprehensive review, hysteroscopy can diagnose endometrial cancer with an 86.4% specificity and a 99.2% sensitivity (Sorosky et al., 2012; Clark et al., 2002). When transvaginal ultrasonography is insufficient and saline infusion sonohysterography is intolerable, magnetic resonance imaging may offer further information on endometrial thickness or structural abnormalities such as fibroids or adenomyosis. In most cases, positron emission tomography and computed tomography are not helpful during the preliminary assessment (Podrasky et al., 2013).

Suppose a woman has invasive carcinoma and is premenopausal and still wants to have children. In that case, she may be eligible for a conservative treatment trial if the histology report shows a well-differentiated carcinoma (grade I) without evidence of myometrial invasion. Patients for such fertility-preserving treatments should be made aware of the fact that they will require frequent clinical follow-up due to the 25% primary failure rate and the

approximately 30% likelihood of recurrence associated with it. The rule out of ovarian involvement or myometrial infiltration using transvaginal ultrasonography and magnetic resonance imaging is a requirement for such treatment. The preferred course of treatment is taking oral gestagen continuously for a minimum of three months, after which transvaginal ultrasonography, hysteroscopy, and curettage are used as part of a follow-up inquiry. After having as many children as they choose, some women are advised to have a hysterectomy due to the high likelihood of recurrence following conservative treatment (Chiva et al., 2008).

Total abdominal hysterectomy, bilateral salpingo-oophorectomy and peritoneal washings are the surgical treatments for endometrial cancer. Omentectomy with pelvic and para-aortic lymphadenectomy may be necessary in some circumstances. There are two types of surgical procedures: laparoscopic (standard or robotically assisted) and laparotomy (entrance via a transverse or midline incision) (Baekelandt et al., 2009; Emons et al., 2009). Both the uterus and the cervix are removed during a total hysterectomy. In addition, the adnexa (ovaries and fallopian tubes) may or may not be removed; in a supracervical or subtotal hysterectomy, the cervix is not removed. There are three primary methods for performing these procedures: laparoscopic hysterectomy (LH), vaginal hysterectomy (VH), or abdominal hysterectomy (AH). The idea behind partial hysterectomy is that if the cervix is kept in place, women may have improved sexual and pelvic floor function. The less comprehensive dissection can lower the risk of complications, but there is a chance of cyclical bleeding that could require a cervix excision (trachelectomy). When the cervix is kept, there is still a chance of developing invasive cancer later on, but in people who have undergone appropriate screening, this risk is shallow (Clayton, 2006). In order to prevent ovarian cancer in the future, bilateral salpingo-oophorectomy—the surgical removal of both the fallopian tubes and ovaries—has historically been offered at the time of hysterectomy for non-malignant conditions. However, because of the possible risks associated with the loss of ovarian hormone production, this surgery is now being avoided more and more (Evans et al., 2016). The age at which surgery was conducted determined the relationship between death and bilateral salpingo-oophorectomy in this population-based cohort study involving over 200,000 women receiving non-malignant hysterectomy. Bilateral salpingo-oophorectomy did not appear to be associated with significantly higher all-cause mortality when compared to ovarian conservation in women under 50, but it did not appear to be associated with significantly higher all-cause mortality in women over 50; in fact, women 50–54 and over 55 years old showed marginally significant decreases in all-cause and cancer mortality, respectively (Tuesley et al., 2020; Mytton et al., 2017). Premature oestrogen insufficiency will arise from bilateral salpingo-oophorectomy

performed prior to menopause but not from bilateral salpingo-oophorectomy performed after menopause has begun. Loss of oestrogen at specific critical moments may contribute to the onset or progression of disease since oestrogen signalling affects several organ systems in genomic and non-genomic ways (Deroo et al., 2006). The question of whether performing a pelvic and para-aortic lymphadenectomy in addition to treating endometrial carcinoma surgically actually has any general benefits, therapeutic—because the removal of involved lymph nodes may prolong survival—or diagnostic—because adjuvant therapy decisions may be made based on the presence or absence of lymph node involvement (Denschlag et al., 2011).

2.1.4. Classification and Staging of Uterine Cancer

The endometrial layer of the uterus is the epithelial layer from which carcinomas of uterine malignancies originate. According to reports, this tissue's most common pathological subtypes are uterine papillary serous carcinomas, clear cell tumours, and adenocarcinomas. Sarcomas, including leiomyosarcomas, endometrial stromal sarcomas, and carcinosarcomas, comprise the remainder of uterine malignancies (Ratner et al., 2010).

The classification of endometrial carcinomas into two categories of tumours with significantly different characteristics and prognoses clarifies the gap in overall patient survival (Bokhman, 1983). Bokhman's work resulted in the description of two different types concerning molecular and histologic features. Eighty to ninety percent of all sporadic endometrial malignancies are Type I EC, also known as the endometrioid type, and the remaining ten to twenty percent are Type II EC or non-endometrioid tumours (Bokhman, 1983). Histologically, Type I endometrial tumours are frequently highly differentiated and might be either an adenocarcinoma or an adenocarcinoma with a squamous differentiation (Ryan et al., 2005). They have a multistep carcinogenic process that begins with simple endometrial hyperplasia, advances to complicated atypia hyperplasia, and finally develops into the precursor lesion, endometrial intraepithelial neoplasia (EIN) (Lacey et al., 2008). Type II EC has two histologies: uterine papillary serous carcinoma (UPSC) and clear-cell carcinoma. Endometrial glandular dysplasia (EmGD), a precursor lesion to both malignancies, appears to proceed from an atrophic endometrium (Yi et al., 2008). In addition to histological variations, the origin and survival of these two subgroups are drastically different. Type I cancers are the most common estrogen-dependent tumours; risk factors that enhance a woman's exposure to circulating estrogen levels are linked to an increased risk of Type I EC. Similarly, conditions that lower progesterone are linked to an increased risk of

Type I EC. Obesity, estrogen replacement therapy (ERT), nulliparity, and health issues that result in high estrogen levels, such as estrogen-secreting ovarian tumours and polycystic ovarian syndrome, have traditionally been identified as risk factors for Type I EC. Furthermore, Type I tumours are more prevalent in pre and perimenopausal women than Type II tumours (Doll et al., 2008). Compared to Type I cases, Type II cases are more likely to be older, of average weight, and multiparous. The estrogen route is not thought to be involved in the carcinogenesis of Type II EC, as normal-weight and parous women have lower estrogen exposure than obese and nulliparous women (Cirisano et al., 1999).

The classification method recommended by the International Federation of Gynecology and Obstetrics Committee (FIGO) is preferred for the staging procedure. This method is also stated in (Table 2.1.), along with its equivalent in the Tumour Node Metastasis (TNM) system provided by the International Organization for Cancer Control (UICC).

Table 2. 1. Staging of uterine cancer according to FIGO and TNM equivalents (Prat; FIGO Gynecological Oncology Committee, 2023)

FIGO	Description	TNM
Stage I	Confined to the uterine corpus	T1 N0 M0
IA	The disease is limited to the endometrium OR non-aggressive histological type, i.e., low-grade endometroid.	T1a N0 M0
IB	Non-aggressive histological types with invasion of half or more of the myometrium.	T1b N0 M0
IC	Aggressive histological type is limited to a polyp or confined to the endometrium.	T1c N0 M0
Stage II	Invasion of cervical stroma without extrauterine extension OR aggressive histological types with myometrial invasion	T2 N0 M0
IIIA	Invasion of the cervical stroma of non-aggressive histological types	T2a N0 M0
IIB	Substantial lymphovascular space involvement (LVSI) LVSI of non-aggressive histological types	T2b N0 M0
IIC	Aggressive histological type with any myometrial involvement	T2c N0 M0
Stage III	Local and regional spread of the tumour of any histological subtype	T3 N0 M0
IIIA	Invasion of uterine serosa, adnexa, or both by direct extension or metastasis	T3a N0 M0
IIIB	Metastasis or direct spread to the vagina and the parametria or pelvic peritoneum	T3b N0 M0
IIIC	Metastasis to the pelvic or para-aortic lymph nodes or both	T3c N1/2 M0
Stage IV	Spread to the bladder mucosa and intestinal mucosa and distance metastasis.	T4 N1/2 M0
IVA	Invasion of the bladder mucosa and the intestinal/bowel mucosa	T4a N1/2 M0
IVB	Abdominal peritoneal metastasis beyond the pelvis	4b N1/2 M0

IVC	Distant metastasis, including metastasis to any extra-or intra-abdominal lymph nodes above the renal vessels, lungs, liver, brain, or bone	T4 N1/2 M1

2.2. Gynecologic Cancers, Ovarian Cancer

2.2.1. Ovarian Cancer and Epidemiology

The ovaries are one of the most essential anatomical parts of the female reproductive system. They are almond-sized structures that are about 2-3 cm tall. And found in the pelvic cavity. Ovarian ligaments attach them to the uterus. They are primarily responsible for oogenesis and hormone synthesis. Endoderm-derived germ cells differentiate into oocytes in the ovarian structure and endocrine and interstitial cells responsible for estrogen and progesterone synthesis. It is supplied by the epithelial cells that surround the ovarian tissue. These three cell types can also be found in the ovary. It has been demonstrated that it may be the cause of cancer (Romero et al., 2012). Cancer usually begins in the ovaries when ovarian cells differentiate into a distinct phenotype and spread to other body areas. It begins by invading the abdominal and pelvic cavities (Kurman et al., 2008). In addition to this, several recent investigations have suggested that the disease may also have its roots in tumours growing at the distal ends of the fallopian tubes (American Cancer Society, 2018).

After cervical and uterine cancer, ovarian cancer is the third most frequent gynaecological disease in the world. However, it is linked to a worse prognosis and fatality rate (Momenimovahed et al., 2019). Around 240,000 new instances of ovarian cancer are reported each year, and more than 150,000 fatalities are attributed to the disease. Western and Central European countries are the most impacted globally (Reid et al., 2017). Numerous researches conducted recently have revealed that different racial groups experience ovarian cancer at varying rates. For instance, in the United States, the diagnoses of White people (12.2 per 100,000), Hispanic people (10.6 per 100,000), Asian/Pacific people (9.5 per 100,000), and Black people (9.4 per 100,000) are the most common (Peres et al., 2018). GLOBOCAN data estimates the mortality rate in ovarian and endometrial cancer, as shown in Figure 2.2.

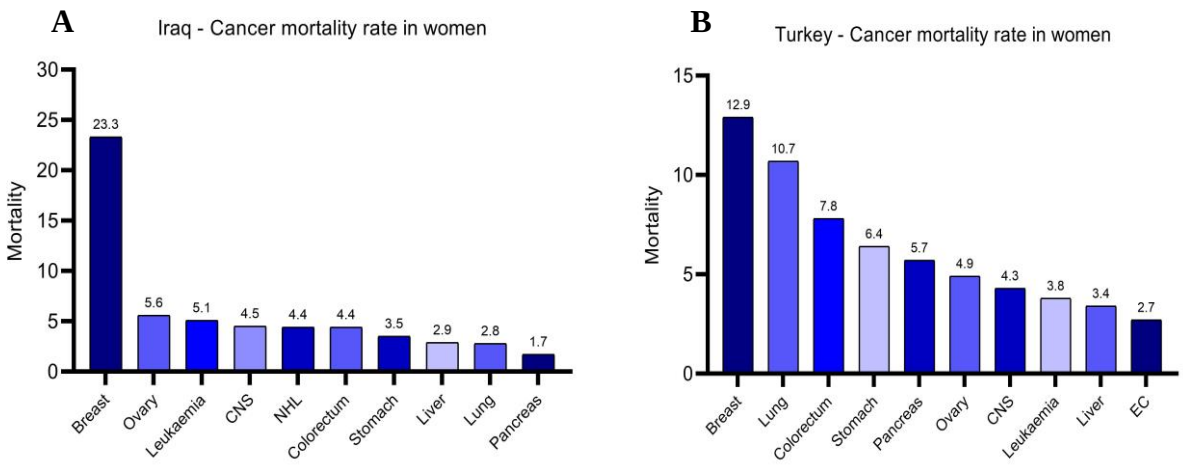

Figure 2. 2. Top ten types of cancer that most frequently cause death in women in A) Iraq and B) Turkiye percentages (GLOBOCAN, 2020).

2.2.2. Ovarian Cancer Etiology and Risk Factors

Ovarian cancer manifests late symptoms and spreads quickly, making it a diverse illness. Even now, the etiology of it is not entirely understood. Nonetheless, it is believed that a significant factor is the patient's age. People in the risk group are known to exist, particularly those 63 years of age or older (Assis et al., 2018). Moreover, ovarian cancer may also occur as a result of several different circumstances.

2.2.2.1. Age

Age-related ovarian cancer is primarily thought to affect women after menopause. The increased incidence of this malignancy is especially noticeable in women who are older than 65 (Mohammadian et al., 2017). It is unclear if age has any bearing on how ovarian cancer will turn out. While numerous researchers have noted that ovarian cancer patients who are diagnosed at a younger age tend to have better outcomes, other researchers have asserted that age is not a reliable predictor of prognosis (Chan et al., 2004). A worse survival rate and a more advanced stage of the disease are linked to older age in this context. The survival rate for older women with ovarian cancer is lower than that of younger patients because they receive less aggressive treatment (Ries, 1993).

2.2.2.2. Parity and Lactation

Numerous research findings indicate that childbearing may offer some protection against ovarian cancer (Kvåle et al., 1988). A case-control study's findings indicate that women who have a live birth ($P<0.001$) or an induced abortion ($P<0.05$) have a lower chance of

developing ovarian cancer; furthermore, this risk declines as the number of live birth cases increases (P<0.001) (Risch et al., 1996). According to the number of pregnancies, older age during pregnancy is linked to a lower risk of ovarian cancer (Moorman et al., 2008).
The number of children breastfed, the length of nursing, and the incidence of ovarian cancer have all been found to be inversely correlated by researchers (Jordan et al., 2010).

2.2.2.3. Nutrition and diet

According to the findings of a case-control study, eating more cholesterol raises the risk of ovarian cancer; however, this risk can be lowered by consuming vegetables, vitamin supplements, beta-carotene, and B-complex vitamins (Pan et al., 2004). the preventive effect of phytoestrogens on the development of ovarian cancer and think that eating a plant-based diet can significantly lower the incidence of cancers linked to hormones (McCann et al., 2003). An elevated vitamin D level in plasma could potentially lower the incidence of ovarian cancer. Calcium consumption also decreases this risk (Goodman et al., 2002).

2.2.2.4. Family history

A family history of breast or ovarian cancer is the most significant risk factor for ovarian cancer. An increased risk of ovarian cancer is linked to a personal history of breast cancer (Kazerouni et al., 2006). Tumour suppressor gene mutations account for almost one-fifth of ovarian cancer cases, while germline mutations in the BRCA gene cause 65–85% of inherited ovarian malignancies (Walsh et al., 2011). While carriers of BRCA1 and BRCA2 mutations have an ovarian cancer risk of less than 3% by age 40, by age 50, that risk rises to 10% (Andrews et al., 2017).

2.2.3. Diagnosis and Treatment of Ovarian Cancer

Early on in the disease's course, there are no symptoms. Nearly all symptoms took longer for women with early-stage cancer to manifest, suggesting that cancer detected at a later stage is a more aggressive entity. Additional open-ended inquiries Allowing women to explain their symptoms in their own words, as well as how they evolved and how they responded to them, would provide extra information that could be beneficial in identifying symptoms of early-stage disease (Olson et al., 2001).

Transvaginal ultrasonography is the most helpful imaging method for detecting whether lesions are benign or malignant in ovarian cancer. In some circumstances, computed tomography or magnetic resonance imaging may be employed, for example, to differentiate between ovarian cancer and a primary gastrointestinal tumour (Kinkel et al., 2005). Currently, there is no apparatus-based diagnostic approach that may substitute surgical staging of ovarian cancer and consistently determine surgical feasibility (Salani et al., 2008). The utilisation of symptom-triggered diagnostic testing, specifically CA125 level and ultrasonography, does not cause a shift in the stage of ovarian cancer. However, it may lead to more patients undergoing complete tumour removal during surgery, indicating a lower tumour load in women identified through such testing (Gilbert et al., 2012). In clinical practice, symptom-triggered testing might be difficult to execute. According to a general practitioner survey, most would still refer patients based on elevated Cancer antigen 125 (CA125) levels, even in cases where the ultrasonography result was expected (Moss et al., 2013). The non-specific marker CA125 can have elevated levels in several illnesses, many of which are benign conditions, including menstruation and endometriosis. When women get counselling, it is essential to keep in mind that the formation of an ovarian cyst is a physiological requirement for ovulation. Only 50% of stage 1 tumours had elevated CA125 levels, which adds to the complexity (Sundar et al., 2015).

Treatment approaches are still mostly ineffective despite recommendations since most individuals with ovarian cancer are discovered when the disease has progressed. Specifically, the diverse behaviour of cancer at the histological level demands that suitable treatment approaches be developed and implemented. It makes the markers less reliable, which is necessary for diagnosis. Controlling the spread of the malignancy and reducing its associated symptoms, however, is the top objective of the recommended course of treatment. Surgery is not always the only option for patients in advanced stages (stages III and IV), as the cancer has already spread to the liver. However, standard therapy in the early stages involves cytoreductive surgery to remove tumour tissue, followed by platinum-based chemotherapy (Cortez et al., 2018).

2.2.4. Classification and Staging of Ovarian Cancer

Ovarian cancer must be classified appropriately and staged due to its heterogeneous nature. By using categorisation and staging techniques, one may ascertain the features of tumour cells in patients and gauge how the disease will progress based on these features. Predictions,

planning suitable treatment regimens, and figuring out a family history of cancer become simpler (Duska & Kohn, 2017). Histologically, ovarian malignancies are categorised into four categories: mixed-cell tumours, germ cell tumours, sex cord-stromal tumours, and epithelial tumours. Tumours with a metastatic genesis (Rojas et al., 2016; Kurman et al., 2014).

The bidirectional model comprises Type I and Type II subtype classification approaches and has gained attention due to clinical and genetic investigations conducted on epithelial ovarian malignancies (Kurman & Shih, 2010). Tumours with minimal malignant potential and local growth characterise Type I ovarian cancers (Lengyel, 2010); on the other hand, high-grade serous cancers, carcinosarcomas, and undifferentiated carcinomas are included in Type II ovarian cancers (Terada et al., 2016). Compared to Type II tumours, Type I cancers grow more slowly. They may, nevertheless, progress into tumours that are on the verge of becoming invasive. Additionally, despite being somatically more stable in terms of the genome than Type II cells, these cell mutations might be present in them (Koshiyama et al., 2014).

Ovarian neoplasms comprise less than 1% of Brenner's tumours. It can be classified as malignant, borderline, or benign (Zhang et al., 2019). Brenner tumours often cluster as a transitional epithelial layer encircled by fibrous stroma, with over 80% of these tumours occurring in women 50 and older (Zheng & Heller, 2019). Among the kinds of epithelial ovarian cancer, mucinous ovarian cancer MOC is an uncommon carcinoma. MOC is included in this class despite the absence of mucinous cells in normal ovarian tissue because of mucinous metaplasia in the ovary's surface epithelium. MOC is linked to endometriosis and exhibits Kras and p53 mutations and HER2 amplification when transitioning to borderline and invasive features unique to other mucinous carcinomas (Babaier & Ghatage, 2020). Comparing MOC to serous carcinomas, 80% of patients are diagnosed early. This is because there is a significant amount of tumour tissue (Morice et al., 2019). Endometriosis is linked to both endometrioid and clear cell carcinomas. Of all ovarian malignancies, 10% have endometrioid ovarian carcinoma ENOC as a recurring malignancy. In particular, histologically and molecularly, ENOC and uterine cancer are similar (Pierson et al., 2020). Furthermore, it is believed that infertility, late menopause, and early menarche raise the chance of ENOC development (Koshiyama et al., 2017). Like ENOC, clear cell ovarian carcinomas (CCOC) are an epithelial cancer that can be identified early on. Nonetheless, patients with advanced-stage CCOC may have a treatment resistance mechanism that is linked to a poor prognosis (Fujiwara et al., 2016).

Just as crucial as histological classification is the staging of ovarian cancer. By splitting patients into subgroups, early-stage tumours must be categorised to characterise tumour progression, examine therapy options, and provide survival data (Montavon Sartorius et al., 2018). The International Federation of Gynecology and Obstetrics Committee (FIGO) categorisation technique is preferred for the staging procedure. The Tumour Node Metastasis (TNM) system supplied by the International Organization for Cancer Control (UICC) also incorporates this technique. Table 2.2. is expressed in conjunction with its inverse.

Table 2. 2. Staging of ovarian cancer according to FIGO and TNM equivalents (Prat; FIGO Gynecological Oncology Committee, 2023)

FIGO	Description	TNM
Stage I	Tumour tissue is limited to the ovary or fallopian tubes	T1 N0 M0
IA	In a capsule, a single ovary or fallopian tube	T1a N0 M0
IB	In capsule, in two ovaries or fallopian tubes	T1b N0 M0
IC	In capsule, in one or both ovaries or fallopian tubes:	
IC1	Capsular rupture after surgery	T1c1 N0 M0
IC2	Capsular rupture before surgery	T1c2 N0 M0
IC3	Ascites or malignant cells in the peritoneum	T1c3 N0 M0
Stage II	The tumour has spread to one or both ovaries or the fallopian tube and pelvis.	T2 N0 M0
IIA	Spread to the uterus from the fallopian tubes and ovaries	T2a N0 M0
IIB	Spread to other pelvic intraperitoneal tissues	T2b N0 M0
Stage III	Tumour in one or both ovaries/fallopian tubes or primary peritoneal in case of cancer confirmed spread outside the peritoneum and lymph nodes.	T1T2 N1 M0
IIIA1	Positive retroperitoneal lymph nodes are present	T3a1 N0 M0
IIIA2	Microscopic extra pelvic peritoneal metastasis, with or without retroperitoneal lymph metastasis	T3a2 N0/1M0
IIIB	Macroscopic peritoneal metastasis up to 2 cm, with or without retroperitoneal lymph metastasis	T3b N0/1 M0
IIIC	macroscopic peritoneal metastasis more than 2 cm, retroperitoneal lymph with or without metastasis, extension to the spleen or liver capsule	T3c N0/N1 M0
Stage IV	Presence of metastasis to distant areas beyond peritoneal metastasis	T1/2/3 N0/1 M1
IVA	Tumour in pleural effusion	T4 N0/1 M0
IVB	Parenchymal metastasis or metastasis to extra-abdominal organs	T4 N0/1 M1

2.3. Cancer Suppresser genes

2.3.1. Liver kinase B1 (LKB1)

Liver kinase B1 (LKB1) is located on chromosome 19p13.3. It is a multifunctional serine/threonine kinase (STK11) that regulates cell polarity, proliferation, apoptosis, cell

cycle progression, and energy metabolism by phosphorylating and boosting AMP-dependent kinase (AMPK) and other substrates. Peutz-Jeghers syndrome is a rare, autosomal dominant, hereditary polyposis syndrome defined by gastrointestinal hamartomas and mucocutaneous pigmentations caused by germline mutations in the LKB1 gene, which is characterised by an increased risk of several cancers, including gynecologic cancers (van Lier et al., 2010). The heterotrimeric complex formed by the association of LKB1 with two proteins, sterile-20-related adaptor (STRAD) and mouse protein 25(MO25), regulates LKB1 kinase activity. MO25 is a scaffolding protein that binds to the C-terminus of STRAD, increasing its affinity for LKB1. STRAD is a pseudo kinase that promotes LKB1 active confirmation (Zeqiraj et al., 2009). The most potent growth and tumour-promoting phenotypes require biallelic inactivation of the LKB1 alleles. However, evidence shows that LKB1 can function as a haploinsufficient tumour suppressor. Many intestinal polyps, for example, do not experience loss or mutation of the second allele (Miyaki et al., 2000). LKB1 encodes an mRNA of approximately 2.4kb transcribed in a telomere-to-centromere orientation and a protein of 433 amino acids and roughly 48kDa (Hemminki et al., 1998). The protein has serine-threonine kinase activity, a kinase domain, and a nuclear localisation signal in the N-terminal noncatalytic region. Although LKB1 protein expression is mainly found in the cytoplasm, it can sometimes be found in the nucleus (Alessi et al., 2006). LKB1 protein levels are high in most epithelia, the follicles and corpus luteum of the ovary, the seminiferous tubules of the testis, myocytes from skeletal muscle, and glia cells in adult tissues (Rowan et al., 2000).

Furthermore, LKB1 regulation by various epigenetic or posttranslational mechanisms has been strongly linked to the malignant transformation of many organs, including the breast, colon, lung, skin, and cervix (Esteller et al., 2000; Trojan et al., 2000). LKB1 phosphorylation in the regulatory domains can occur at 11 different sites, Thr185, Thr189, Thr336 and Ser404 being direct targets of LKB1 (autophosphorylation). In vitro, phosphorylation of these sites does not affect kinase activity or subcellular localisation. However, it does serve as an indicator of catalytically active LKB1, while other sites (Ser31, Ser307, Ser325, Thr366, Ser399, Ser 428, and Ser431) are phosphorylated by upstream kinases and influence LKB1 cytoplasmic translocation as well as LKB1-dependent growth suppression (Zhu et al., 2013; Sapkota et al., 2002). The LKB1 gene has previously been studied for hypermethylation in cervical, lung, colon, head and neck, pancreatic, and breast cancers. Methylation silencing of the LKB1 gene does not appear to be the primary cause of LKB1 loss in these tumour types, and the same for EC (Co et al., 2014). Deacetylation can be used to modify LKB1 after it has been translated. SIRT1, which is a conserved NAD+-dependent deacetylase, can deacetylate

LKB1. SIRT1 promotes deacetylation, ubiquitination, and proteasome-mediated degradation of LKB1 in primary endothelium cells, acting as a regulator of LKB1/AMPK signalling (Lan et al., 2008).

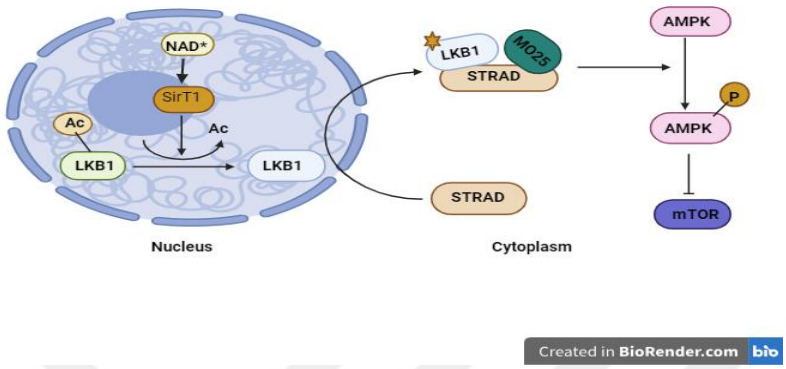

Figure 2.3. LKB1 deacetylation by NAD+-dependent deacetylase SIRT1 and localisation in the cytoplasm. (https://biorender.com)

Sex hormones like androgen and estrogen can influence the LKB1 gene. Estrogen is a steroid hormone that plays essential roles in cell proliferation and differentiation in various target tissues (Bjornstrom et al., 2005). Estrogen exerts its effects by binding to its receptor ERα, causing it to be activated. This, in turn, causes it to change conformation, dimerise, and bind to specific estrogen response elements (EREs) located in the targeted gene promoter regions (Nilsson et al., 2001). Estrogen has been shown to regulate LKB1 gene expression via transcriptional regulation, and an estrogen receptor (ER) binding site has been discovered in the promoter region of LKB1. 17β-Estradiol can downregulate both mRNA and protein levels of LKB1 in MCF-7 breast cancer cells by inhibiting LKB1 promoter activity by reducing ER binding to the LKB1 promoter (Brown et al., 2011). Besides this, estrogen can regulate LKB1 protein level in the cytoplasm; the LKB1 binding site present on ERα after binding LKB1's ability to phosphorylate its substrates is impaired, altering its anti-tumoral activity (Bouchekioua-Bouzaghou et al., 2014).

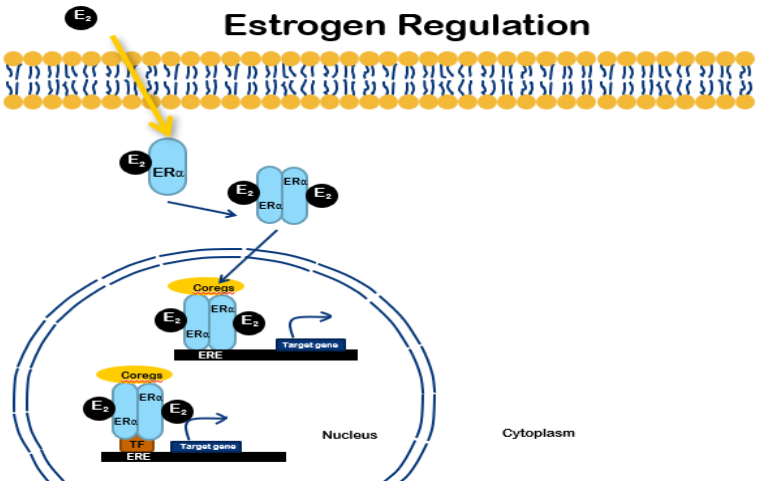

Figure 2.4. Mechanisms for estrogen signalling. Via a genomic mechanism, estrogen binds directly to estrogen-responsive elements (EREs) or indirectly through other transcription factors on responsive elements (RE), causing its receptor, Estrogen receptor α (Erα), to dimerise and translocate into the nucleus. Following the recruitment of coregulator complexes, this transcription of target genes is initiated. E2: 17 β-oestradiol; Coregs: Coregulators; TF: Transcription factor (Lattouf et al., 2016).

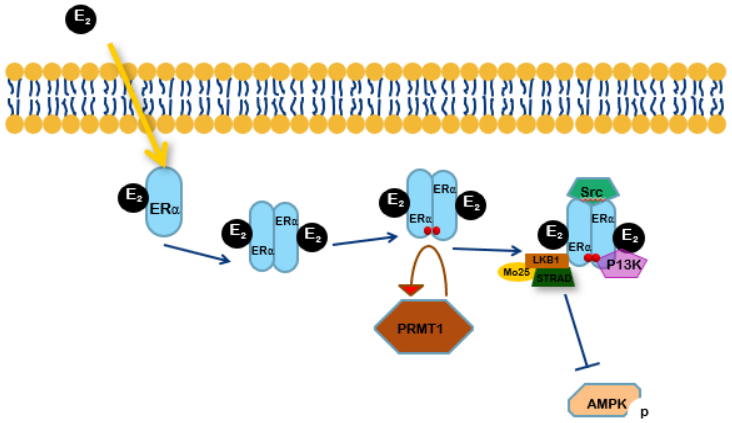

Figure 2.5. Diagram illustrating the connection between the non-genomic ERα/Src/PI3K complex and cytoplasmic LKB1. LKB1's connection with the estrogen non-genomic complex cannot inhibit the mTOR signalling pathway since it cannot phosphorylate its substrates as AMPK. E2: 17 β-oestradiol; ERα: Estrogen receptor α; PRMT1: Protein arginine methyltransferase 1; PI3K: Phosphatidylinositide 3-kinase (Lattouf et al., 2016).

2.3.2. Stimulator of Interferon Genes (STING)

STING (stimulator of interferon genes; also known as TMEM173, MPYS, ERIS, and MITA) is an endoplasmic reticulum (ER)-associated multi-transmembrane protein that operates as an essential innate immunity signalling molecule required for activating dsDNA-mediated gene induction (Ishikawa et al., 2008; Ishikawa et al., 2009). Cyclic GMP-AMP synthase (cGAS) detects abnormal cytoplasmic dsDNA and creates the second messenger cGAMP, which

activates STING and promotes its cellular relocalisation (Kitajima et al., 2016). While STING signalling developed as an innate immune response to protect against viral and other infections, it has become increasingly clear that STING is commonly triggered as a result of a variety of different abnormalities that cause cytoplasmic dsDNA build-up (Barber, 2015). STING signalling has now been proven to be critical for defending cells from a range of infections, as well as for preventing cancer growth by increasing antitumor immune responses (Woo et al., 2015). When pathogenic DNAs or their upstream DNA sensors activate STING, it translocates to perinuclear endosomes with TANK-binding kinase 1 (TBK1). This process activates IRFs and NF-κB, which causes the expression of type I interferon (IFN-I) and other immune response genes (Ishikawa et al., 2009). A positive feedback loop based on the ability of IFNβ and IFNα to trigger multiple IFN-stimulated genes (ISGs) regulates the initial generation of IFN-I (Liu et al., 2012). Immunotherapy is most successful when an immune response, including activated T cells and killing tumour cells, is already underway. The process of developing immunity against cancer is cyclical. It has the potential to spread, resulting in the build-up of immune-stimulatory substances that, in theory, ought to enhance and expand the T-cell response (Chen et al., 2013). One key goal of anticancer treatment approaches is to induce strong tumour-specific cytotoxic T-cell responses. To trigger native CD8+ T lymphocytes, antigen-presenting cells (APCs) must present tumour-associated antigens (Ag) on their MHC class-I molecule. This procedure is known as cross-priming. The most significant APCs that present tumour-derived antigens are dendritic cells (DCs) (Engelhardt et al., 2012). According to recent in vitro and in vivo research, Type-I interferon (IFN), which includes IFN-α and IFN-β, can be targeted to increase anti-tumour CD8+ T-cell responses8. IFN-α and IFN-β activate cross-priming by DC against tumour-associated antigens, a crucial mechanism for cancer immune surveillance (Schiavoni et al., 2013). cGAMP causes STING to undergo a conformational shift, which attracts and activates protein kinase TBK1 at the signalling complex. TBK1 then recruits the transcription factor interferon regulatory factor 3 (IRF3) to the signalling complex, where it is phosphorylated. IFN-β, which controls the expression of more than two hundred interferon-inducible genes and can inhibit protein synthesis, cause cell growth arrest, and trigger apoptosis, is triggered by phosphorylated IRF3 (Tanaka et al., 2012).

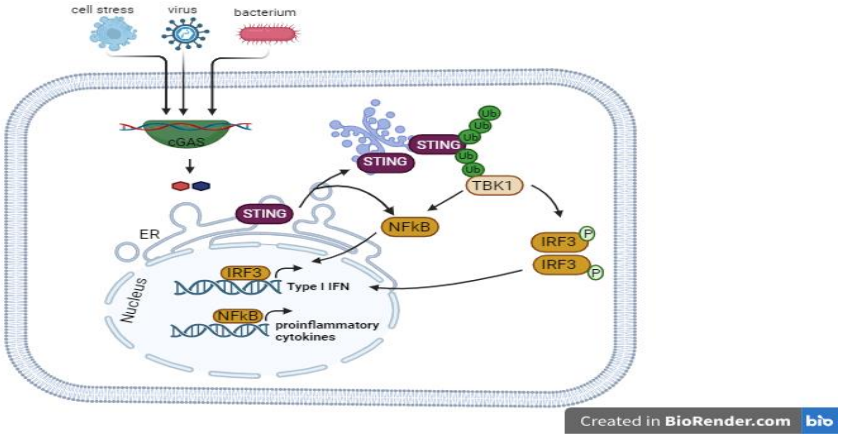

Figure 2.6. cGAS-STING signalling mechanism. The DNA sensor cGAS recognises pathogenic or abnormally localised DNA and creates 2′3′-cGAMP, which binds to STING. STING dimerises and translocates from the ER to the Golgi apparatus when activated. STING is then ubiquitinated, acting as an anchor for TBK1. This causes IRF3 activation and homodimer formation. When IRF3 is activated, it translocates into the nucleus and induces the production of type I IFN. Activated STING causes NF-kB-dependent synthesis of proinflammatory cytokines before transport to the Golgi (Stempel et al., 2019) (https://biorender.com).

Moreover, epigenetic regulation of STING in colon cancer and melanoma cells causes silencing of the promoter region and, as a result, suppresses STING expression (Xia et al., 2016; Xia et al., 2016). DNA methylation, the most extensively researched type of epigenetic alteration, can significantly influence gene expression. It consists of covalently modifying the nucleotide cytosine at the five positions at sites preceding guanine (CpG) [1]. It is duplicated on the daughter strand cytosine at the corresponding CpG by the maintenance enzyme DNA methyltransferase 1 (DNMT1) during mammalian cell division, frequently leading to gene silence (Feinberg et al., 2018). DNA methylation is generally used to silence genes. When methyl groups bind to specific locations in the STING promoter region, they disrupt protein binding required for gene transcription. This results in lower STING gene expression and, as a result, decreased STING protein levels. STING methylation is widespread in a variety of malignancies, including melanoma, glioblastoma, and lung cancer. This silence enables cancer cells to avoid immune identification and decrease antitumor responses, encouraging tumour development and treatment resistance (Lin et al., 2022). A deeper exploration of the complex STING regulation reveals that deacetylation is a counterbalance to acetylation and is essential for adjusting the immune response. Deacetylation acts as a brake, reducing STING signalling and averting over-inflammation, whereas acetylation typically increases STING activity. Histone deacetylases (HDACs) are specialised enzymes that remove acetyl groups from lysine residues on the STING protein. Distinct HDACs may target different locations on

STING, which could affect how it functions differently. It could make it harder for STING to attach to foreign DNA, reducing the activation threshold and stopping the immune system from being overstimulated. It might prevent STING from interacting with other signalling molecules, preventing the downstream immune response machinery from being assembled. This could encourage the deterioration of STING (Hong et al., 2022). Phosphorylation of STING happens after autophagosome formation and Golgi trafficking. Further research revealed that STING phosphorylation inhibits IRF3 activity but not NF-kB activity. In order to further inhibit sustained function, phosphorylation may also aid in STING breakdown. After phosphorylating IRF3, STING appears to be phosphorylated in autophagosome/endosomal compartments and destroyed, which allows phosphorylated TBK1 to be broken down by proteases (Konno et al., 2013).

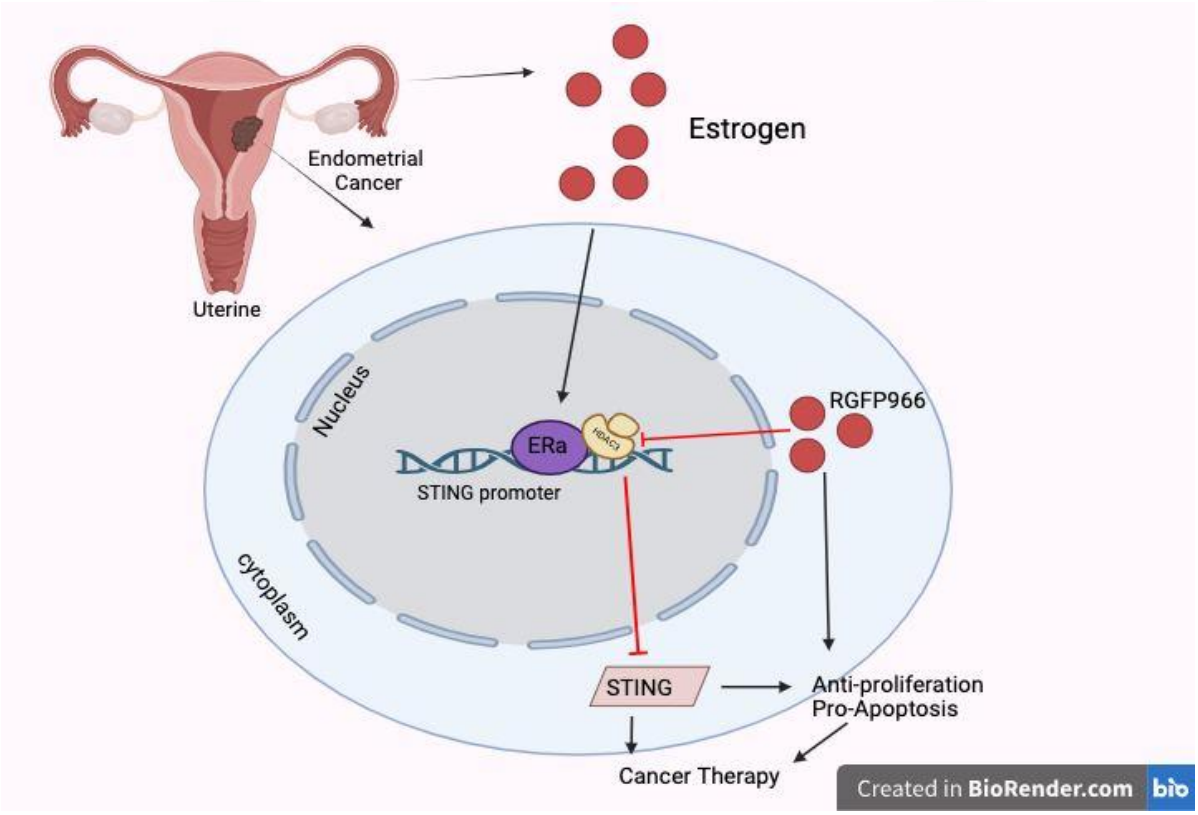

Figure 2.7. The mechanism of β-estradiol-ERα-mediated endometrial carcinogenesis through HDAC3-dependent STING expression. Inducing apoptosis and reducing proliferation are two effects of activating the STING signalling system. Furthermore, β-estradiol-ERα may aid in the repression of STING, while HDAC3-selective inhibition preferentially suppresses proliferation, speeds up EC death, and derepresses STING expression. By increasing STING's expression and decreasing tumour growth in endometrial cancer cells, RGFP966, an HDAC3-selective inhibitor, knocks down or inhibits HDAC3. Utilising mechanical identification, we ascertained that β-estradiol-ERα attracted HDAC3 and promoted the deacetylation of histone three lysine 4 by binding to the STING promoter. This, in turn, decreased the expression of STING (Chen et al., 2022) (https://biorender.com).

IFN pathways in breast cancer cells are dependent on STING levels. It has been noted that ER-negative cells exhibit high STING positivity, whereas ER-positive cells express low STING or negative (Vasiyani et al., 2021). The STING gene promoter's histone deacetylation can be facilitated by estrogen binding to ERα, effectively silencing and lowering the expression of the gene. According to studies, estrogen increases HDAC3, which causes histone deacetylation to inhibit STING expression even further.

2.3.3. Interferon Gamma Protein 16 (IFI16)

Hematopoietic interferon-inducible nuclear, or HIN, is a 200-amino acid signature pattern shared by evolutionarily related proteins that IFI16 and the other members of the IFN-inducible PYHIN-200 gene family encode (Ludlow et al., 2005). Four distinct members of this family exist in humans: IFI16, Myeloid cell Nuclear Differentiation Antigen (MNDA), interferon-inducible protein X (IFIX), and absent in melanoma (AIM) (Cridland et al., 2012). For the first time, IFI16 in lymphoid cells has been characterised (Trapani et al., 1992). It was later found in the epithelium of the genitourinary tract, the skin, the gastrointestinal tract, and the breast glands and ducts (Wei et al., 2003). The control of transcription, apoptosis, cell division and growth, autoimmune, resistance to viruses, and reaction to damaged or viral DNA are among the cellular processes (Veeranki et al., 2012). IFI16's participation in cellular senescence-associated cell growth inhibition is linked to its increased expression in older cell populations. This is partially due to the Rb/E2F and p53/p21 pathways (Choubey et al., 2008). Research has looked into IFI16 expression in several malignancies. The development of cancer in cases of breast and prostate cancer is caused by the epithelial cells' decrease of IFI16 expression (Alimirah et al., 2007). On the other hand, elevated IFI16 expression in ovarian cancer patients was linked to resistance to chemotherapy (Ju et al., 2009). IFNs (α, β, or γ) stimulate the expression of IFI16 protein in various cells. The nuclear localisation signal (NLS) of the IFI16 protein is bipartite, just like that of several other family members. A negative regulator of cell growth is the IFI16 protein (Johnstone et al., 1999). Cell growth arrest linked to cellular senescence is partially caused by elevated IFI16 protein expression in older cell populations via the p53/p21 pathways (Choubey et al., 2008). Comparing human breast cancer cell lines to normal mammary epithelial cells, it was found that most of them expressed lower levels of IFI16 mRNA and protein. Compared to cultured normal human prostate epithelial cells, most human prostate cancer cell lines and prostate cancer tumours

either do not express IFI16 mRNA and protein or express it at reduced levels (Xin et al., 2003; Fujiuchi et al., 2004).

CpG islands, which are collections of cytosine and guanine nucleotides and excellent candidates for DNA methylation, are found in the IFI16 promoter region. Gene expression is essentially silenced when DNA methyltransferases (DNMTs) add methyl groups to these CpG islands. Methyl-CpG binding proteins (MeCP2) and other repressor proteins are drawn to methylated CpG islands (Ali et al., 2013; Caldiran & Cacan, 2022). These repressors physically prevent the enzyme RNA polymerase II, which starts gene transcription, from binding to DNA. By stopping the IFI16 gene from being translated into mRNA, this blockage suppresses the expression of the gene (Zhang et al., 2021). Ironically, deacetylation—removing acetyl groups from histone proteins- can be a silencing mechanism for some genes, including IFI16. Histones are DNA beads that are strung together. When the string is loosened by acetylation, transcription factors can now reach the beads or genes. Deacetylation makes the string tighter, making it harder to see the beads and gain access. The deacetylation-induced compaction of chromatin hinders the ability of RNA polymerase, the transcription-related enzyme, to bind to the IFI16 promoter, hence leading to the silencing of the gene (Choubey et al., 2008). Phosphorylation and IFI16 expression are intertwined processes with multifaceted consequences. Phosphorylation, or the addition of phosphate groups to proteins, can both activate and repress the production of IFI16. However, this may appear paradoxical depending on the situation and the particular phosphorylated sites. For IFI16 to engage its antiviral activities, it must move from the cytoplasm into the nucleus, where phosphorylation can operate as a passport. IFI16 partners with other proteins drawn to specific phosphorylation sites, enhancing the protein's capacity to bind to viral DNA and initiate an immune response. IFI16's antiviral activity can be prolonged, and phosphorylation can prevent degradation. By exporting IFI16 from the nucleus back to the cytoplasm, phosphorylation at particular locations can function as a one-way ticket, thereby eliminating IFI16 from the site of action. Certain phosphorylations cause IFI16's partner proteins to become less bound, which impairs the protein's ability to function and reduces its antiviral response. IFI16 can be marked for destruction by phosphorylation at particular locations, which lowers the protein's overall expression and function (Justice et al., 2021).

Complex variables like cell type, estrogen levels, and the presence of other stimuli can all affect how estrogen affects IFI16 expression. Its dual ability to increase and decrease IFI16 expression illustrates the complexity of its involvement in controlling this gene. When estrogen attaches itself to its receptor ERα, HDAC3, a histone deacetylase that suppresses

gene expression, is drawn to the area and can directly restrict IFI16 transcription. IFI16 can indirectly suppress by estrogen by encouraging DNA methylation of its promoter region, which reduces transcriptional accessibility. Estrogen may play a context-specific activation role in immune cells by enhancing IFI16 expression in concert with the cytokine IFNγ. Indirect effects of estrogen on IFI16 expression can arise from its modulation of other immunological pathways, including NF-κB signalling (Ka et al., 2022).

2.4. Interactions between cancer suppresser genes

Deleting LKB1 can potentially disrupt the delicate balance of cellular defence systems by considerably impacting STING expression in multiple ways. LKB1 is a crucial transcriptional activator of the STING gene. STING protein levels drop directly due to its loss, which lowers STING mRNA synthesis. The cell's capacity to detect and react to internal danger signals or invasive infections is compromised by this downregulation. The regulation of metabolism by LKB1 affects the expression of STING. Loss of LKB1 interferes with energy metabolism, which raises S-adenosyl methionine (SAM) levels. DNA methyltransferases (DNMTs), enzymes that add methyl groups to DNA, utilise SAM as a substrate. By silencing the STING gene promoter, this methylation can further inhibit the production of the gene. In addition to suppressing gene expression, LKB1 deletion also encourages histone deacetylation, which may impact STING levels (Kitajima et al., 2019).

The connection between IFI16 and STING: IFI16 interacts with STING when it binds to foreign DNA in the cytoplasm. STING is activated by this contact, which causes a conformational change in the protein. After that, activated STING attracts and stimulates additional signalling molecules, synthesising other immune-stimulating proteins, including type I interferons (IFNs). Targeting contaminated cells and triggering immune cells to fight infection, these IFNs and signalling molecules start a robust antiviral response. Additionally, they cause inflammation, which aids in drawing immune cells to the infection site (Li et al., 2022).

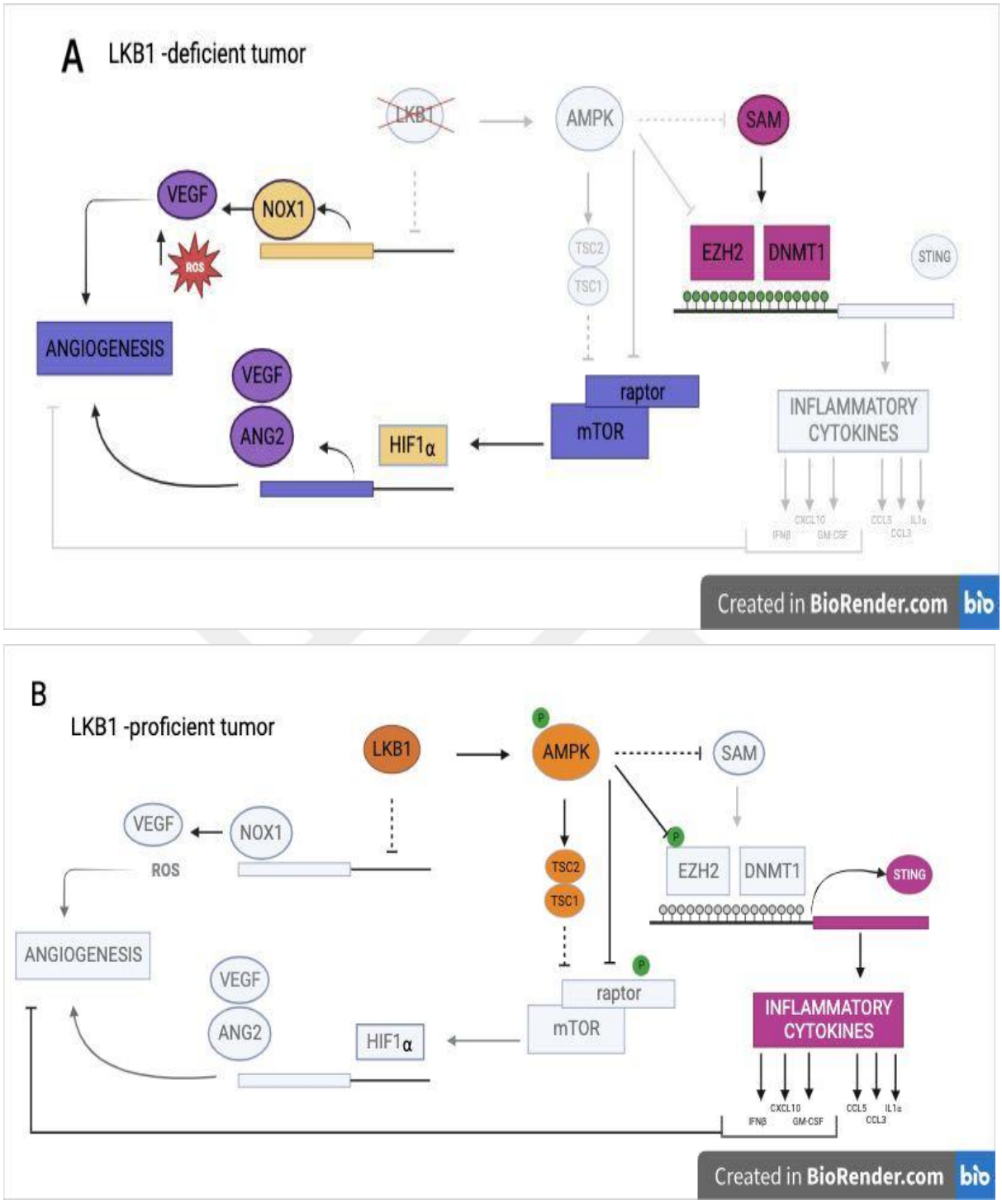

Figure 2.8. A functional model for regulating tumour angiogenesis and immune evasion by LKB1. (A). Increased NADPH oxidase 1 (NOX1) transcript expression is linked to LKB1 loss. By boosting the production of redox oxygen species (ROS) and vascular endothelial factor (VEGF), NOX1 encourages the angiogenic switch. Lack of AMPK activation increases hypoxia-inducible factor 1 subunit alpha (HIF-1α) production and downstream targets, including VEGF and angiopoietin 2 (ANG2), by inducing mTOR activity. Furthermore, the absence of LKB1 stimulates the production of S-adenosyl methionine (SAM), a substrate for several epigenetic silencing enzymes, including DNMT1 and EZH2. The expression of the stimulator of interferon genes (STING) is thereby silenced. Immune escape is facilitated by STING suppression, which downregulated chemokines that encourage T-cell recruitment. (B). In addition to suppressing NOX1, LKB1 also suppresses mTOR by activating AMPK.

As a result, angiogenesis and VEGF expression are decreased. Methyltransferases DNMT1 and EZH2 cannot methylate the STING promoter when AMPK is activated. Additionally, EZH2 is directly phosphorylated and inhibited by AMPK. Increased antitumor innate immunity signals result from the production of immune-inflammatory cytokines, which are caused by the activation of the STING intracellular phosphorylation cascade (Bonanno et al., 2019) (https://biorender.com).

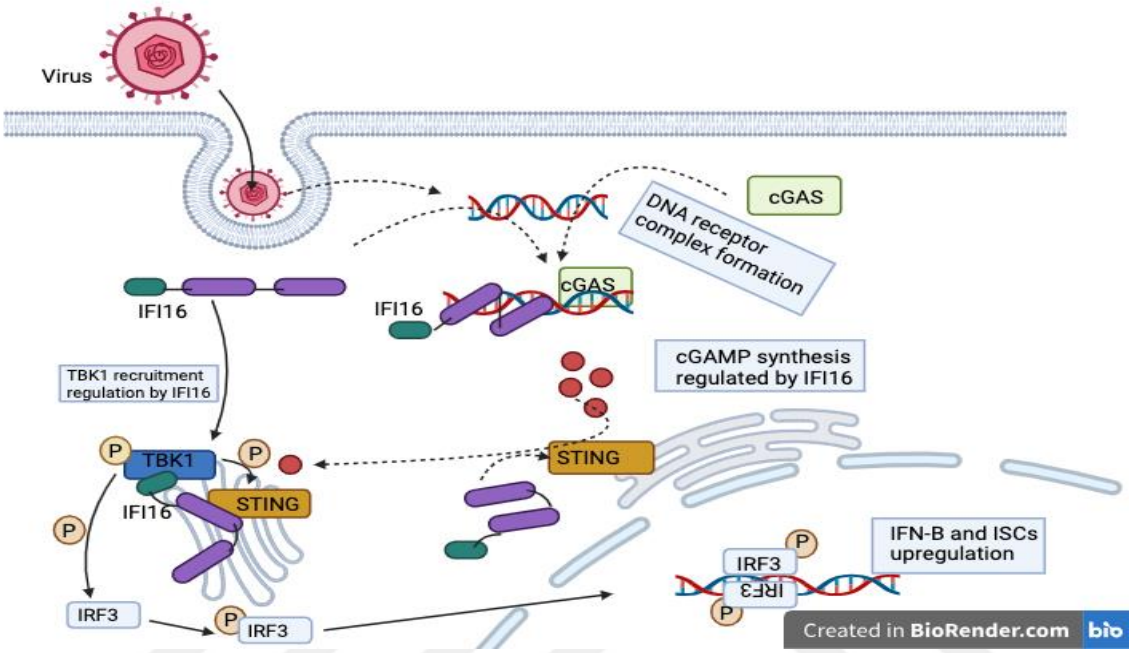

Figure 2.9. IFI16 dictating STING function (Jønsson et al., 2017) (https://biorender.com)

2.5. Drugs Mediated Epigenetics Changes

2.5.1. 17β-Estradiol

The primary female sex hormone, 17β-Estradiol, influences genes in a complex way involving several pathways. Two nuclear receptors, ERα (estrogen receptor alpha) and ERβ (estrogen receptor beta) are the primary receptors with which estrogen interacts. These receptors function as transcription factors that are ligand-activated. They undergo structural changes and become activated upon binding with 17β-Estradiol. The target gene promoters include specific DNA sequences known as estrogen response elements (ERE), activating ER binding. ERs bind to the ERE and then recruit more coactivator proteins to help in the transcription of genes. This causes the target gene to produce more mRNA, which raises the amount of protein in the end (Lobenhofer et al., 2002). Additionally, through their interactions with other transcription factors and signalling cascades, ERs can indirectly control the expression of specific genes. Binding to repressor proteins, preventing the transcription of target genes, adjusting the stability and translation of mRNA molecules, and

changing the accessibility of DNA to other transcription factors. Apart from nuclear signalling, 17β-Estradiol can also act quickly via G-protein-coupled and membrane-associated estrogen receptors. These receptors set off signalling cascades that affect metabolism, apoptosis, and cell division, among other biological functions (Russo et al., 2002).

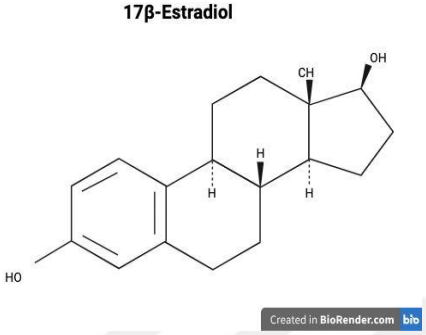

Figure 2.10. 17β-Estradiol structure (C18H24O2) (Lamminmaki et al., 2001) (https://biorender.com).

2.5.2. Vorinostat (SAHA)

A novel medication called Vorinostat, often called suberoylanilide hydroxamic acid (SAHA), treats cutaneous T cell lymphoma when it does not go away, worsens, or recurs in contrast, or after other medications have been taken. It has been regarded as a unique medicine for treating this condition and is effective and well-tolerated (Grant et al., 2007). Both class I and class II HDAC enzymes are inhibited by Vorinostat, a broad inhibitor of HDAC activity (Marks et al., 2005). Nevertheless, class III HDACs are not inhibited by Vorinostat. Crystallographic studies have revealed that Vorinostat attaches to the zinc atom of the HDAC enzyme's catalytic site, protruding its phenyl ring onto the enzyme's surface from the catalytic domain (Finnin et al., 1999). Histones and other acetylated proteins accumulate upon binding to the HDAC enzyme, which has a variety of physiological consequences (Secrist et al., 2003). Both transcriptional and non-transcriptional effects are observed. Vorinostat's direct HDAC binding may have the desired transcriptional or indirect effects by influencing different transcriptional variables. Some genes' expression may change (Bereshchenko et al., 2002). The categories of Vorinostat's non-transcriptional actions are the downregulation of immunosuppressive interleukins, inhibition of angiogenesis, apoptosis, and cell cycle arrest (Zhao et al., 2005; Lin et al., 2007).

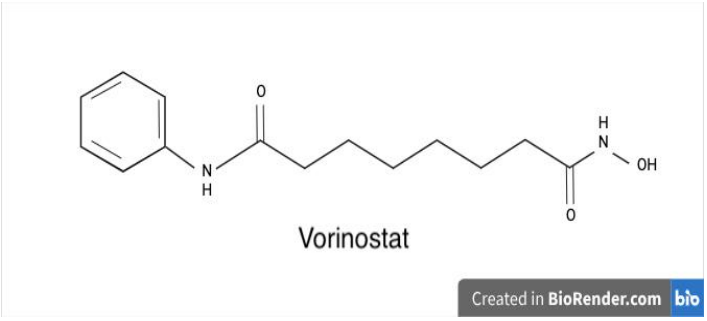

Figure 2.11. Vorinostat (SAHA) structure (C14H20N2O3) (Marks et al., 2007).

2.5.3. Decitabine (5-aza-2′-deoxycytidine)

It is a hypomethylating drug that functions in two ways: at low dosages, it reactivates silenced genes and promotes differentiation; at significant levels, it causes cytotoxicity (Jabbour et al., 2008). Decitabine's ability to bind to freshly produced DNA is what gives it its anticancer properties. With two distinct, dose-dependent modes of action, it is an agent exclusive to the S-phase. Its lethal action at large concentrations result from the enzyme DNA methyltransferase being covalently trapped within DNA. Its capacity to prevent DNA hypermethylation and reactivate tumour suppressor genes is probably the reason for its anticancer action at lower dosages. Decitabine does not impede G1 phase cells' ability to continue through the cell cycle and enter the S phase at low doses. DNA methyltransferase is trapped and eventually depleted by low concentrations of decitabine integrated into DNA (Jones et al., 1980). It normalises the acetylation: methylation ratio and restores gene expression by increasing H3-lysine 9 acetylation and decreasing H3-lysine 9 methylation. Decitabine's simultaneous action on histone acetylation and methylation explains why it is more efficient than histone-deacetylase inhibitors, which do not alter histone methylation, at reactivating suppressed gene expression (Issa, 2003).

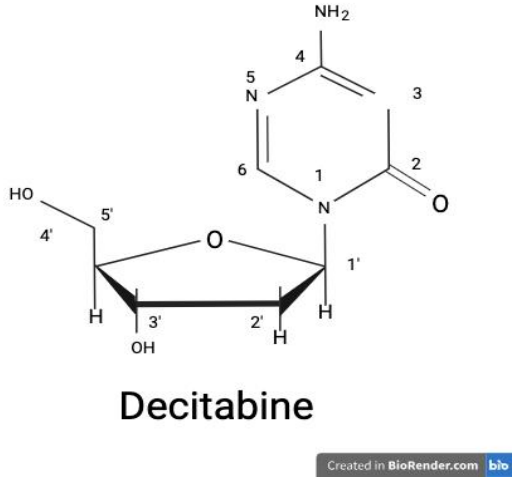

Figure 2.12. Decitabine (5-aza-2′-deoxycytidine) structure ($C_8H_{12}N_4O_4$) (Jabbour et al., 2008)

3. MATERIAL AND METHOD

3.1 MATERIAL

The equipment, chemicals and kits used in this thesis study are given in the Tables below.

Table 3.1. The instruments used in this study.

instrument /Equipment	**Brand**
security cabin	ESCO, Class II, Type A2
Automatic Cell Counting Device	Countess TM 3, Invitrogen, ThermoFisher Scientific
Pro Pipette Controller	accu-jetR pro, BRAND
Centrifuge	micro 200 R Hettich Zentrifugen
Vortex	Velp Scientifica
Mini Centrifuge-Vortex	Combi-Spin, BIOSAN
Humidified CO2 Incubator with Water Jacket	NuAire, NU-4850
Heater and Magnetic Stirrer	VELP Scientifica
Microplate Shaker Incubator	PST-60HL, BOECO
Light Microscope	Leica DM IL LED
Fluorescence Microscope	Leica DFC295 S 40/0.45
Precision Scale	Denver Instrument
ELISA License Plate Reader	Thermo Scientific, Multiskan go
Ice Machine	Scotsman, AF 80
Micropipette Set	İsolab
-20°C Deep Freezer	Vestel
-80°C Freezer	new brunswick scientific
Autoclave	HMC HIRAYAMA
Homogenizer	IKA T10 basic/ ULTRA-TURRAX

PCR plate reader	Analytikjena
PCR plate	Bioplastic

Table 3.2 The chemicals used in this study.

Chemicals and Consumables	**Brand**
Dulbecco's Modified Eagle's Medium (DMEM)/F12(HAM)1:1	SARTORIUS
RPMI-1640 Medium	Sigma Life Science
RPMI-1640 Medium (Non-Phenol Red)	Capricorn Scientific
L-Glutamine solution	Sigma Life Science
Penicillin-streptomycin	Biological Industries
Fetal Bovine Serum (FBS)	Biological Industries
Phosphate Buffered Saline (PBS)	Capricorn scientific
Dimethyl Sulfoxide (DMSO)	serva
Trypsin EDTA Solution A	Biological Industries
MTT (methylthiazoldiphenyl-tetrazolium bromide) dye	serva
Vorinostat (SAHA)	CAYMAN CHEMICAL COMPANY
Decitabine (5-Aza)	AK Scientific
17β-Estradiol	CAYMAN CHEMICAL COMPANY
Isopropyl Alcohol	AMRESCO
Chloroform	EMSURE
RiboEX	GeneAll
Ripa Buffer	Thermo Scientific
Protease inhibitor – EDTA-free	Complete Mini/Roche
ethanol	isolab
methanol	isolab

Acetic acid	isolab
Rnase free water	Thermo Scientific
Forward Reverse primers	Macrogen
Antibacterial-Antifungal Solution Zefiran	Dermocept
Pasteur Pipette	isolab
15ml Centrifuge Tubes	Nest Scientific
50 ml Centrifuge Tubes	Nest Scientific
10 ml Sterile Serological Pipette	Nest Scientific
25 ml Sterile Serological Pipette	Nest Scientific
100-1000 µl, 20-200 µl and 0.5-10 µl Micropipette	isolab
Sterile filter tip (0.45 µm)	sartorius
Pasteur Pipette	isolab
6-Well Cell Culture Dish	Nest Scientific
12-Well Cell Culture Dish	Nest Scientific
96-Well Cell Culture Dish	Nest Scientific
2ml Cryovial Tube	Nest Scientific
T75 Culture Flask	Nest Scientific
T25 Culture Flask	Nest Scientific
Microtube tube	isolab
Sterile Injector	baby
Powder-Free Nitrile Gloves	baby

Table 3.3. The kits used in this study.

Kit	**Brand**
One Step qRT-PCR kit for 400 Reactions	Snp Bioteknoloji
Human Liver Kinase B1 ELISA Kit	BT LAB

3.2 METHODS

3.2.1. Cell Culture and Preparation of Drug Concentrations

Cell Culture

All cell culture procedures were performed in a safety cabinet (ESCO, Class II, Type A2). To minimise the risk of contamination in the cell culture laboratory, pre-experimental and, afterwards, ultraviolet light was applied. The work area and materials with 70% ethanol were cleaned and used. Additionally, cabin environment and used consumables are 10%. While cleaned regularly with bleach, disposable materials after autoclaving were removed.

This study used ovarian cancer cell line A2780 and its chemoresistance clone A2780AD cells, available in the cancer research laboratory stocks at Tokat Gaziosmanpasha University, Department of Molecular Biology and Genetics and endometrium cancer cell line RL95-2 gained from the cancer research laboratory stocks at Erciyes University Kayseri from assistant professor Ayshe Kubra Karaboga. For culture procedures, 10% fetal bovine serum (FBS, Biological Industries) and 5mM penicillin-streptomycin (Biological Industries) solution RPMI-1640 (Sigma-Aldrich) medium for ovarian cancer cell lines and DMEM-F12 (Sigma-Aldrich) medium for endometrium cancer cell line enriched with was preferred. The cryovial cells removed from the cooler at -80°C were thawed with the help of medium in 50 ml centrifuge tubes and settled to the bottom after centrifugation at 3000 rpm for 3 minutes. The medium was removed from the resulting pellet, suspended with approximately 15 ml of fresh media, and the solution was transferred to a 75 cm^2 culture flask (Corning). Then, the flasks were placed in an incubator environment with 37°C, 5% CO_2 and 80-90% humidity saturation for the cells to become adherent and proliferate. On the third day of incubation, the medium was removed from the environment. After washing with 1X phosphate buffered salt solution (PBS), the fresh medium was transferred back into it. In addition, the culture processes of chemoresistant A2780AD were continued in a medium containing cisplatin (Koçak Farma) at a concentration of 3 μM. When the cells reached confluency, passage procedures were started. For this purpose, the culture dishes were first washed with PBS, and approximately 5 ml of trypsin-EDTA solution was added. Then, resuspension was achieved by separating from the base and adding fresh medium. Some of the A2780 and A2780AD were counted with the help of a hemocytometer and transferred to new culture media as 1,000,000/15 ml and passaged. Specific to the first passage process, the remaining cells, after counting, were transferred to new 150 cm2 culture flasks and incubated for cell freezing. The steps in the passaging process were repeated, and a different cell concentration of 1,000,000/ml was transferred to cryovial tubes in a freezing solution of 1% Dimethyl

sulfoxide (DMSO) and 9% fetal bovine serum (FBS, Biological Industries). After the cryovial tubes were kept at -20 °C for half an hour, they were transferred to the -80°C freezer for long-term storage.

Preparation of Drug Concentrations

17β-Estradiol, Vorinostat from (CAYMAN Chemical Company) and Decitabine from (AK Scientific) were available at Tokat Gaziosmanpasha University. Each drug stock solution was prepared from their powder by measuring a specific amount and dissolved in 1000µL Dimethyl sulfoxide (DMSO) from the stock solutions; different concentrations for each drug were prepared. It is detailed in the table below.

The drugs in a powder form, stock solutions and prepared different concentrations were stored at -20ºC, and the prepared different concentrations thawed before being used in procedures.

Table 3.4. Preparation of Drug Concentrations

Drug	Concentrate	Drug Amount	Dilution Rate	DMSO	Total
17β-Estradiol	1600nM	3.13 µL	1:300	996.87 µL	1000µL
	6400nM	12.5 µL	1:80	987.5 µL	1000µL
	25600nM	50 µL	1:20	950 µL	1000µL
Decitabine	2000µM	50 µL	1:20	950 µL	1000µL
	4000µM	100 µL	1:10	900 µL	1000 µL
	8000µM	200 µL	1:5	800 µL	1000 µL
Vorinostat	20µM	1 µL	1:1000	999 µL	1000 µL
	200µM	10 µL	1:100	990 µL	1000 µL
	1000µM	50 µL	1:20	950 µL	1000 µL
	2000µM	100 µL	1:10	900 µL	1000 µL

3.2.2. MTT ((3-(4, 5-dimethyl thiazolyl-2)-2, 5-diphenyltetrazolium bromide) assay

Analysis using the MTT (3-(4,5-dimethylthiazol-2-yl)-2,5-diphenyl-2H-tetrazolium bromide) test to determine the potential effects of 17β-Estradiol, Vorinostat and Decitabine on the endometrium cancer cell line RL95-2 and ovarian cancer cell lines A2780 and A2780AD done. MTT test, one of the cytotoxicity determinations tests, measures based on the colouration of cells using tetrazolium salt. Tetrazolium salts are broken down by

mitochondrial dehydrogenases, thus reducing to formazan crystals and showing the colour change. However, only living cells can be created since living mitochondria can break down the tetrazolium ring. MTT salts are yellow, but the resulting formazan crystals are purple and insoluble in water. Therefore, it is dissolved in a suitable solvent, Dimethyl sulfoxide (DMSO), to measure absorbance. The dissolved formazan and cell viability are directly proportional, and the spectrophotometer makes measurements at specific wavelengths.

Cells that reached sufficient density during incubation were removed from the incubator, and the old medium was poured into a container in the laminar cabinet. In order to demonstrate trypsin activity, the inside of the flask was washed with 10 ml of 1X phosphate buffer saline (PBS). 3ml trypsin was added and placed in the 37ºC incubator for 2-5 minutes. After incubation, a new medium containing the cells to inactivate trypsin was added to the flask, and after pipetting, it was transferred to a 50ml falcon tube. It was centrifuged at 3000rpm for 3 minutes. After centrifugation, the pellet in which the supernatant was shed was dissolved with a new 10ml medium and measured with the help of a hemocytometer. MTT analyses were applied as stated previously (Berkel et al., 2020; Al-Janabi et al., 2020; Berkel & Cacan, 2021; Kucuk et al., 2021; Saygi & Cacan, 2021). After calculating 10000 cells per well, 10000 cells were planted in 200 µl per well of 96-well plates. The 96-well plate was placed in the incubator and incubated for 24 hours. After 24 hours of incubation, the drugs (17β-Estradiol, Vorinostat, Decitabine) used were removed from -20ºC and, after thawing, vortexed before adding, and drugs with their different concentrations and three repetitions for each concentration were added to the wells containing the cells. After adding drugs, it was left to incubate for 48 hours. After 48 hours, the remaining part of the MTT steps was carried out: 10 mg of MTT powder was weighed using a precision balance. 10 mg MTT powder was dissolved in 2 ml 1X PBS in the laminar cabinet. It was then filtered before being combined with RPMI 1640 media, which does not contain phenol red, and the solution was made ready. The media in the 96-well plate removed from the incubator was removed with the help of a micropipette. Then, 100 µl 1X PBS was added into the wells and washed. Then, 100 µl of the prepared MTT mixture was added to each well and incubated for 4 hours. After 4 hours, a dark purple colour change was observed in living cells. All the MTT mixture in the wells was withdrawn, and 100 µl of DMSO solvent was added and pipetted. It was kept in a shaking incubator for an hour. At the end of 1 hour, measurements were made at 540 and 570 nm on the spectrophotometer. The values obtained in the measurement were analysed in Excel and GraphPad programs graphed, and the appropriate concentration to be used in other procedures was determined. The highest concentration of each drug was used.

3.2.3. Cell Migration Assay

Migration assay took place by using 2-well insert silicones. First, the silicones had to be sterilised, and the steps of sterilisation are like below:

1. All silicones were put into a beaker containing distilled water
2. Tweezer was used, and silicones were taken out from distilled water and put into a beaker containing 100% ethanol
3. Silicones were put into another beaker containing distilled water
4. Silicones were taken out from distilled water and put into a beaker containing 70% ethanol
5. Again, silicones were put into another beaker containing distilled water
6. After drying the silicones, they were left under ultraviolet light for a few minutes and became ready to use.

The silicones were put on a 12-well plate. On the other hand, cells were passaged and counted, and 50000 cells were put on each side of the silicones. Each side contained 100µl of the specific media, then incubated for 24 hours. After 24 hours, the cells were observed to be adherent, and the silicones were taken out carefully. 1000µl media were poured into each well; after that, 5µl of the drugs were put into their specific well. Before drug addition, the cells were photographed under a fluorescent microscope, and after the drug addition, photographing was continued for five days.

3.2.4. Blood and Tissue Sample Collection

For this study, tumour and regular tissue collection from gynecologic cancer patients took place in Iraq and blood was taken from each patient. Tissue samples were collected in a 15ml tube containing PBS after being saved in a -80°C refrigerator. 5 ml of blood was taken from each patient, 2 ml of it was poured into an EDTA tube after mixing properly with EDTA, it was poured into a Microtube tube, and another 3 ml of blood was poured into biochemistry tube and separated to serum and blood cells after that the serum was poured into Microtube tube, both saved in the -80°C refrigerator. Each tube was labelled with the patient's name and the cancer type. Samples were brought to Turkey in a container with the help of 10kg of dry ice and kept frozen after reaching Tokat Gazi Osmanpasha University. They were kept in a -80°C refrigerator.

3.2.5. RNA Isolation from Blood, Tissue and Cell

RNA Isolation from Blood

The blood was taken from the -80°C freezer and left to thaw at room temperature for a few minutes. When it thawed, it gently turned upside down for a few minutes and 500 µl of the blood from the Microtube tube was taken and added into a new Microtube tube, and 1000µl Trizol was poured over it into the Microtube tube. It was homogenised by a homogeniser for 1 minute, put on a shaker at 400 rpm for 5 minutes, then homogenised again until it became homogenous. To precipitate the proteins, 200 µl of chloroform was added, vortexed for a few seconds, left for 2-3 minutes, and centrifuged at 12000 rpm for 15 minutes at 4ºC. After centrifugation, phase separation (RNA, DNA and protein phase) was observed, and the RNA phase was carefully withdrawn and transferred to the new Microtube. 500 µl of isopropanol was added to precipitate the RNA, which was transferred to a separate Microtube and left overnight at -20ºC freezer. The next day, the Microtube contained the isopropanol, and the RNA was taken out from the -20ºC freezer and left at room temperature for thawing. The microtube was vortexed for a few seconds and then centrifuged at 12000 rpm for 10 minutes at 4ºC. The supernatant in the Microtube tubes removed from the centrifuge was poured. 1 ml of 75% ethanol was added to obtain pure RNAs in the tubes. RNAs treated with ethanol were centrifuged at 7500 rpm for 5 minutes at 4ºC. After centrifugation, the supernatant was poured out and left in the laminar cabin for 5-10 minutes to dry with the lids of the Microtubes open. Then, 40 µl of Nuclease Free H_2O was added to dissolve the pellet and pipetted. The concentration was measured by 1µl of the solution and loaded into the microplate reader. Absorbance values were measured at 230, 260 and 280 nm wavelengths, and the concentration calculation was made in Excel as ng/µl by multiplying the 260 nm wavelength values from the obtained absorbance values by 40.

The isolated RNA samples were stored in the -80◦C freezer. Unnecessary freeze-thaw steps were avoided in order not to reduce the quality of the RNA.

RNA Isolation from Tissue

The sample was taken out from the -80◦C freezer and left to thaw at room temperature for a few minutes. Before it was wholly thawed, a small piece was cut off from the sample, and the remaining part of the sample was put back into the tube containing PBS and put back into the -80◦C freezer again. The small piece which was cut before was put into the Microtube tube, and 700µl Trizol was poured over it into the Microtube tube. A homogeniser homogenised them till they totally became homogenous. To precipitate the proteins, 200 µl of chloroform

was added, vortexed for a few seconds, left for 2-3 minutes, and centrifuged at 12000 rpm for 15 minutes at 4ºC. After centrifugation, phase separation (RNA, DNA and protein phase) was observed, and the RNA phase was carefully withdrawn and transferred to the new Microtube. 500 µl of isopropanol was added to precipitate the RNA, which was transferred to a separate Microtube. The microtube was vortexed for a few seconds, incubated for 10 minutes at room temperature, and then centrifuged at 12000 rpm for 15 minutes at 4˚C. The supernatant in the Microtube tubes removed from the centrifuge was poured. 1 ml of 75% ethanol was added to obtain pure RNAs in the tubes. RNAs treated with ethanol were centrifuged at 7500 rpm for 5 minutes at 4ºC. After centrifugation, the supernatant was poured out and left in the laminar cabin for 5-10 minutes to dry with the lids of the Microtubes open. Then, 40 µl of Nuclease Free H_2O was added to dissolve the pellet and pipetted. The concentration was measured by 1 µl of the solution and loaded into the microplate reader. Absorbance values were measured at 230, 260 and 280 nm wavelengths, and the concentration calculation was made in Excel as ng/µl by multiplying the 260 nm wavelength values from the obtained absorbance values by 40.

The isolated RNA samples were stored in the -80˚C freezer. Unnecessary freeze-thaw steps were avoided in order not to reduce the quality of the RNA.

RNA Isolation from Cell

The passage technique mentioned above was used for ovarian cancer cell lines (A2780 and A2780AD) and endometrium cancer cell line (RL95-2) that reached sufficient density in the incubator. Then, cell counting was done with the help of a hemocytometer. 500000 cells were seeded per well of 6-well plates and incubated for 24 hours. At the end of 24 hours, drugs (17β-Estradiol, Vorinostat and Decitabine) were added to the wells at the concentration determined according to the data obtained from the MTT test and incubated for 48 hours. After the incubation, the RNA isolation protocol was started, as stated previously (Morgan et al., 2015; Cacan & Ozmen, 2020; Karatas et al., 2021). According to the applied protocol, the media of the cells in the plate wells was first withdrawn, and 1 ml of PBS was added to each well, waited and carefully withdrawn. To ensure that the cells were separated from the surface and disrupted, thus allowing the molecules inside the cell to pass into the external environment, 1 ml of Trizol was added, and the plate was shaken slowly. Then, the cells removed from the surface after treatment with Trizol were transferred to a Microtube and gently turned upside down for a few minutes. To precipitate the proteins, 200 µl of

chloroform was added, vortexed for a few seconds, left for 2-3 minutes and centrifuged at 12000 rpm for 15 minutes at 4ºC.

After centrifugation, phase separation (RNA, DNA and protein phase) was observed, and the RNA phase was carefully withdrawn and transferred to the new Microtube. 500 µl of isopropanol was added to precipitate the RNA, which was transferred to a separate Microtube. The microtube was vortexed for a few seconds, incubated for 10 minutes at room temperature, and then centrifuged at 12000 rpm for 10 minutes at 4ºC. The supernatant in the Microtube tubes removed from the centrifuge was poured. 1 ml of 75% ethanol was added to obtain pure RNAs in the tubes. RNAs treated with ethanol were centrifuged at 12000 rpm for 2 minutes at 4ºC. After centrifugation, the supernatant was poured out and left in the laminar cabin for 5-10 minutes to dry with the lids of the Microtubes open. Then, 50 µl of Nuclease Free H_2O was added to dissolve the pellet and pipetted. The concentration was measured by 1 µl of the solution and loaded into the microplate reader. Absorbance values were measured at 230, 260 and 280 nm wavelengths, and the concentration calculation was made in Excel as ng/µl by multiplying the 260 nm wavelength values from the obtained absorbance values by 40.

The isolated RNA samples were stored in the -80°C freezer. Unnecessary freeze-thaw steps were avoided in order not to reduce the quality of the RNA.

3.2.6. Protein Isolation from Tissue and Cell

Protein Isolation from Tissue

The sample was taken out from the -80°C freezer and left to thaw at room temperature for a few minutes. Before it was wholly thawed, a small piece was cut off from the sample, and the remaining part of the sample was put back into the tube containing PBS and put back into the -80°C freezer again. The small piece which was cut before was put into the Microtube tube. RIPA buffer for protein isolation from tissues was prepared before, and a proteinase inhibitor was added. 300 µl of prepared RIPA buffer was added into the Microtube tube. The piece of the tissue sample inside the Microtube tube was homogenised with the RIPA buffer by homogeniser for a few minutes and then by sonicator for 30 seconds to be completely homogenous. 400 µl of the RIPA buffer was added. The Microtube tubes were put on an ice shaker for 2 hours. Then, the Microtubes were centrifugated at 14000 rpm for 20 minutes at 4°C, and the supernatant, which is the protein phase, was carefully withdrawn and transferred to the new Microtube.

Bovine serum albumin (BSA) and Bradford assay were done to determine the concentration of isolated proteins. 2mg BSA crystals, which is a known protein concentration measured and dissolved in 1ml Phosphate-buffered saline (PBS) by using a vortex, and the standards (2mg/ml, 1.5mg/ml, 1mg/ml, 0.75mg/ml, 0.5mg/ml, 0.25mg/ml, 0.125mg/ml) were prepared. Proteins were brought to room temperature, and a 96-well plate was used to measure the concentrations of the proteins. By using a multichannel pipet 250µl of the Bradford solution which was used as a colour reagent, was added to each well, 5µl of standards was added to standard wells in duplicate form, 5µl of proteins which concentrations were unknown were also added in duplicate form directly after using proteins they were stored in -80◦C freezer, and 5µl PBS was added to two wells and used as a blank. When the standards and the isolated proteins were added to the w, the colour of the Bradford was changed from reddish brown to blue colour, and the darkness of the blue colour depended on the concentration of the proteins. After pipetting of each well the plate was left at room temperature for 5 minutes. At the end of 5 minutes, measurements were made at 595 nm on the spectrophotometer. The values obtained in the measurement were analysed in Excel, and a standard curve was drawn using standards absorbance. The curve equation was found to find the concentrations of unknown concentration proteins after subtracting the blank absorbance value from the standards and proteins absorbance values.

Protein Isolation from Cell

The passage technique mentioned above was used for ovarian cancer cell lines (A2780 and A2780AD) and endometrium cancer cell line (RL95-2) that reached sufficient density in the incubator. Then, cell counting was done with the help of a hemocytometer. 500,000 cells were seeded per well of 6-well plates and incubated for 24 hours. At the end of 24 hours, drugs (17β-Estradiol, Vorinostat and Decitabine) were added to the wells at the concentration determined according to the data obtained from the MTT test and incubated for 48 hours. After 48 hours before taking the cells from the wells, protein lysate was prepared by mixing RIPA buffer and proteinase inhibitor. Then, the cells were taken from the wells by adding 500 µl trypsin into each well, and the plate was put into the incubator for 3 minutes. After 3 minutes, the plate was checked under a microscope to be sure the cells separated from the bottom of the plate, and the cell + trypsin mixture was taken from the wells and put into the Microtube tube and centrifugate at 3000 rpm for 3 minutes at 4°C. The supernatant is withdrawn carefully, and the pellet remains below. 500 µl cold PBS was added to each Microtube tube and centrifugated at 3000 rpm for 3 minutes at 4°C to wash the pellet from the

remaining trypsin. The supernatant was withdrawn carefully, and the pellet remained below. The 500 µl protein lysate buffer was poured into the Microtubes and put on an ice shaker at 400-500 rpm for 30 minutes. Then, the Microtubes were centrifugated at 12000 rpm for 20 minutes at 4°C, and the supernatant, which is the protein phase, was carefully withdrawn and transferred to the new Microtube.

Bovine Serum Albumin (BSA) and Bradford assay were done as mentioned above to ensure the presence of protein in the cells. The isolated protein samples were stored in the -80°C freezer. Unnecessary freeze-thaw steps were avoided not to reduce the quality of the proteins.

3.2.7. Quantitative Real-time Polymerase Chain Reaction (qRT-PCR)

Before the experiment, primers were ordered to amplify transcripts in quantitative real-time PCR and Eva Green one-run real-time PCR kit 2X. The components' concentrations and the technique corresponding with this kit were processed. Humanising genomics macrogen gave information on the methods utilised to dissolve and alter the primer concentrations for the qRT-PCR study.

The GAPDH gene was utilised as a calibrator to compare the gene expressions of the various groups. Table 3.5. provides the primer sequences utilised in the qRT-PCR analysis.

Table 3.5. Primer sequences for qRT-PCR analysis

Gen	Forward Primer	Reverse Primer	Reference
LKB1	CTACTGAGGAGGTTACGGCACA	ACGCTGTCCAGCATTTCCTGCA	Koivunen et al., 2008
STING	CCTGAGTCTCAGAACAACTGCC	GGTCTTCAAGCTGCCCACAGTA	Balagunaseelan, 2014
IFI16	GATGCCTCCATCAACACCAAGC	CTGTTGCGTTCAGCACCATCAC	Baggetta et al., 2010
GAPDH	AATGAATGGGCAGCCGTTA	TAGCCTCGCTCCACCTGACT	Cacan, 2016

The total volume of component concentrations prepared according to the protocol was completed to 10.5µl in a PCR 96-well microplate. The amounts and concentrations used for each reaction are given in Table 3.6.

Table 3.6. Volumes of each reaction used in qRT-PCR experiments.

Ingredients Utilized	**Amount Utilized for Every Reaction**
Eva Green One step qRT-PCR master mix	5µl
Forward primer	0.75µl
Reverse primer	0.75µl
RNA template	4µl

The components prepared according to the protocol were transferred to a PCR 96-well microplate and placed in the PCR device (Analytik Jena) to perform the PCR steps. PCR steps are given in Table 3.7.

Table 3.7. Steps required for the one-step PCR process

Program Phases	Number of Cycles	Analysis Mode	Temperature (°C)	Duration	Acquisition Mode
Reverse Transcription Step	1	None	45°C	15:00	none
Initial Denaturation	1	None	95°C	03:00	none
Amplification Stage	40	Quantification	Denaturation, 95°C	00:10	none
			Binding, 55°C	00:30	none
			Amplification, 72°C	00:30	single
Cooling Phase	1	None	37°C	00:15	none

Following the completion of the experiment, the procedure was followed in accordance with the Ct values discovered. Nevertheless, the housekeeping gene, GAPDH, was identified as

the Ct calibrator when examining the Ct values of related genes. Relative gene expression was performed using the Livak (2-ΔΔct) technique.

3.2.8. Enzyme-Linked Immunosorbent Assay (ELISA)

Before the experiment, a Human Liver Kinase B1 ELISA kit was ordered. The components' concentrations and the technique corresponding with this kit were processed. Furthermore, the protein concentrations from cells, serum and tissue were measured by Bovine Serum Albumin (BSA) and Bradford assay, as mentioned above. The amounts and concentrations of reagents used for the reaction are given in Table 3.8.

Table 3.8. Volume of each reagent provided in the kit.

Components	Quantity (96 tests)
Standard Solution (16ng/ml)	0.5ml x1
Standard Diluent	3ml x1
Streptavidin-HRP	6ml x1
Stop Solution	6ml x1
Substrate Solution A	6ml x1
Substrate Solution B	6ml x1
Wash Buffer Concentrate (25x)	20ml x1
Biotinylated Human LKB1 Antibody	1ml x1

To start the assay, standards were prepared according to the instructions in the kit. Table 3.9 summarises the standards preparation by standard solution and standard diluent, and standard diluent was used as zero standard.

Table 3.9. Standards preparation.

8ng/ml	Standard No.5	120µl Original Standard + 120µl Standard Diluent
4ng/ml	Standard No.4	120µl Standard No.5 + 120µl Standard Diluent
2ng/ml	Standard No.3	120µl Standard No.4 + 120µl Standard Diluent

1ng/ml	Standard No.2	120µl Standard No.3 + 120µl Standard Diluent
0.5ng/ml	Standard No.1	120µl Standard No.2 + 120µl Standard Diluent

All steps of the assay procedure were done according to the instructions; at the end of the procedure, the 96-well microplate had to be read in 10 minutes. At the end of 10 minutes, measurements were made at 450 nm on the spectrophotometer. The values obtained in the measurement were analysed in Excel, and a standard curve was drawn by using standards absorbance and the curve equation was found to find the concentrations of LKB1 protein in each sample after subtracting the blank absorbance value from the standards and protein absorbance values.

3.2.9. Data Analysis and Visualization

This study compared and examined MTT tests between the experimental and control groups. Since the controls had 100% viability, the alterations in the experimental groups were thus noted. Analysis was carried out in qRT-PCR assays using the Livak (2-ΔΔct) method. In the Livak technique, on the other hand, the target genes' observed expression levels were assessed, and the control groups were set to 1. The results between the target genes and the control group were statistically compared using the Student's T-test method. When a situation was statistically significant, an asterisk symbol visualised P values of 0.05 and lower. ($P \leq 0.0001$ in ****, $P \leq 0.001$ in ***, $P \leq 0.01$ in **, and $P \leq 0.05$ in *). The ELISA study used an Excel formula for standard absorbance to determine the protein concentration. The GraphPad software was the one of choice for visuals of the results of qRT-PCR and ELISA assays. 0-24-48-96-120 are the microscope pictures following drug applications. A Leica DFC295 S 40/0.45 was used to capture time intervals. Software called Leica Application Suite v+ was used to prepare the photos.

4. RESULTS

4.1. Cell Viability Assays

4.1.1. Determination of the cytotoxic effects of 17β-Estradiol, Vorinostat and Decitabine on the chemosensitive ovarian cancer cell line.

Cell culture investigations examined the survival responses of chemosensitive ovarian cancer cell line A2780 against drugs (17β-Estradiol, Vorinostat and Decitabine) at varying doses. In order to do this, A2780 was treated with (8 nM, 32 nM and 128 nM) of 17β-Estradiol, (0.1 μM, 1 μM, 5 μM and 10 μM) of Vorinostat and (10 μM, 20 μM and 40 μM) 0f Decitabine for 24 hours.

Using MTT tests, the percentage of viable cells following (17β-Estradiol, Vorinostat and Decitabine) treatment was ascertained. At 8μM, 17β-Estradiol exhibited significant cytotoxicity in chemo-resistant A2780. Vorinostat and Decitabine's effect on viability was significant in all concentrations, statistically shown in (Figure 4.1) A2780 was not very sensitive to any of the drugs.

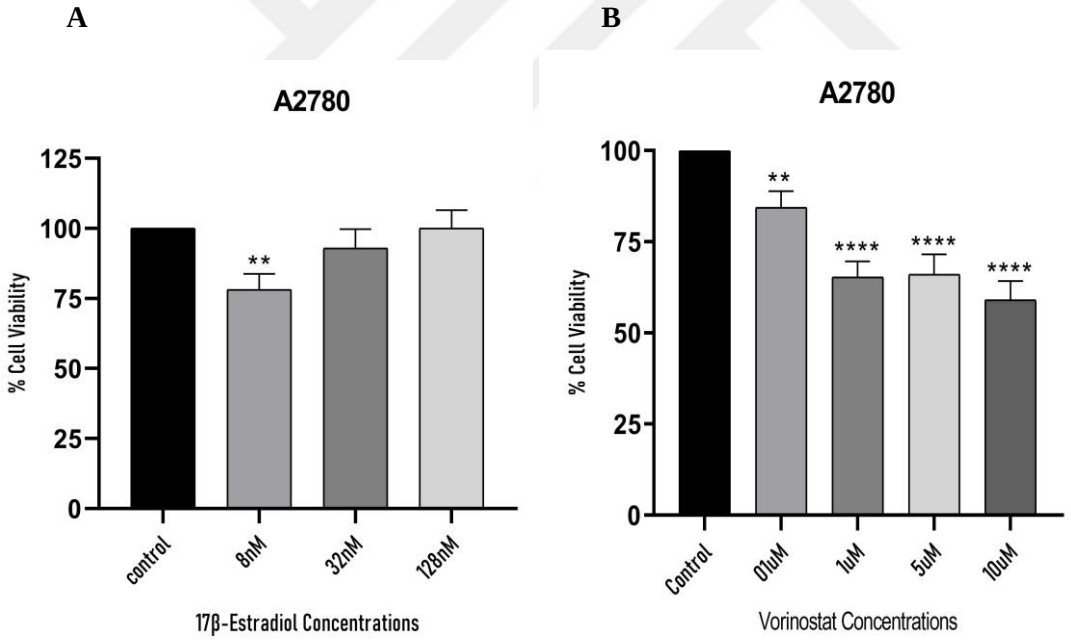

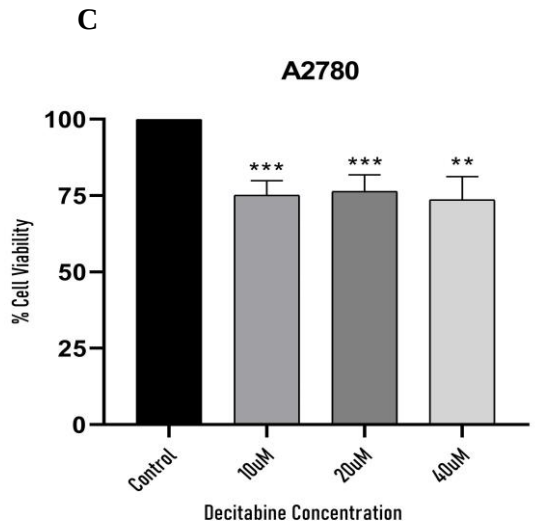

Figure 4.1. Effect of drugs on the proliferation of ovarian cancer cell line A2780. Variations in the percentage proliferation data of A2780 following applications of A) 17β-Estradiol (8 nM, 32 nM and 128 nM). B) Vorinostat (0.1 μM, 1 μM, 5 μM and 10 μM). C) Decitabine (10 μM, 20 μM and 40 μM). Mean % proliferation is shown by bars, and +SEM is indicated by error bars. Statistical comparisons were performed with the control group as a point of reference (****: $P \leq 0.0001$; ***: $P \leq 0.001$; **: $P \leq 0.01$; *: $P \leq 0.05$).

4.1.2. Determination of the cytotoxic effects of 17β-Estradiol, Vorinostat and Decitabine on the chemoresistant ovarian cancer cell line.

The survival responses of chemoresistant ovarian cancer cell line A2780AD against different doses of drugs (17β-Estradiol, Vorinostat, and Decitabine) were investigated by cell culture experiments. To do this, 8 nM, 32 nM, and 128 nM of 17β-Estradiol, 0.1 μM, 1 μM, 5 μM, and 10 μM of Vorinostat, and 10 μM, 20 μM, and 40 μM of Decitabine were administered to A2780 for 24 hours.

Using MTT tests, the percentage of viable cells following (17β-Estradiol, Vorinostat and Decitabine) treatment was ascertained. In all concentrations, 17β-Estradiol increases cancer cell line viability significantly. In exposure to Vorinostat and Decitabine, the cell viability declined significantly, as the A2780 cell line A2780AD was not that sensitive to a decline in the cell viability by less than 50%, as statistically shown in (Figure 4.2).

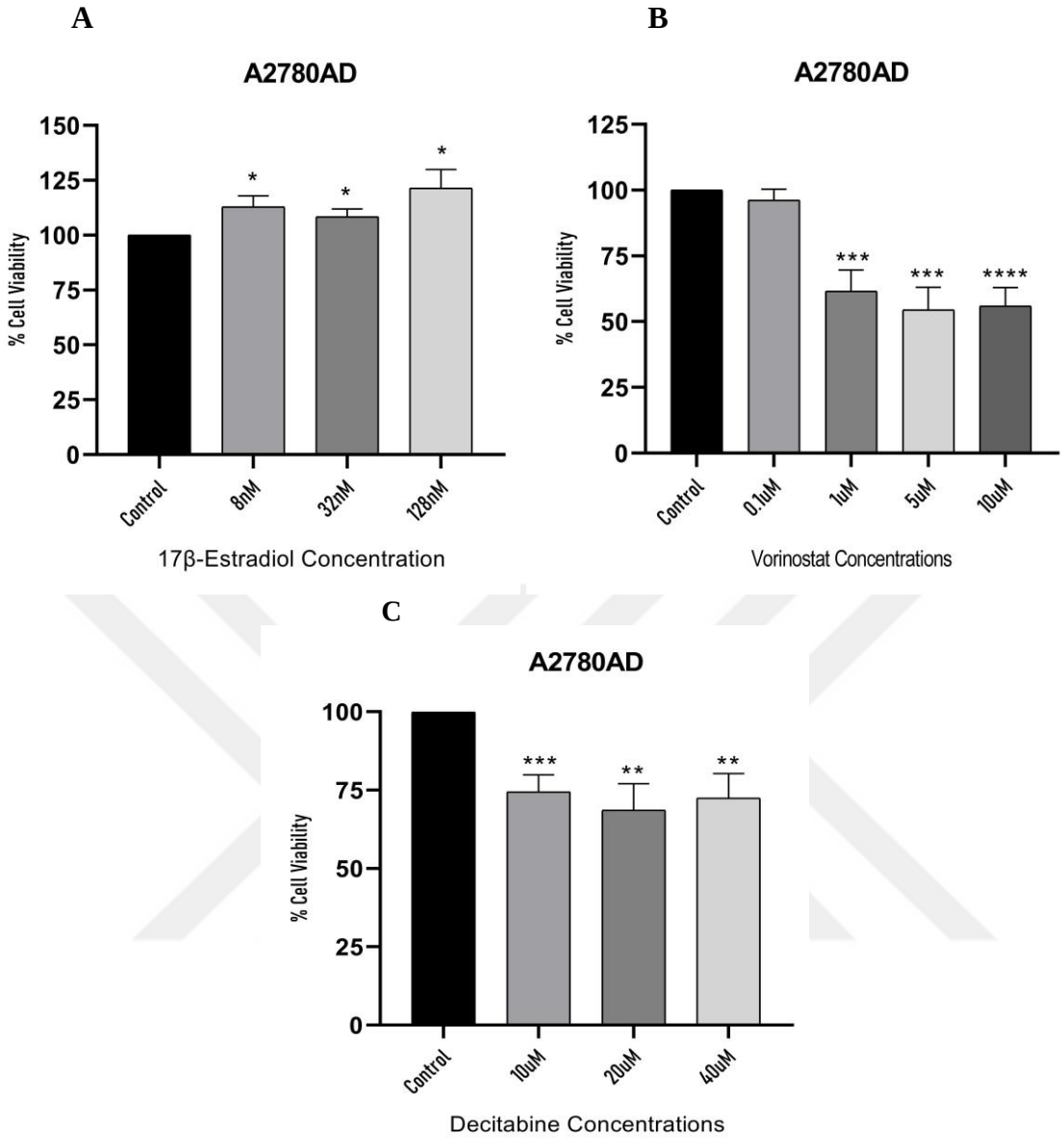

Figure 4.2. Effect of drugs on the ovarian cancer cell line A2780AD proliferation. Variations in the percentage proliferation data of A2780AD following applications of A) 17β-Estradiol (8 nM, 32 nM and 128 nM). B) Vorinostat (0.1 μM, 1 μM, 5 μM and 10 μM). C) Decitabine (10 μM, 20 μM and 40 μM). Mean % proliferation is shown by bars, and +SEM is indicated by error bars. Statistical comparisons were performed with the control group as a point of reference (****: $P \leq 0.0001$; ***: $P \leq 0.001$; **: $P \leq 0.01$; *: $P \leq 0.05$).

4.1.3. Determination of the cytotoxic effects of 17β-Estradiol, Vorinostat and Decitabine on the endometrium cancer cell line.

Cell culture tests examined the survival responses of the endometrium cancer cell line RL95-2 against various drug dosages (17β-Estradiol, Vorinostat, and Decitabine). In order to do this, RL95-2 was given 8 nM, 32 nM, and 128 nM of 17β-Estradiol, 0.1 μM, 1 μM, 5 μM, and 10 μM of Vorinostat, and 10 μM, 20 μM, and 40 μM of Decitabine over a day. The percentage of viable cells after treatment with 17β-Estradiol, Vorinostat, and Decitabine was

determined using MTT assays. 17β-Estradiol considerably boosts the viability of the cancer cell line at all doses. The cells of endometrium cancer cell lines were more sensitive to Vorinostat and 5 µM, and 10 µM of this drug decreased the cell proliferation by less than 50%. The cells were significantly sensitive to Decitabine but not as sensitive as Vorinostat. Presented statistically in (Figure 4.3).

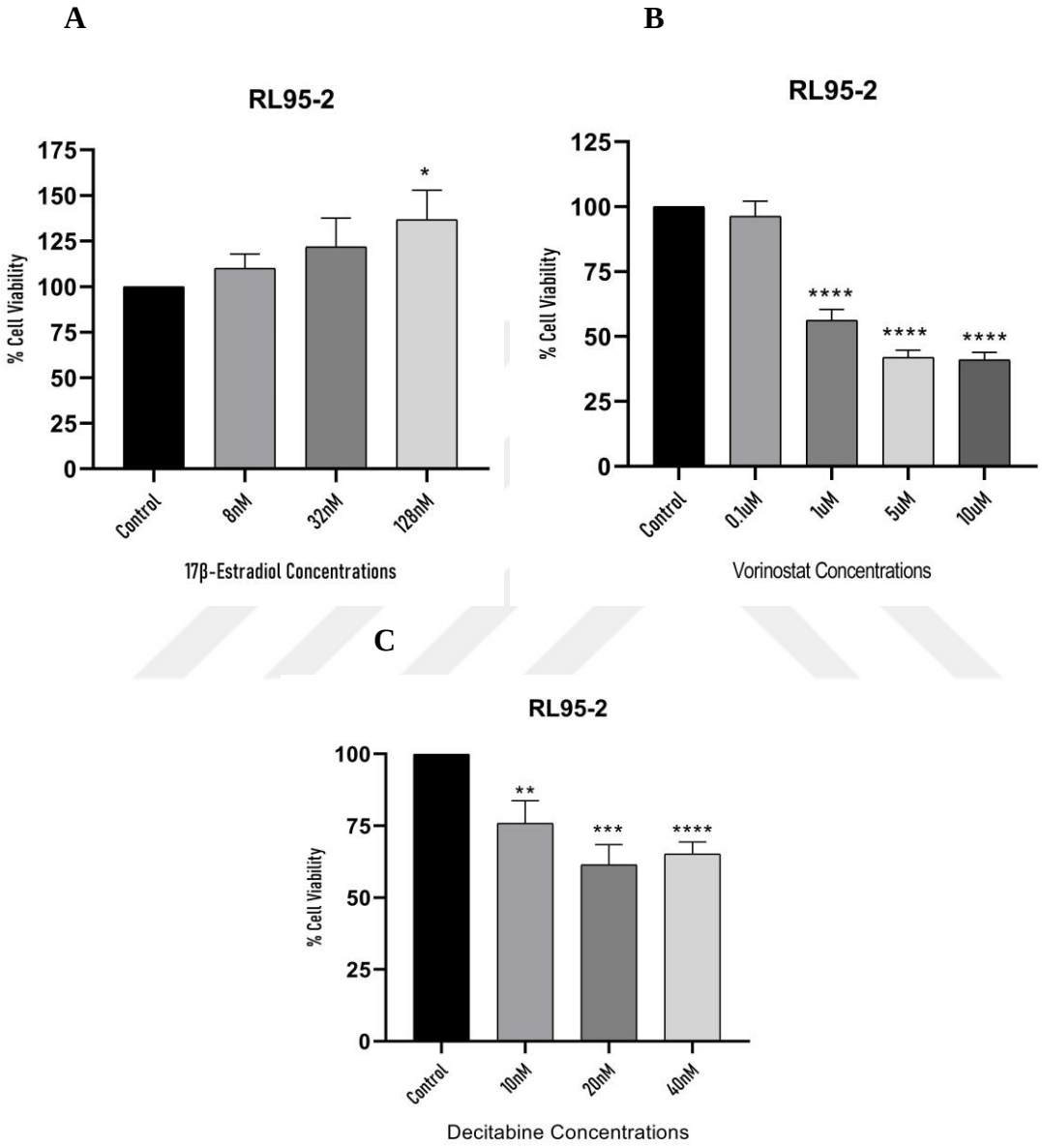

Figure 4.3. Effect of drugs on the endometrium cancer cell line RL95-2 proliferation. Variations in the percentage proliferation data of RL95-2 following applications of A) 17β-Estradiol (8 nM, 32 nM and 128 nM). B) Vorinostat (0.1 µM, 1 µM, 5 µM and 10 µM). C) Decitabine (10 µM, 20 µM and 40 µM). Mean % proliferation is shown by bars, and +SEM is indicated by error bars. Statistical comparisons were performed with the control group as a point of reference (****: $P \leq 0.0001$; ***: $P \leq 0.001$; **: $P \leq 0.01$; *: $P \leq 0.05$).

Totally, the cell line's viability toward drugs was not that sensitive to decrease the cell line's proliferation below 50%, and the IC50 concentration was not determined for any drug.

Furthermore, the highest concentration of each drug was determined to be used in other procedures. Figure 4.4 - 4.6 displays microscope pictures of the highest concentration applications in the experimental groups of these cells.

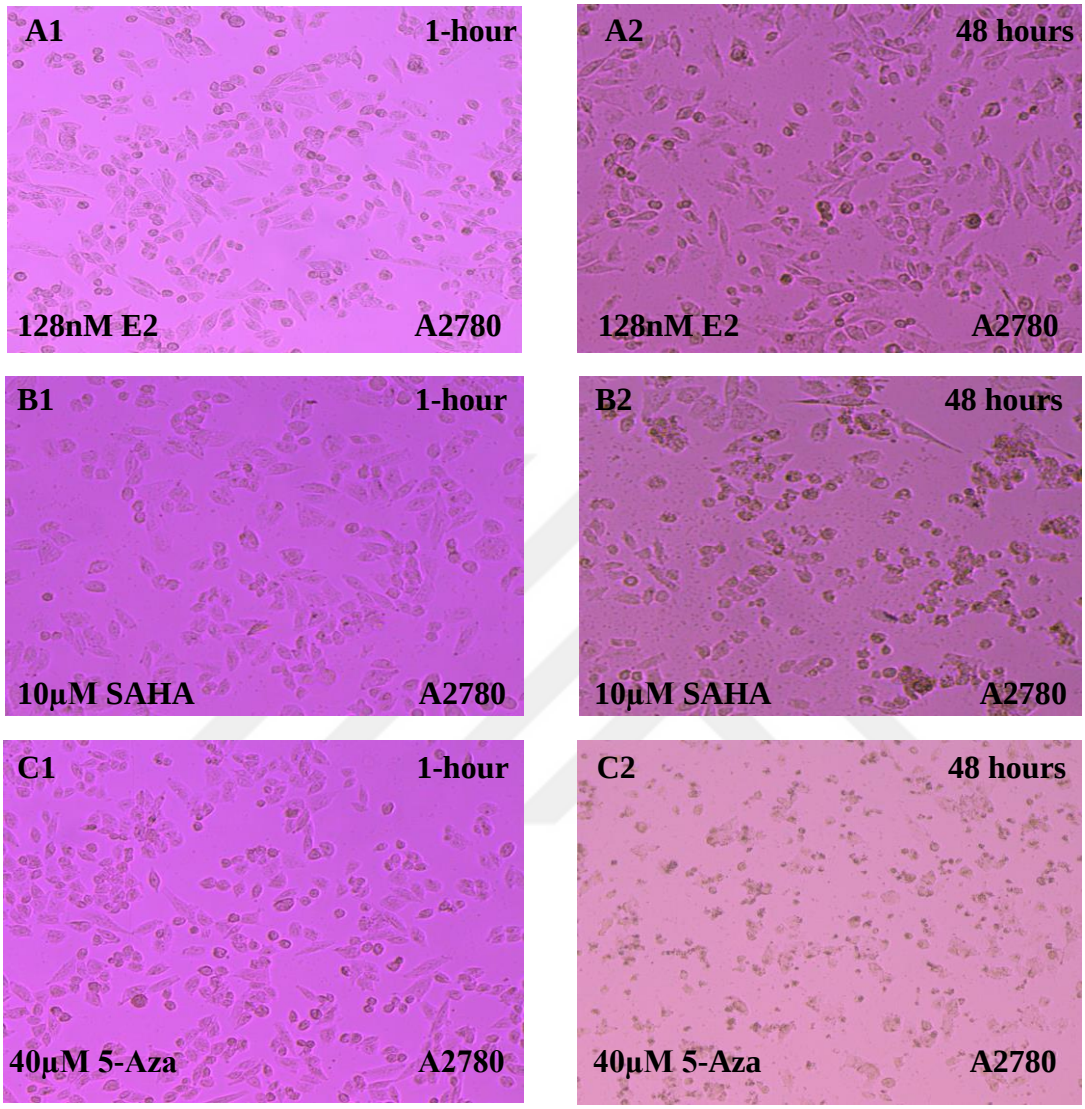

Figure 4.4. Microscope images of ovarian cancer cell line A2780 after drug application. A1- Microscopic image of A2780 cells after 1 hour of E2 application A2- Microscopic image of A2780 cells after 48 hours of E2 application B1- Microscopic image of A2780 cells after 1 hour of SAHA application B2- Microscopic image of A2780 cells after 48 hours of SAHA application C1- Microscopic image of A2780 cells after 1 hour of 5-Aza application C2- Microscopic image of A2780 cells after 48 hours of 5-Aza application (10x objective, 200 µm scale) (E2 = 17β-Estradiol, SAHA = Vorinostat, 5-Aza = Decitabine)

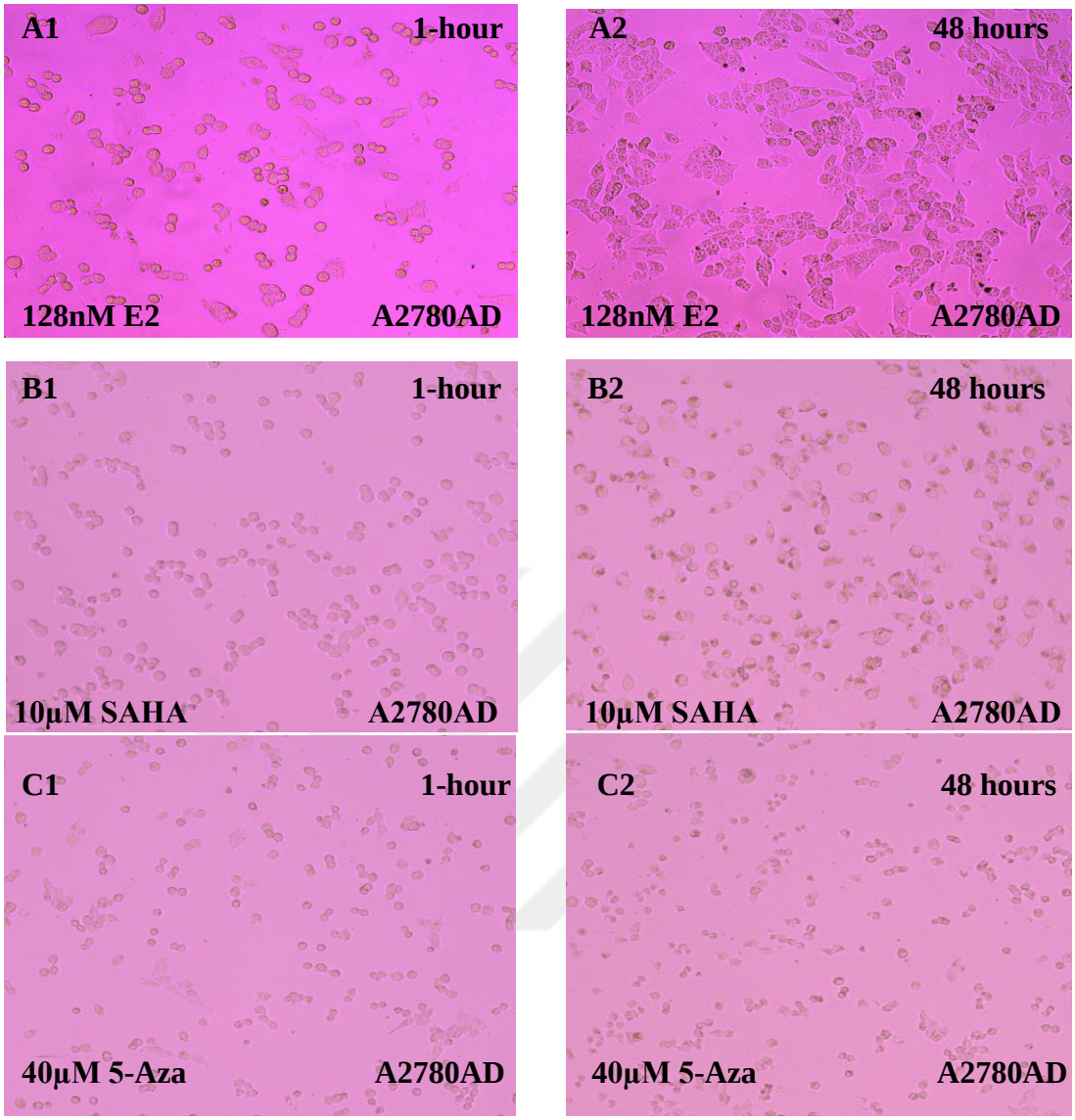

Figure 4.5. Microscope images of ovarian cancer cell line A2780AD after drug application. A1- Microscopic image of A2780AD cells after 1 hour of E2 application A2- Microscopic image of A2780AD cells after 48 hours of E2 application B1- Microscopic image of A2780AD cells after 1 hour of SAHA application B2- Microscopic image of A2780AD cells after 48 hours of SAHA application C1- Microscopic image of A2780AD cells after 1 hour of 5-Aza application C2- Microscopic image of A2780AD cells after 48 hours of 5-Aza application (10x objective, 200 µm scale) (E2 = 17β-Estradiol, SAHA = Vorinostat, 5-Aza = Decitabine)

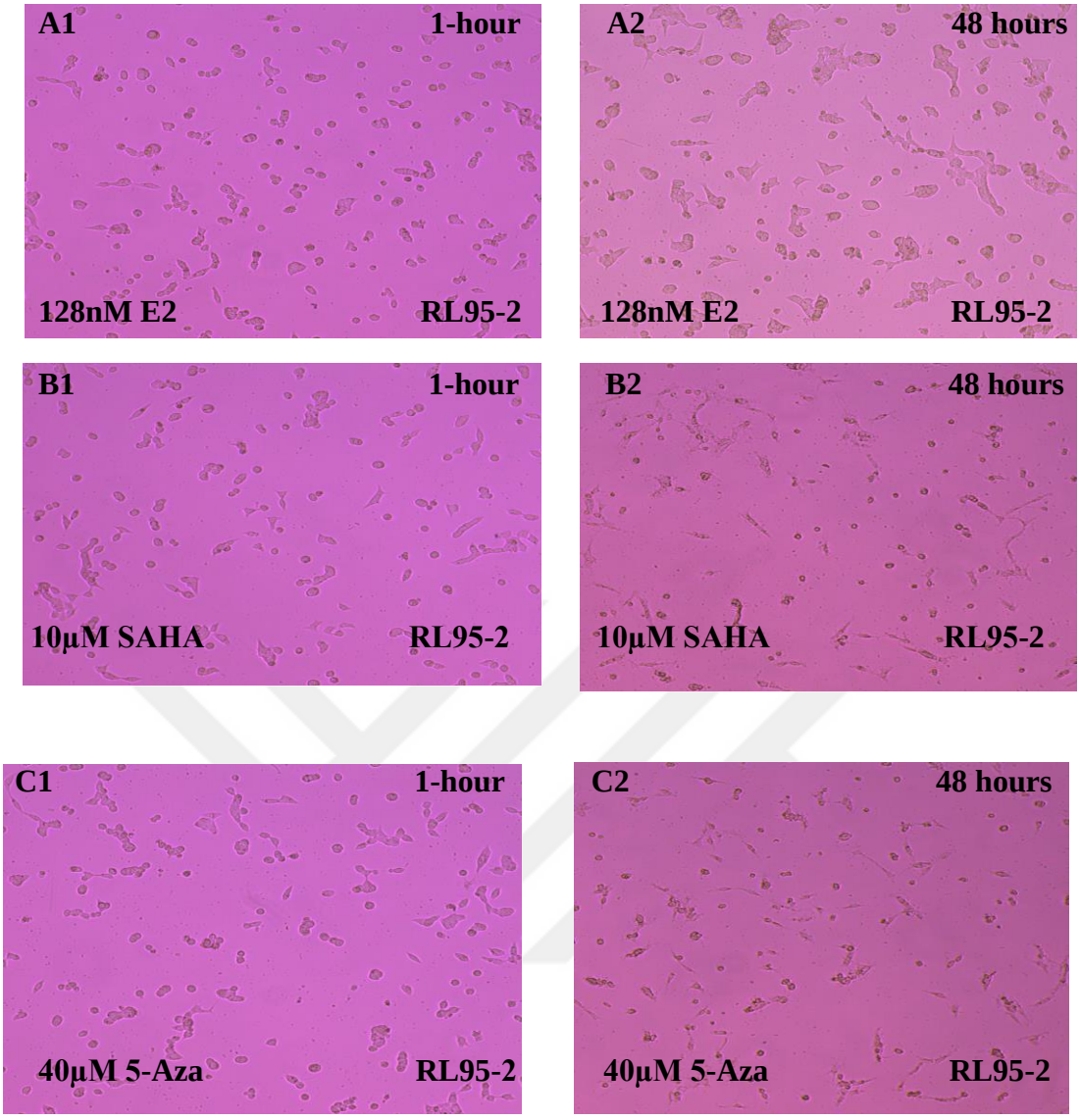

Figure 4.6. Microscope images of endometrium cancer cell line RL95-2 after drug application. A1- Microscopic image of RL95-2 cells after 1 hour of E2 application A2- Microscopic image of RL95-2 cells after 48 hours of E2 application B1- Microscopic image of RL95-2 cells after 1 hour of SAHA application B2- Microscopic image of RL95-2 cells after 48 hours of SAHA application C1- Microscopic image of RL95-2 cells after 1 hour of 5-Aza application C2- Microscopic image of RL95-2 cells after 48 hours of 5-Aza application (10x objective, 200 µm scale) (E2 = 17β-Estradiol, SAHA = Vorinostat, 5-Aza = Decitabine)

4.2. Impact of 17β-Estradiol, Vorinostat and Decitabine treatment on cell lines migration

4.2.1. Impact of 17β-Estradiol, Vorinostat and Decitabine treatment on chemosensitive ovarian cancer cell line migration (A2780)

The concentrations of (128nM of estrogen, 10µM of Vorinostat and 40µM of Decitabine) were chosen after the MTT results. In 12-well plates, cells were sown. Drugs were introduced after the 24-hour incubation period. Using a fluorescence microscope, the effects on the migration of cells were seen at 0 hours, 24 hours, 48 hours, 72 hours, 96 hours and 120 hours.

We evaluated microscopic images from cell migration studies done on the A2780 ovarian cancer cell line at the first hour and at the end of the 24th hour after treatment with specific concentrations of drugs. Cell migration experiments revealed that treatment with 10μM and 40μM concentrations of Vorinostat and Decitabine, respectively, slowed cell growth and proliferation compared to the control group, resulting in reduced cell migration. However, it was vice versa with estrogen treatment (Figure 4.7).

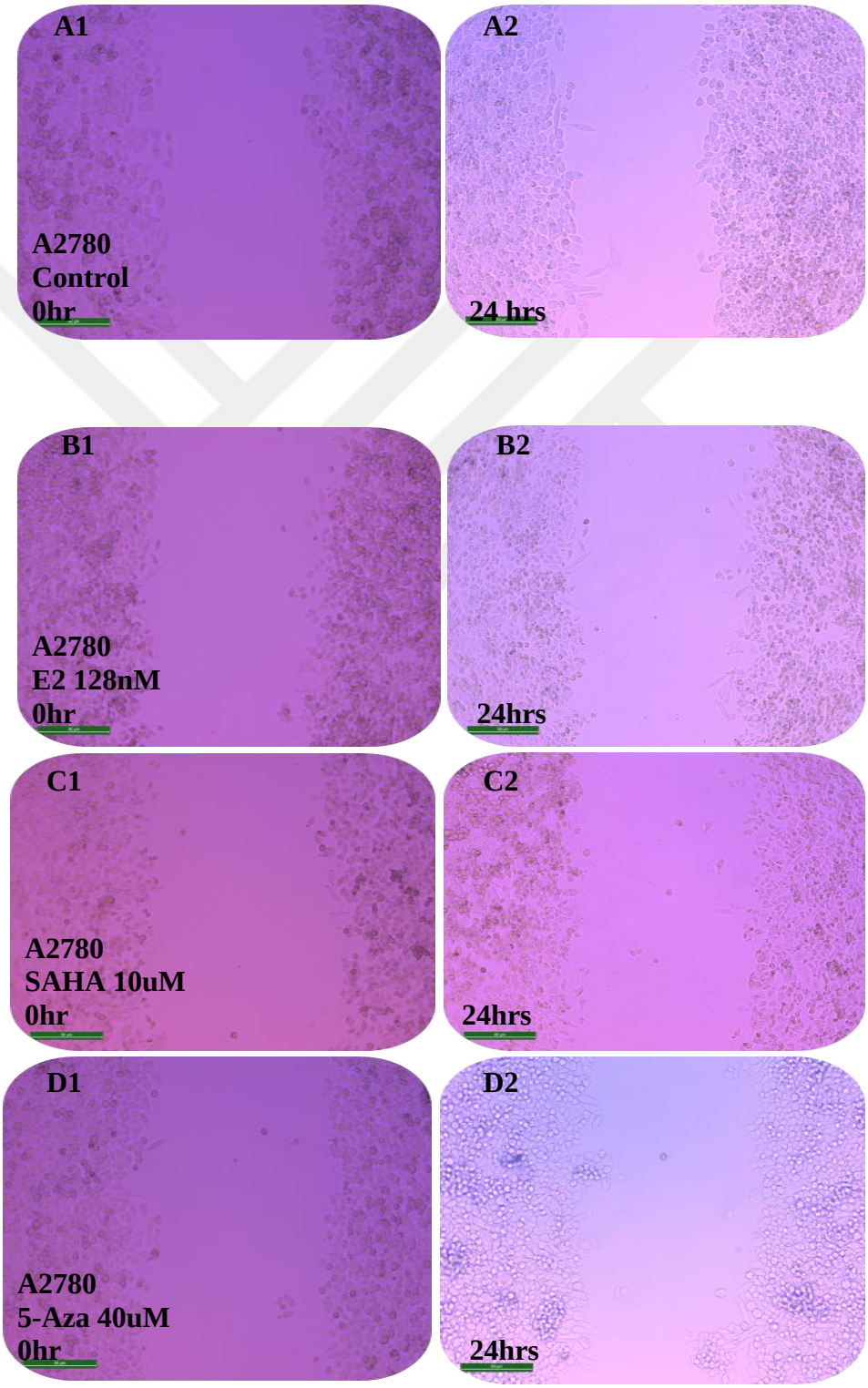

Figure 4.7. Cell microscopic images at the first 0 and 24 hours after treatment with 17β-Estradiol, Vorinostat and Decitabine in the A2780 chemosensitive ovarian cancer cell line. A1- Microscopic image of A2780cell lines in the control group at 0-hour A2- Microscopic image of the control group after 24 hours B1- Microscopic image of A2780 cells after treatment with E2 (128 nM) in the experimental groups at 0-hour B2-Microscopic image of A2780 cells treated with E2 (128 nM) at 24 hours C1- Microscopic image of A2780 cells treated with SAHA (10 μM) for 0 hour C2- Microscopic image of A2780 cells treated with SAHA (10 μM) for 24 hours D1- Microscopic image of A2780 cells treated with 5-Aza (40 μM) for 0 hour D2- Microscopic image of A2780 cells treated with 5-Aza (40 μM) for 24 hours (10x objective 200 μm scale).

We evaluated the microscopic images at the 48th and 72nd hours following treatment with concentrations of drugs in cell migration studies done on the A2780 ovarian cancer cell line. After the 72nd hour, there was apparent cell movement in the control and estrogen-treated groups, and the migration gap would be closed. Cell migration decreased in the groups treated with 10μM concentration of Vorinostat and 40μM concentration of Decitabine compared to the control group, and the cells leading to death increased in the shape of the cells. (See Figure 4.8).

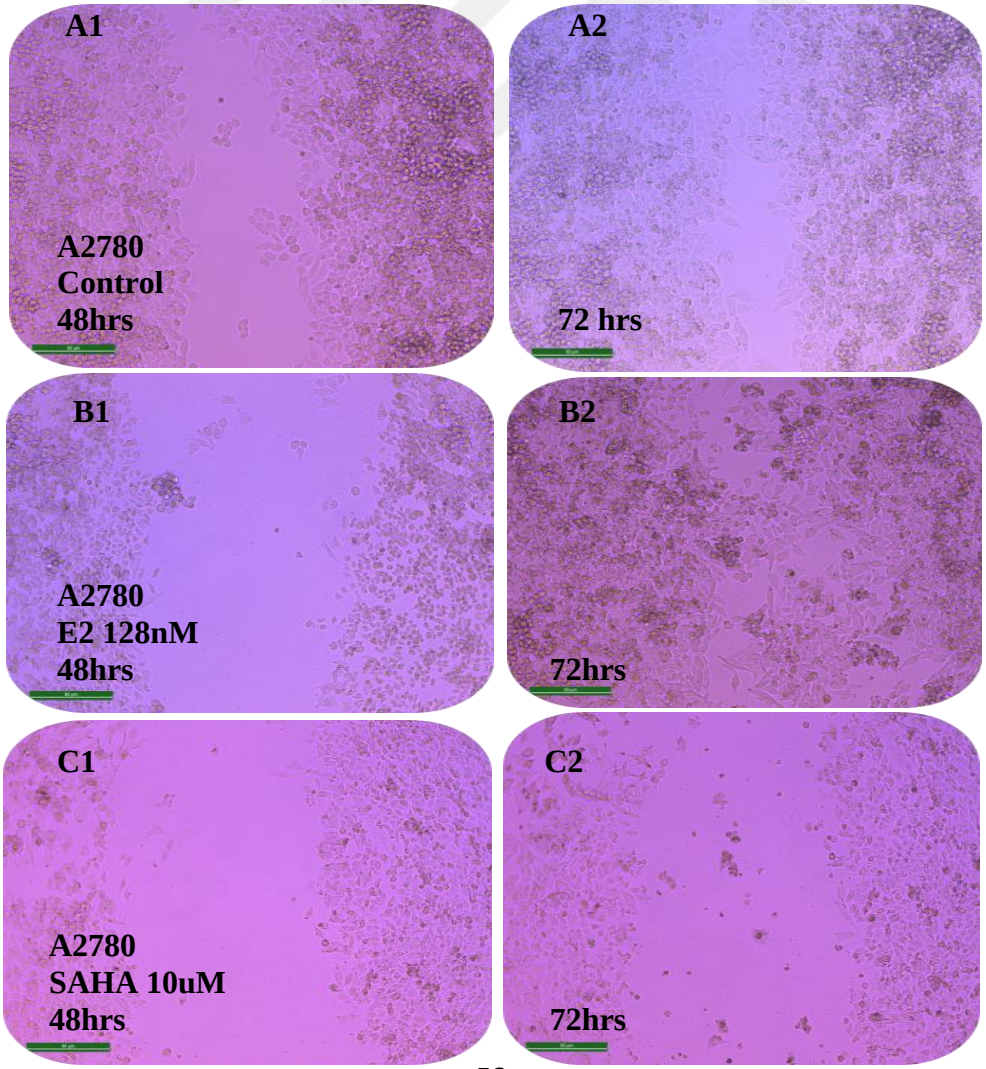

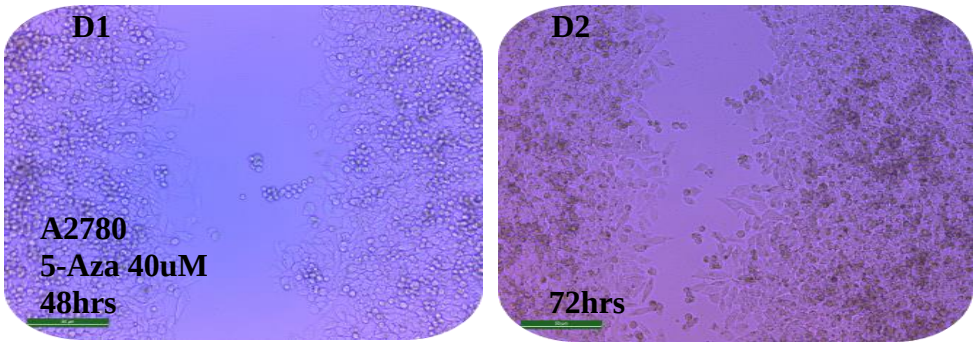

Figure 4.8. Cell microscopic images at 48 and 72 hours after treatment with 17β-Estradiol, Vorinostat and Decitabine in the A2780 chemosensitive ovarian cancer cell line. A1- Microscopic image of A2780 cell lines in the control group at 48 hours A2- Microscopic image of the control group after 72 hours B1- Microscopic image of A2780 cells after treatment with E2 (128 nM) in the experimental groups at 48 hours B2-Microscopic image of A2780 cells treated with E2 (128 nM) at 72 hours C1- Microscopic image of A2780 cells treated with SAHA (10 μM) for 48 hours C2- Microscopic image of A2780 cells treated with SAHA (10 μM) for 72 hours D1- Microscopic image of A2780 cells treated with 5-Aza (40 μM) for 48 hours D2- Microscopic image of A2780 cells treated with 5-Aza (40 μM) for 72 hours (10x objective 200 μm scale).

We analysed the microscopic images taken 96 and 120 hours after treating the A2780 ovarian cancer cell line with specific concentrations of drugs as part of cell migration tests. By the conclusion of the 120th hour, there was a noticeable cell movement in the control group and 128nM estrogen-treated group, and the migration gap was closed. On the other hand, it was noted that in the groups administered 10μM concentration of Vorinostat and 40μM concentration of Decitabine, there was less cell movement than in the control group, and the shape of the cells that ultimately led to death increased. (See Figure 4.9).

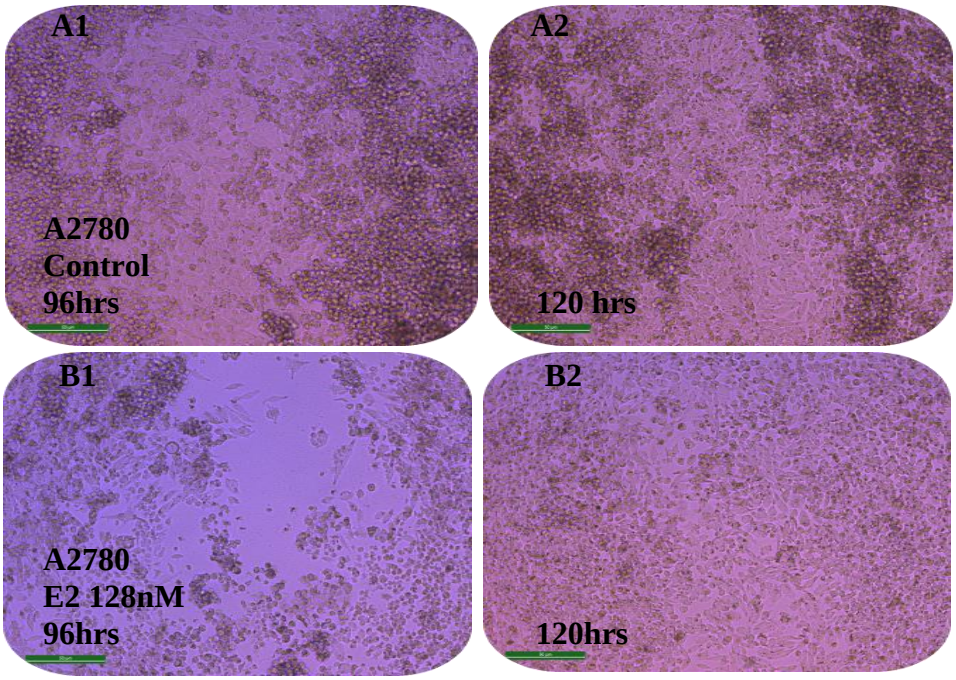

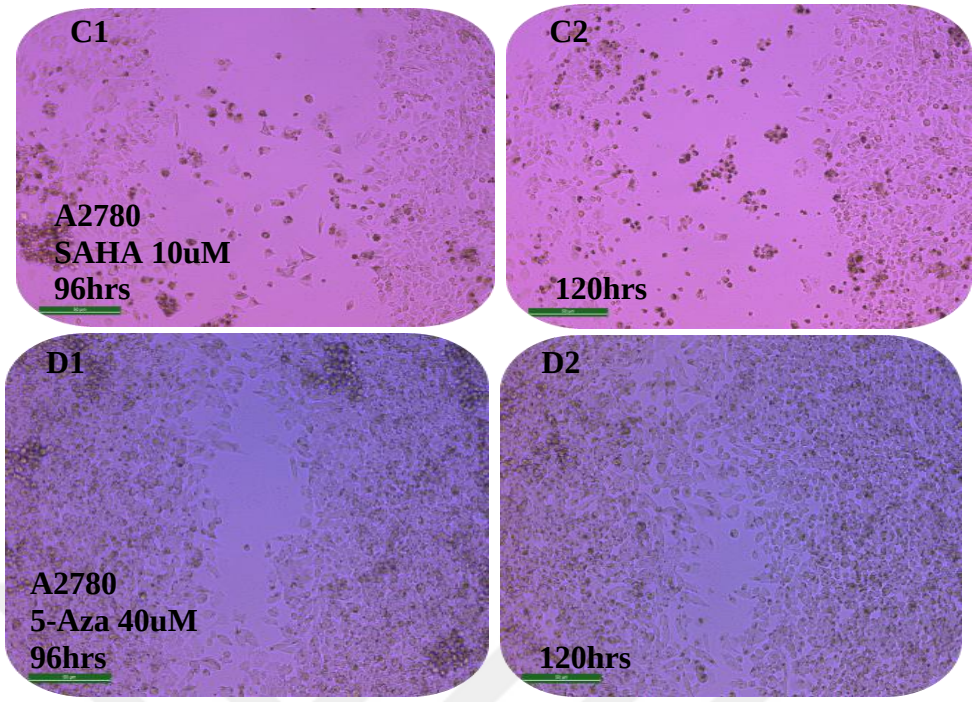

Figure 4.9. Cell microscopic images at 96 hours and 120 hours after treatment with 17β-Estradiol, Vorinostat and Decitabine in the A2780 chemosensitive ovarian cancer cell line. A1- Microscopic image of A2780 cell lines in the control group at 96 hours A2- Microscopic image of the control group after 120 hours B1- Microscopic image of A2780 cells after treatment with E2 (128 nM) in the experimental groups at 96 hours B2-Microscopic image of A2780 cells treated with E2 (128 nM) at 120 hours C1- Microscopic image of A2780 cells treated with SAHA (10 μM) for 96 hours C2- Microscopic image of A2780 cells treated with SAHA (10 μM) for 120 hours D1- Microscopic image of A2780 cells treated with 5-Aza (40 μM) for 96 hours D2- Microscopic image of A2780 cells treated with 5-Aza (40 μM) for 120 hours (10x objective 200 μm scale).

4.2.2. Impact of 17β-Estradiol, Vorinostat and Decitabine treatment on chemoresistant ovarian cancer cell line migration (A2780AD)

We analysed microscopic pictures from cell migration experiments conducted on the ovarian cancer cell line A2780AD at the beginning and conclusion of the 24th hour following treatment with particular drug concentrations. According to cell migration experiments, treatment with 10μM and 40μM concentrations of Decitabine and Vorinostat, respectively, slowed down cell proliferation and growth in comparison to the control group, which in turn led to less cell migration; however, when estrogen was administered, the opposite occurred (Figure 4.10).

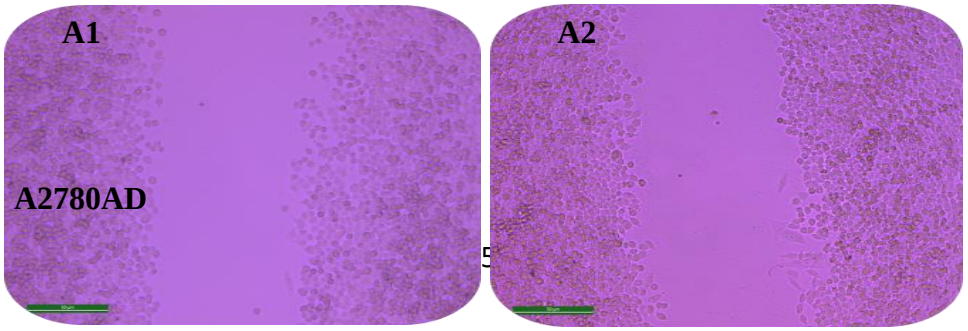

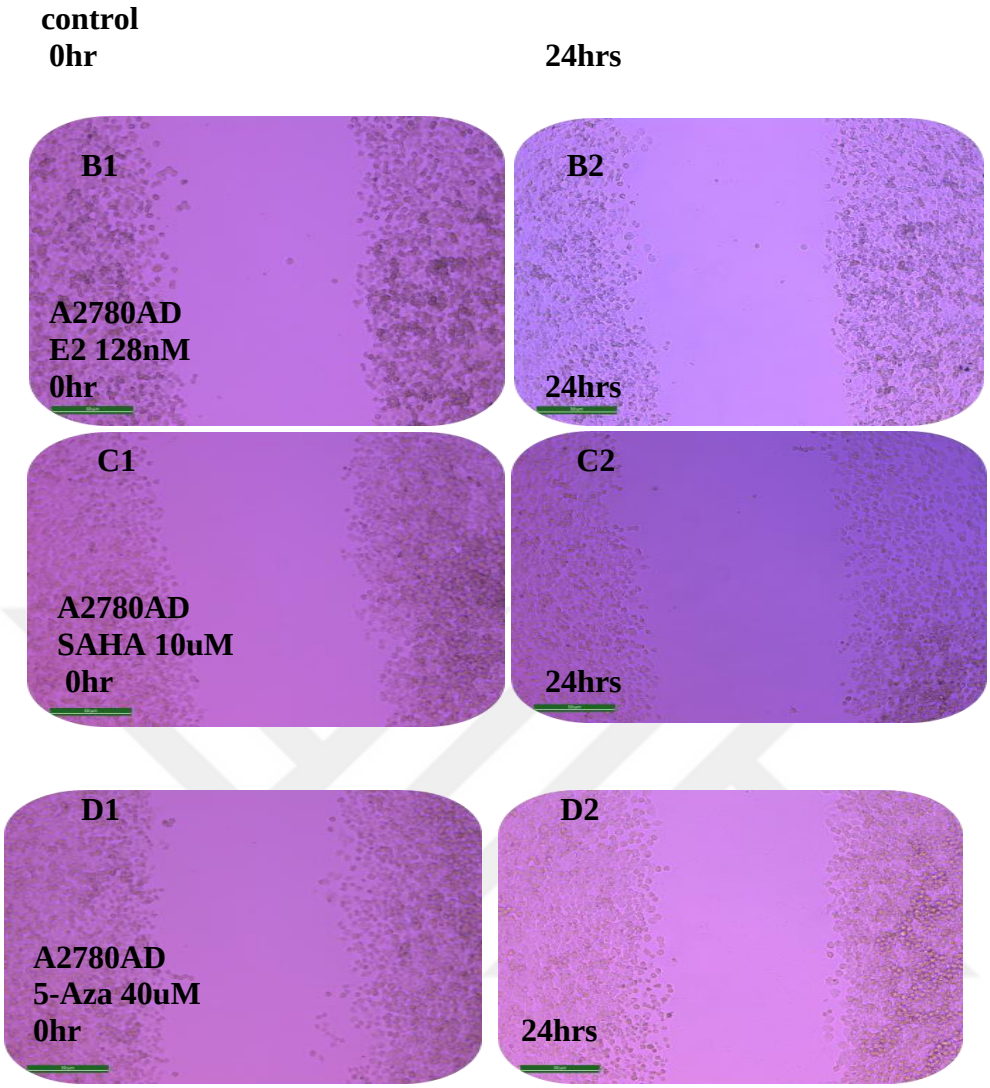

Figure 4.10. Cell microscopic images at the first 0 and 24 hours after treatment with 17β-Estradiol, Vorinostat and Decitabine in the A2780AD chemoresistant ovarian cancer cell line. A1- The control group at 0-hour A2- The control group after 24 hours B1- A2780AD cells after treatment with E2 (128 nM) in the experimental groups at 0-hour B2- A2780AD cells treated with E2 (128 nM) at 24 hours C1- A2780AD cells treated with SAHA (10 μM) for 0-hour C2- A2780AD cells treated with SAHA (10 μM) for 24 hours D1- A2780AD cells treated with 5-Aza (40 μM) for 0-hour D2- A2780AD cells treated with 5-Aza (40 μM) for 24 hours (10x objective 200 μm scale).

In cell migration tests on the A2780AD ovarian cancer cell line, we assessed microscopic pictures 48 and 72 hours after treatment with different drug concentrations. At the end of the 72nd hour, there was visible cell movement in both the control and estrogen-treated groups, and the migration gap was closing. Cell migration was reduced in the groups treated with 10M Vorinostat and 40M Decitabine compared to the control group, and the number of cells that died rose in the form of the cells. (See Fig. 4.11).

A2

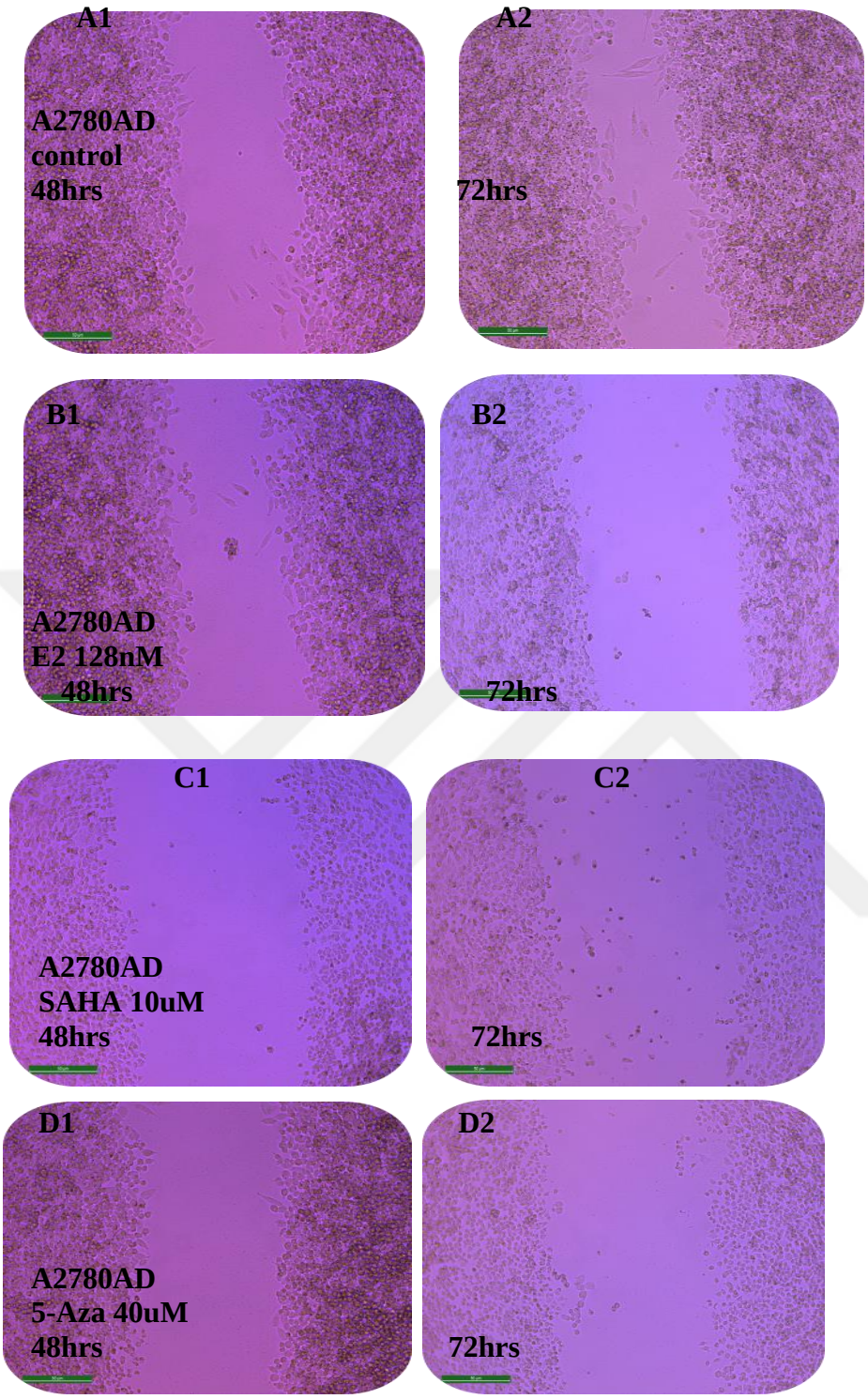

Figure 4.11. Cell microscopic images at 48 hours and 72 hours after treatment with 17β-Estradiol, Vorinostat and Decitabine in the A2780AD chemoresistant ovarian cancer cell line. A1- The control group at 48 hours A2- The control group after 72 hours B1- A2780AD cells after treatment with E2 (128 nM) in the experimental groups at 48 hours B2- A2780AD cells treated with E2 (128 nM) at 72 hours C1- A2780AD cells treated with SAHA (10 μM) for 48 hours C2- A2780AD cells treated with SAHA (10 μM) for 72 hours D1- A2780AD cells treated with 5-Aza (40 μM) for 48 hours D2- A2780AD cells treated with 5-Aza (40 μM) for 72 hours (10x objective 200 μm scale).

We examined microscopic images obtained 96 and 120 hours after the A2780AD ovarian cancer cell line was treated with specific drug concentrations as part of cell migration assays. By the 120th hour, there was considerable cell movement in both the control and 128nM estrogen-treated groups, and the migration gap had narrowed. On the other hand, it was discovered that in the groups given 10M Vorinostat and 40M Decitabine, there was less cell mobility than in the control group, and the form of the cells that eventually led to death increased. (See Fig. 4.12).

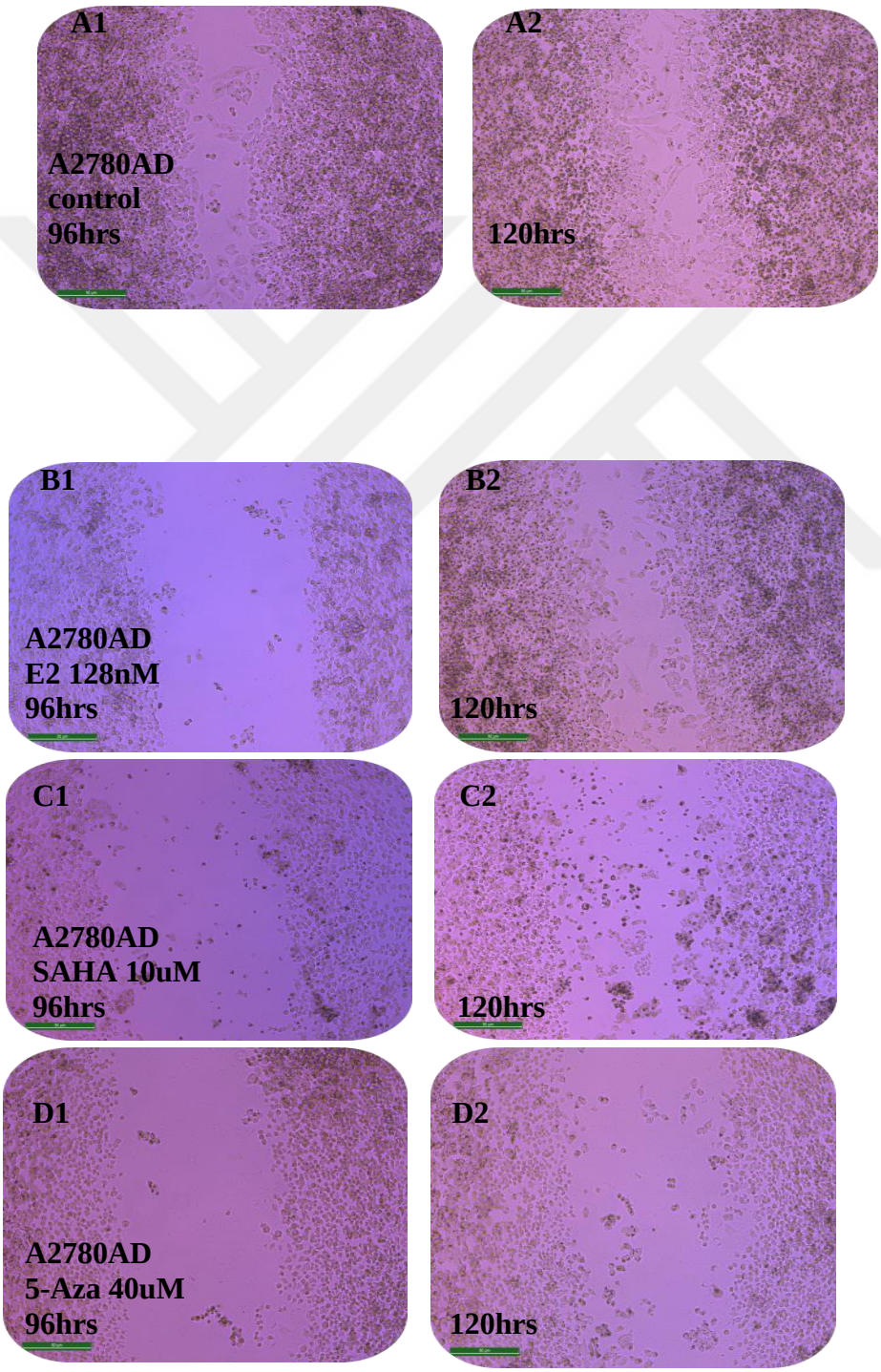

Figure 4.12. Cell microscopic images at 96 hours and 120 hours after treatment with 17β-Estradiol, Vorinostat and Decitabine in the A2780AD chemoresistant ovarian cancer cell line.

A1- The control group at 96 hours A2- The control group after 120 hours B1- A2780AD cells after treatment with E2 (128 nM) in the experimental groups at 96 hours B2- A2780AD cells treated with E2 (128 nM) at 120 hours C1- A2780AD cells treated with SAHA (10 μM) for 96 hours C2- A2780AD cells treated with SAHA (10 μM) for 120 hours D1- A2780AD cells treated with 5-Aza (40 μM) for 96 hours D2- A2780AD cells treated with 5-Aza (40 μM) for 120 hours (10x objective 200 μm scale).

4.2.3. Impact of 17β-Estradiol, Vorinostat and Decitabine treatment on endometrium cancer cell line migration (RL95-2)

We evaluated microscopic images from cell migration studies done on the RL95-2 endometrium cancer cell line at the first hour and at the end of the 24th hour after treatment with specific concentrations of drugs. Cell migration experiments revealed that treatment with 10μM and 40μM concentrations of Vorinostat and Decitabine, respectively, slowed cell growth and proliferation compared to the control group, resulting in reduced cell migration. However, it was vice versa with estrogen treatment (Figure 4.13).

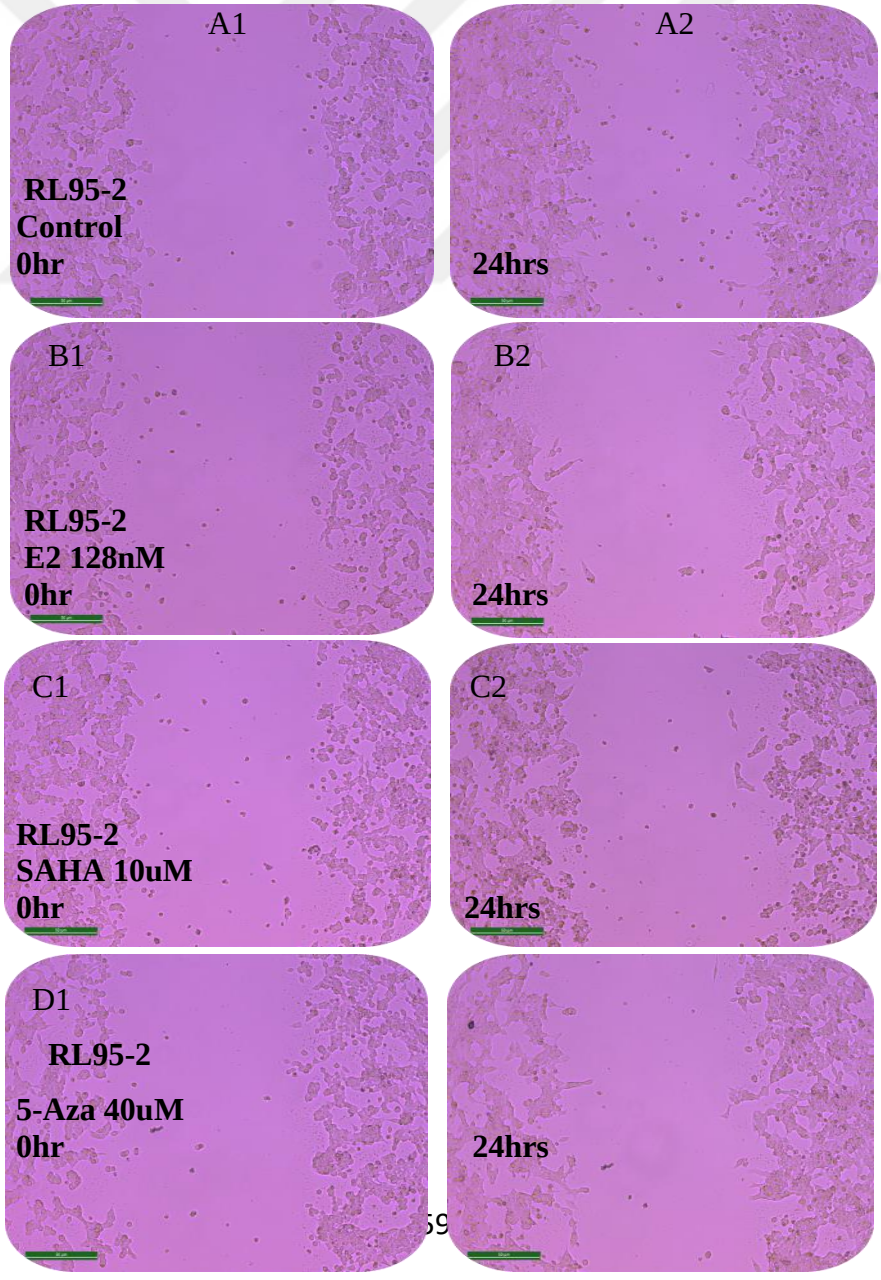

Figure 4.13. Cell microscopic images at the first 0 and 24 hours after treatment with 17β-Estradiol, Vorinostat and Decitabine in the RL95-2 endometrium cancer cell line. A1- The control group at 0-hour A2- The control group after 24 hours B1- RL95-2 cells after treatment with E2 (128 nM) in the experimental groups at 0-hour B2- RL95-2 cells treated with E2 (128 nM) at 24 hours C1- RL95-2 cells treated with SAHA (10 μM) for 0-hour C2- RL95-2 cells treated with SAHA (10 μM) for 24 hours D1- RL95-2 cells treated with 5-Aza (40 μM) for 0-hour D2- RL95-2 cells treated with 5-Aza (40 μM) for 24 hours (10x objective 200 μm scale).

In cell migration tests on the RL95-2 endometrium cancer cell line, we assessed microscopic pictures 48 and 72 hours after treatment with different drug concentrations. At the end of the 72nd hour, there was visible cell movement in both the control and estrogen-treated groups, and the migration gap was closing. Cell migration was reduced in the groups treated with 10μM Vorinostat and 40μM Decitabine compared to the control group, and the number of cells that died rose in the form of the cells. (See Fig. 4.14).

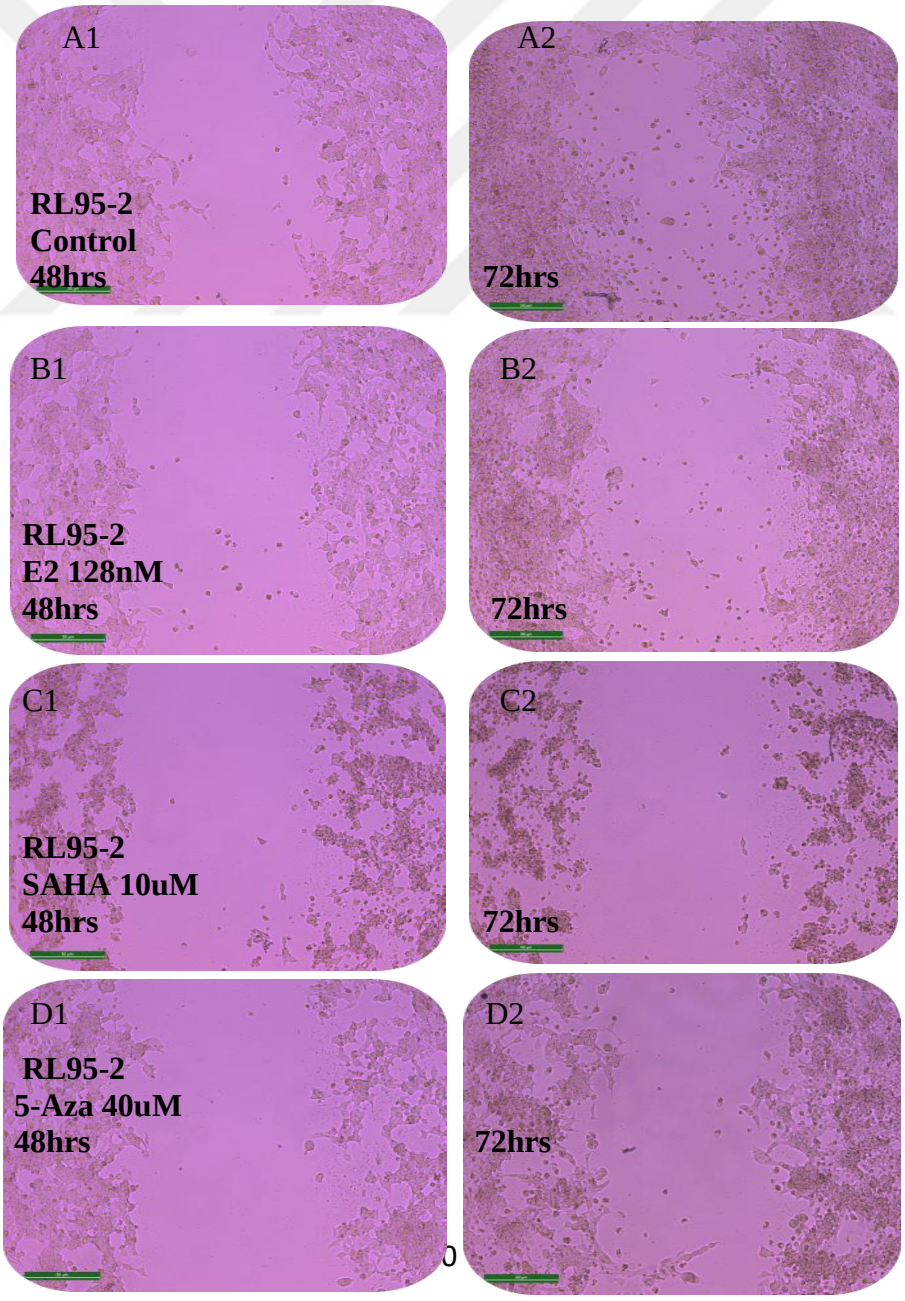

Figure 4.14. Cell microscopic images at 48 hours and 72 hours after treatment with 17β-Estradiol, Vorinostat and Decitabine in the RL95-2 endometrium cancer cell line. A1- The control group at 48 hours A2- The control group after 72 hours B1- RL95-2 cells after treatment with E2 (128 nM) in the experimental groups at 48 hours B2- RL95-2 cells treated with E2 (128 nM) at 72 hours C1- RL95-2 cells treated with SAHA (10 μM) for 48 hours C2- RL95-2 cells treated with SAHA (10 μM) for 72 hours D1- RL95-2 cells treated with 5-Aza (40 μM) for 48 hours D2- RL95-2 cells treated with 5-Aza (40 μM) for 72 hours (10x objective 200 μm scale).

We analysed the microscopic images taken 96 and 120 hours after treating the RL95-2 endometrium cancer cell line with specific concentrations of drugs as part of cell migration tests. By the conclusion of the 120th hour, there was a noticeable cell movement in the control group and 128nM estrogen-treated group, but the migration gap was not closed. On the other hand, it was noted that in the groups administered 10μM concentration of Vorinostat and 40μM concentration of Decitabine, there was significantly less cell movement in Decitabine-treated cells, and there was no cell movement in Vorinostat-treated cells in comparison to the control group, and the shape of the cells that ultimately led to death increased. (See Figure 4.15).

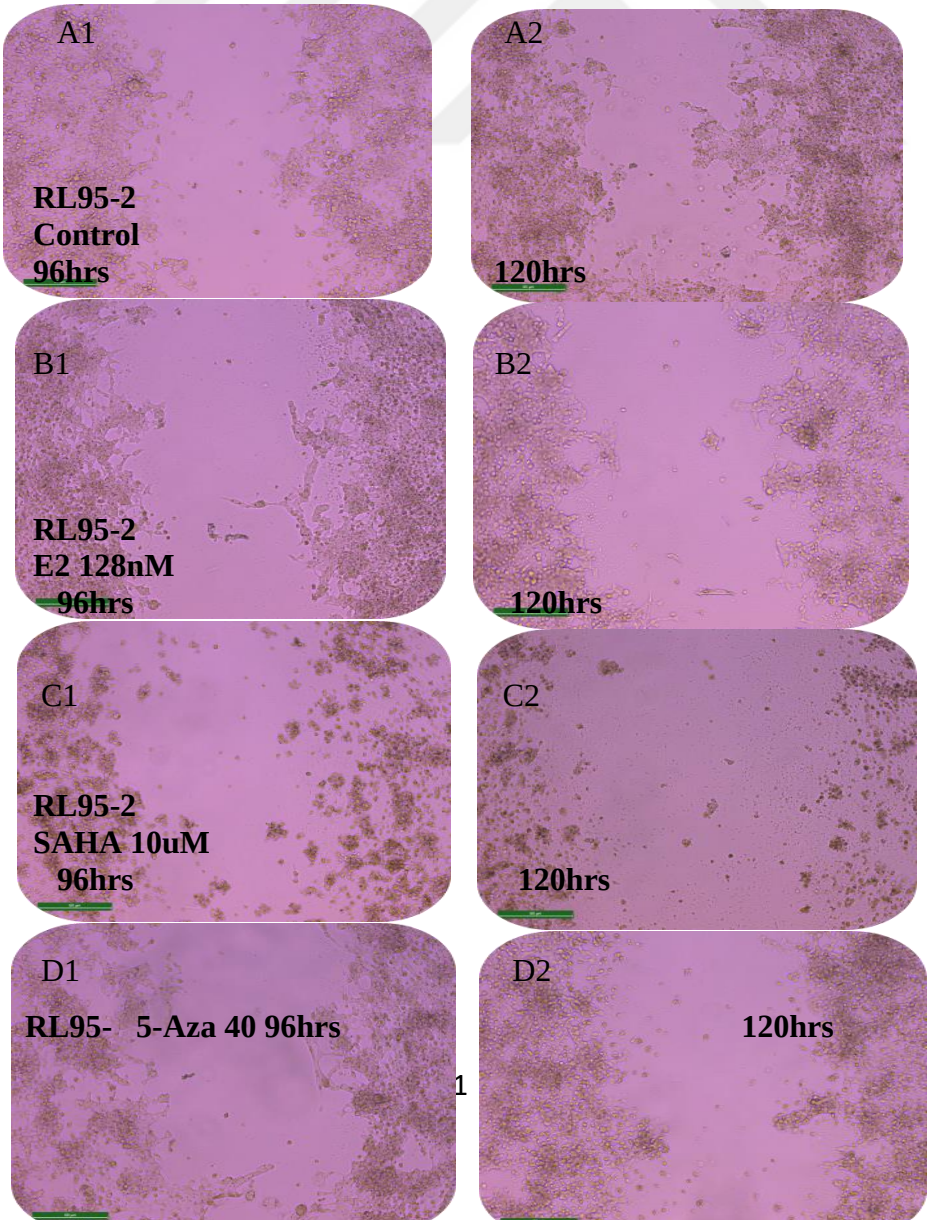

Figure 4.15. Cell microscopic images at 96 hours and 120 hours after treatment with 17β-Estradiol, Vorinostat and Decitabine in the RL95-2 endometrium cancer cell line. A1- The control group at 96 hours A2- The control group after 120 hours B1- RL95-2 cells after treatment with E2 (128 nM) in the experimental groups at 96 hours B2- RL95-2 cells treated with E2 (128 nM) at 120 hours C1- RL95-2 cells treated with SAHA (10 μM) for 96 hours C2- RL95-2 cells treated with SAHA (10 μM) for 120 hours D1- RL95-2 cells treated with 5-Aza (40 μM) for 96 hours D2- RL95-2 cells treated with 5-Aza (40 μM) for 120 hours (10x objective 200 μm scale).

4.3. Investigations on the Effects of Drugs on Some Cancer Suppresser Gene Expression

The effects of 17β-Estradiol, Vorinostat and Decitabine on regulating LKB1, STING and IFI16 genes involved in inhibiting tumour growth were then investigated. To investigate the potential effects of 17β-Estradiol, Vorinostat and Decitabine on the identified genes, the concentrations of (128nM of estrogen, 10μM of Vorinostat and 40μM of Decitabine) that affect cell viability above 50% in ovarian cancer cell lines (A2780 and A2780AD) and endometrium cancer cell line (RL95-2) were chosen, and RNA isolation experiments were carried out. qRT-PCR analyses were carried out immediately following the RNA isolation step.

4.3.1 Potential effects of 17β-Estradiol, Vorinostat and Decitabine on the modulation of LKB1 gene expression levels in A2780, A2780AD and RL95-2 cells.

A2780, A2780AD ovarian cancer cell lines and RL95-2 endometrium cancer cell line were treated with 17β-Estradiol, Vorinostat and Decitabine. RNA was separated from the treated cells, and qRT-PCR analysis was used to extract cDNA from the separated RNA. Based on the collected data, it was found that when 17β-Estradiol and Vorinostat were applied to the cell lines, the LKB1 gene expression level decreased in A2780 than the control group. At the same time, Decitabine declined the gene expression in A2780 and RL95-2 cell lines, as shown in (figure 4.16).

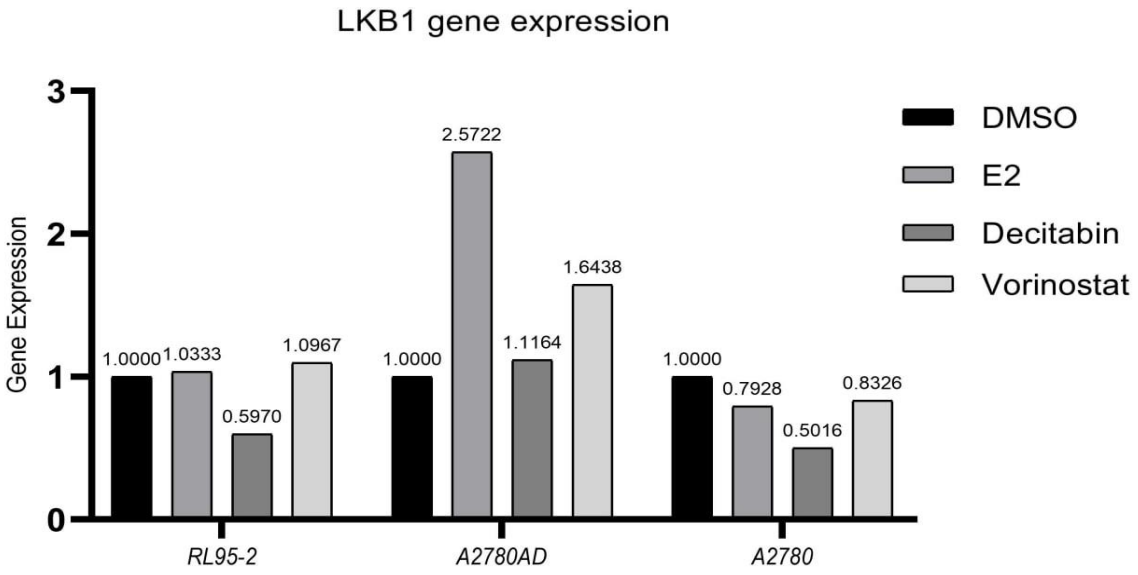

Figure 4.16. LKB1 gene expression in A2780, A2780AD ovarian cancer cell lines and RL95-2 endometrium cancer cell line after treatment with 17β-Estradiol, Vorinostat and Decitabine. The experimental groups were supplemented with 5 µl/mL of drugs. Error bars show +SEM, and comparisons were performed using the Livak (2^-ddCT) method. Normalisation to the GAPDH control gene was used to compute the results, and the control value was maintained at 1. Three iterations of the trials were conducted.

4.3.2 Potential effects of 17β-Estradiol, Vorinostat and Decitabine on the modulation of STING gene expression levels in A2780, A2780AD and RL95-2 cells.

Decitabine, Vorinostat, and 17β-Estradiol were used to treat the ovarian cancer cell lines A2780 and A2780AD and the endometrial cancer cell line RL95-2. After the treated cells' RNA was separated, cDNA was extracted from the separated RNA using qRT-PCR analysis. Based on the data gathered, it was discovered that when 17β-Estradiol and Decitabine were administered to the cell lines, RL95-2 showed a higher level of STING gene expression than the control group. Gene expression decreased in A2780AD after applying all drugs, as seen in (figure 4.17).

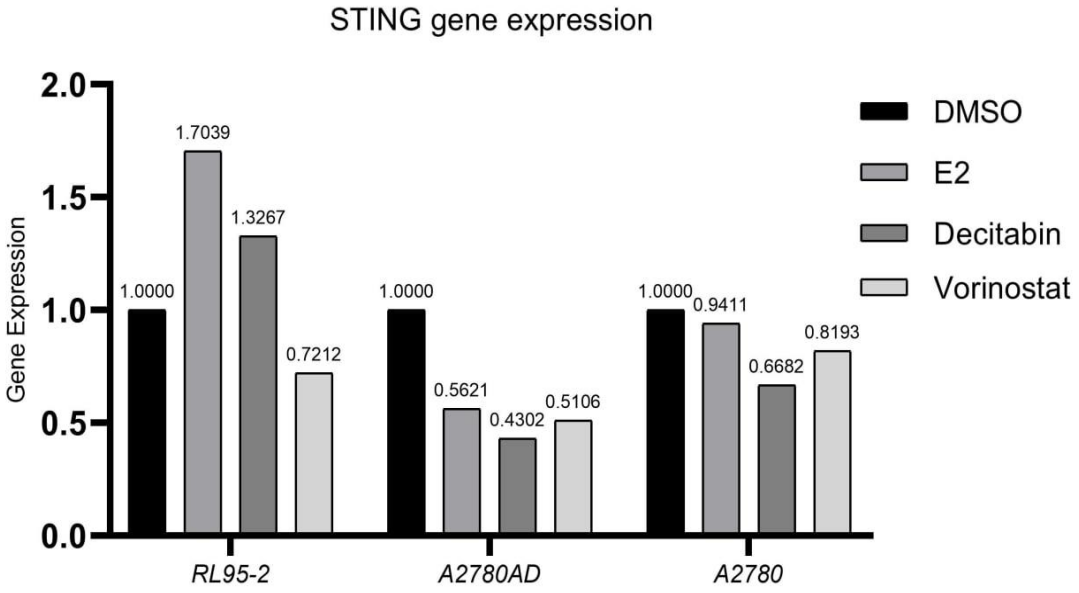

Figure 4.17. STING gene expression in A2780, A2780AD ovarian cancer cell lines and RL95-2 endometrium cell lines after treatment with 17β-Estradiol, Vorinostat and Decitabine. The experimental groups were supplemented with 5 µl/mL of drugs. Error bars show +SEM, and comparisons were performed using the Livak (2^-ddCT) method. Normalisation to the GAPDH control gene was used to compute the results, and the control value was maintained at 1. Three iterations of the trials were conducted.

4.3.3 Potential effects of 17β-Estradiol, Vorinostat and Decitabine on the modulation of IFI16 gene expression levels in A2780, A2780AD and RL95-2 cells.

The ovarian cancer cell lines A2780 and A2780AD and the endometrial cancer cell line RL95-2 were treated with decitabine, vorinostat, and 17β-estradiol. Using qRT-PCR analysis, cDNA was isolated from the separated RNA of the treated cells after the RNA was separated. Based on the data collected, it was found that RL95-2 displayed higher levels of IFI16 gene expression than the control group when 17β-Estradiol was applied to the cell lines, gene expression reduced in all cell lines after applying Decitabine, and when cells treated with Vorinostat IFI16 gene expression declined in RL95-2 and A2780, as shown in (figure 4.18).

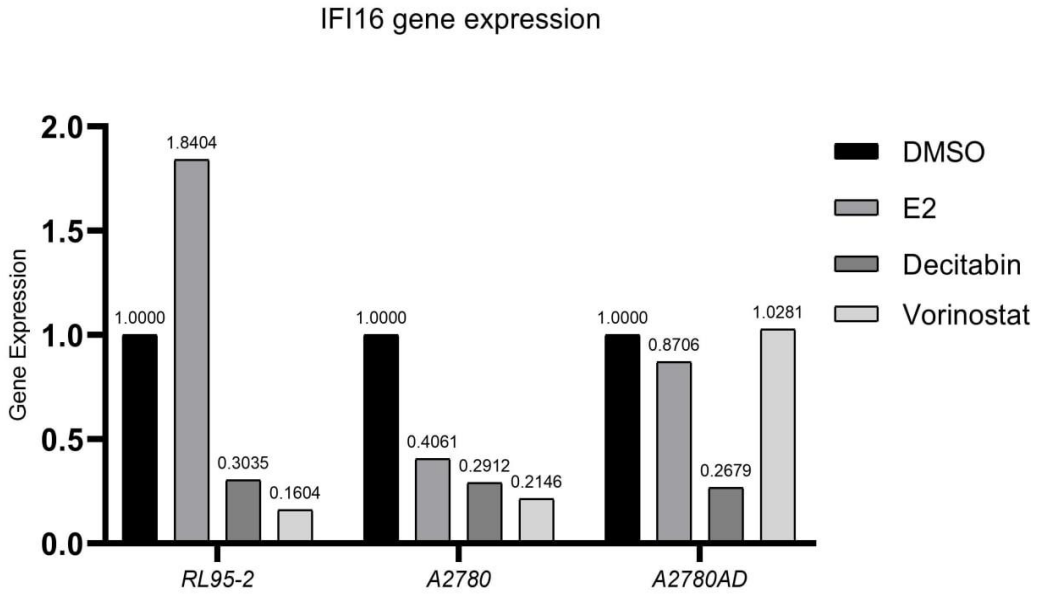

Figure 4.18. IFI16 gene expression in A2780, A2780AD ovarian cancer cell lines and RL95-2 endometrium cancer cell line after treatment with 17β-Estradiol, Vorinostat and Decitabine. The experimental groups were supplemented with 5 µl/mL of drugs. Error bars show +SEM, and comparisons were performed using the Livak (2^-ddCT) method. Normalisation to the GAPDH control gene was used to compute the results, and the control value was maintained at 1. Three iterations of the trials were conducted.

4.4. Studies on the expression of genes in tissue and blood samples from both healthy individuals and patients with gynecologic cancer.

4.4.1 LKB1 gene expression levels in blood samples taken from regular and gynecologic cancer patients.

cDNA was extracted after the RNA from the tissue samples was separated. In the course of this investigation, total RNAs were extracted from a total of 42 patients, comprising 26 patients (n = 8) with ovarian cancer, 18 patients with endometrial cancer, and 16 healthy persons without cancer. Figure 4.19 illustrates that although our qRT-PCR data indicated a tendency toward higher LKB1 gene expression in patients with endometrial and ovarian cancers compared to control groups, statistical significance was not attained.

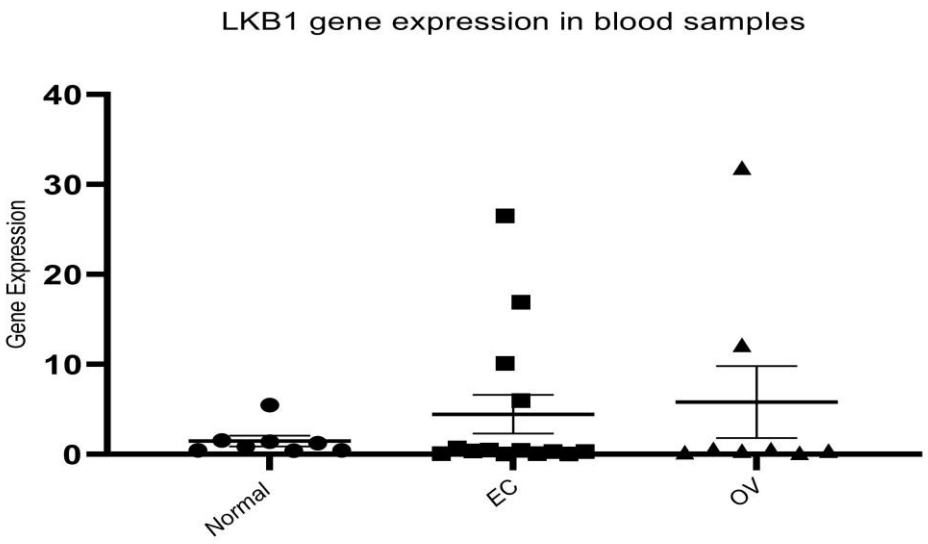

Figure 4.19. Determination of transcription levels of target genes LKB1 in the blood of ovarian cancer, endometrium cancer and control group patients using qRT-PCR. The data obtained were normalised to the GAPDH level, the housekeeping gene. Statistical significance was calculated using One Way ANOVA - t test (non-parametric) Mann Whitney U test (*: $p <= 0.05$; **: $p <= 0.01$, ***: $p <= 0.001$).

4.4.2 STING gene expression levels in blood samples taken from regular and gynecologic cancer patients.

cDNA was extracted after the RNA in the blood samples was separated. Based on collected data, it was found that most patients with gynecologic cancer had gene expressions lower than those found in normal samples, and some showed higher gene expressions relative to the normal samples, as Figure 4.20 illustrates, and there was not statistical significance.

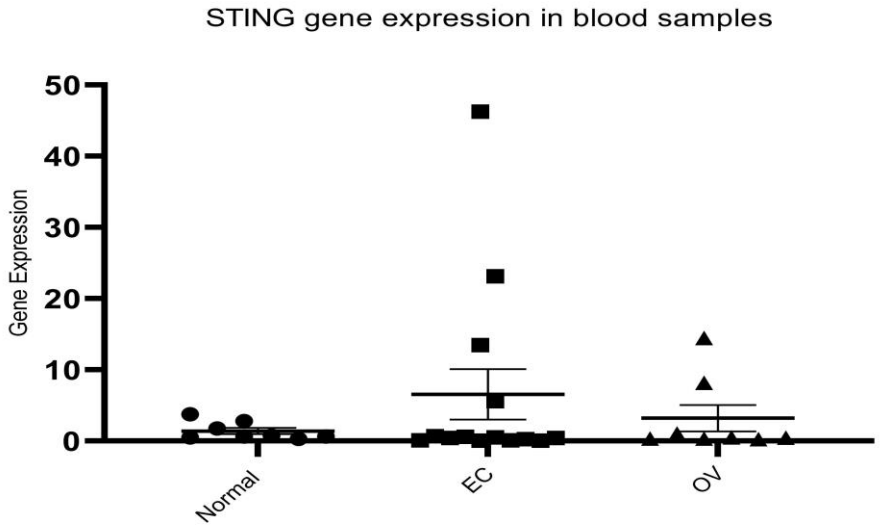

Figure 4.20. Figure 4.19. Determination of transcription levels of target genes STING in the blood of ovarian cancer, endometrium cancer and control group patients using qRT-PCR. The data obtained were normalised to the GAPDH level, the housekeeping gene. Statistical significance was calculated using One Way ANOVA - t test (non-parametric) Mann Whitney U test (*: p < = 0.05; **: p < = 0.01, ***: p < = 0.001).

4.4.3 IFI16 gene expression levels in blood samples taken from regular and gynecologic cancer patients.

Following the separation of the RNA in the blood samples, cDNA was extracted. Figure 4.21 shows that, according to the data gathered, most patients with gynecologic cancer had higher gene expressions than those found in normal samples. In contrast, some had fewer gene expressions than the normal samples. No statistical significance could be reached.

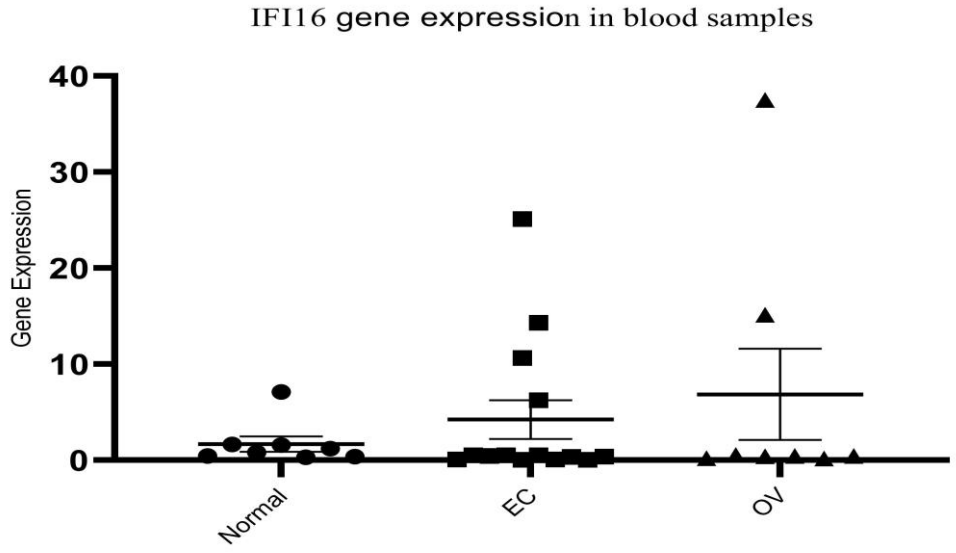

Figure 4.21. Determination of transcription levels of target genes IFI16 in the blood of ovarian cancer, endometrium cancer and control group patients using qRT-PCR. The data obtained were normalised to the GAPDH level, the housekeeping gene. Statistical significance was calculated using One Way ANOVA - t test (non-parametric) Mann Whitney U test (*: p < = 0.05; **: p < = 0.01, ***: p < = 0.001).

When all the genes in patients with gynaecological cancer were examined, the samples with higher levels of gene expression were identical across all genes, and the majority of these samples belonged to the group that received chemotherapy. Paclitaxel, Bevacizumab, and Carboplatin were the chemotherapies used.

4.4.4 LKB1 gene expression levels in tissue samples taken from regular and gynecologic cancer patients.

Following the separation of the RNA from the tissue samples, cDNA was extracted. Within the scope of this study, total RNAs were isolated from a total of 26 patients (n= 8) with ovarian cancer (n= 18) endometrial cancer and (n= 16) healthy individuals without cancer (total n= 42). While our qRT-PCR results noted a trend towards an increase in LKB1 gene expression in ovarian cancer and endometrial cancer patients compared to control groups, statistical significance was not reached, as shown in Figure 4.22.

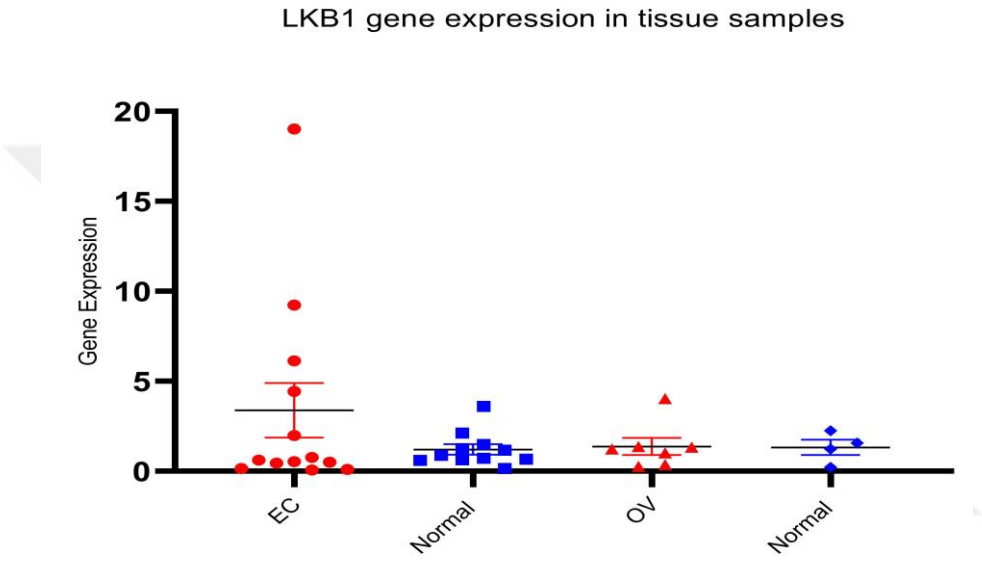

Figure 4.22. Determination of transcription levels of target genes LKB1 in ovarian cancer, endometrium cancer and control group patients using qRT-PCR. The data obtained were normalised to the GAPDH level, the housekeeping gene. Statistical significance was calculated using One Way ANOVA - t test (non-parametric) Mann Whitney U test (*: $p <= 0.05$; **: $p <= 0.01$, ***: $p <= 0.001$).

4.4.5 STING gene expression levels in tissue samples taken from regular and gynecologic cancer patients.

cDNA was extracted after the RNA in the tissue samples was separated. Based on collected data, it was found that most patients with gynecologic cancer had STING gene expressions lower than those found in normal samples, and some showed higher gene expressions relative to the normal samples, as Figure 4.23 illustrates. No statistical significance could be reached.

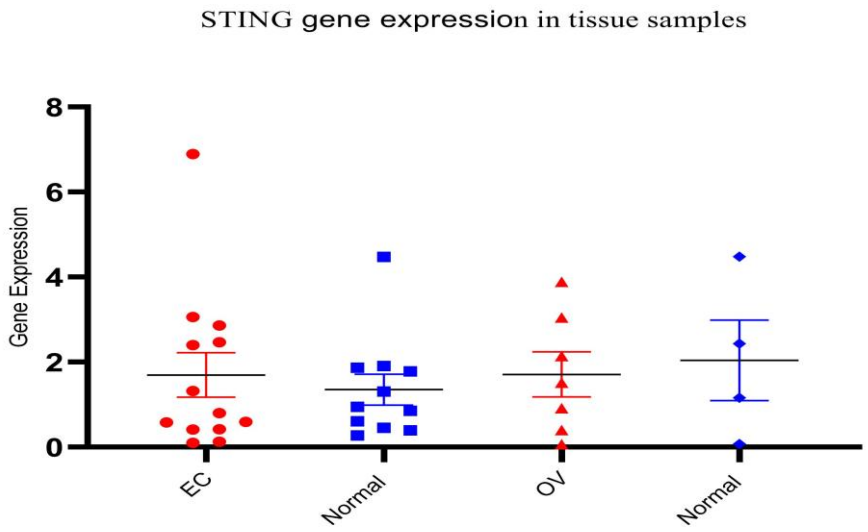

Figure 4.23. Determination of transcription levels of target genes STING in ovarian cancer, endometrium cancer and control group patients using qRT-PCR. The data obtained were normalised to the GAPDH level, the housekeeping gene. Statistical significance was calculated using One Way ANOVA - t test (non-parametric) Mann Whitney U test (*: $p <= 0.05$; **: $p <= 0.01$, ***: $p <= 0.001$).

4.4.6 IFI16 gene expression levels in tissue samples taken from regular and gynecologic cancer patients.

Following the separation of the RNA in the blood samples, cDNA was extracted. Figure 4.24 shows that, according to the data gathered, most patients with gynecologic cancer had IFI16 gene expressions that were higher than those found in normal samples. In contrast, some had fewer gene expressions than the normal samples. There was not a reach of statistical significance.

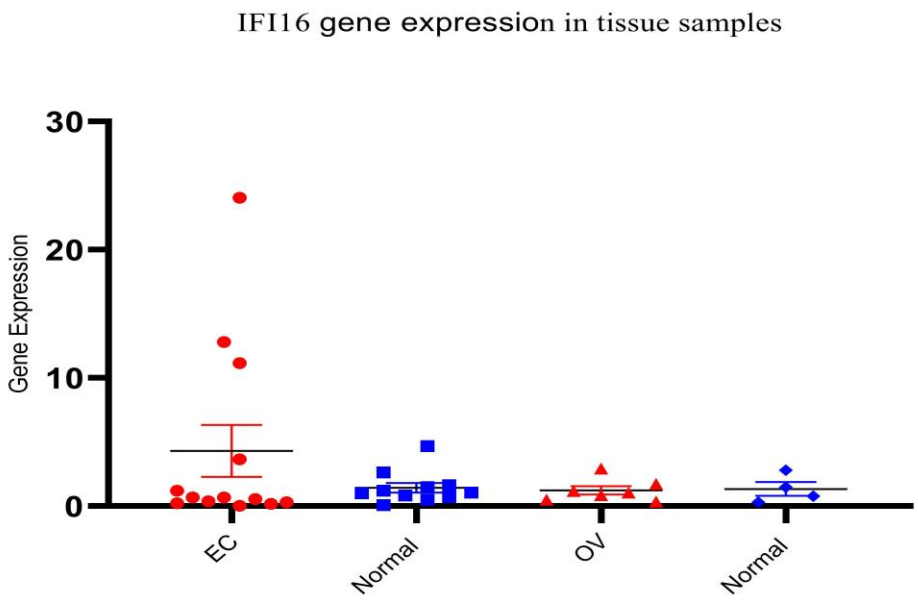

Figure 4.24. Determination of transcription levels of target genes IFI16 in ovarian cancer, endometrium cancer and control group patients using qRT-PCR. The data obtained were normalised to the GAPDH level, the housekeeping gene. Statistical significance was calculated using One Way ANOVA - t test (non-parametric) Mann Whitney U test (*: $p <= 0.05$; **: $p <= 0.01$, ***: $p <= 0.001$).

The samples with greater levels of gene expression were identical across all genes when all the genes in the patients with gynaecological cancer were evaluated; part of these samples was from the treatment group. The two chemotherapy drugs that were employed were bevacizumab and paclitaxel, while the remaining samples had high gene expression levels without the need for chemotherapy.

4.5. Analysis of the Expression of LKB1 Protein in Cells, Serum, and Tissue Samples

4.5.1. Examining How the Drugs Affect the Expression of LKB1 Proteins

It looked at how 17β-Estradiol, Vorinostat, and Decitabine affected the regulation of LKB1, STING, and IFI16 proteins that are important in preventing the growth of tumours. In order to examine the possible impacts of 17β-Estradiol, Vorinostat, and Decitabine on the identified proteins, protein isolation experiments were conducted using concentrations of 128μM estrogen, 10μM Vorinostat, and 40μM Decitabine that impact cell viability over 50% in ovarian cancer cell lines (A2780 and A2780AD) and endometrial cancer cell line (RL95-2). The protein isolation procedure was followed immediately by the ELISA assay.

Based on the data gathered, we compared each treated cell line to its control group. We discovered that when drugs were applied to the RL95-2 cell line, the LKB1 protein

expression level did not appear to change following the control group; in the A2780AD cell line, E2 treatment increased protein expression, while Decitabine and Vorinostat treatment resulted in a decrease in protein expression; and in the A2780 cell line, all drug treatments caused a decline in protein expression, as illustrated in (figure 4.25).

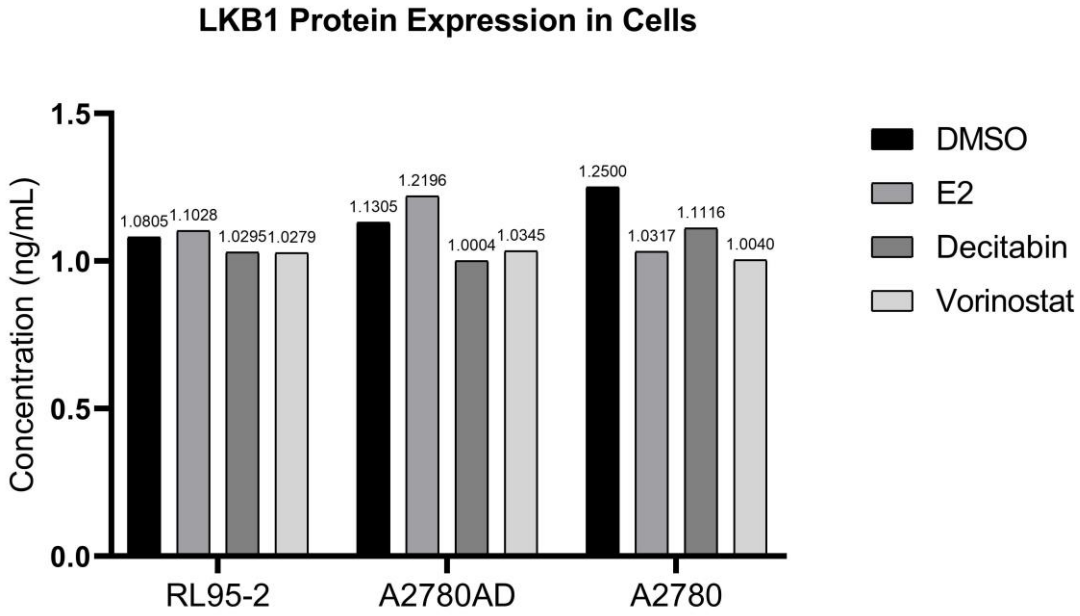

Figure 4.25. LKB1 protein expression in A2780, A2780AD ovarian cancer cell lines and RL95-2 endometrium cancer cell line after treatment with 17β-Estradiol, Vorinostat and Decitabine. The experimental groups were supplemented with 5 µl/mL of drugs. Error bars show +SEM.

4.5.2. Examination of LKB1 Protein Expression in Serum Samples

The concentration of LKB1 protein expression in the serum of gynecologic cancer patients was measured after protein isolation, and an ELISA assay was performed. The results showed that, regarding LKB1 gene expression in both ovarian and endometrial cancer, most of the samples expressed more LKB1 protein than the healthy samples, and some cancer samples expressed low levels. Additionally, some of the samples with elevated LKB1 protein levels received chemotherapy while undergoing treatment, as shown in Figure 4.26.

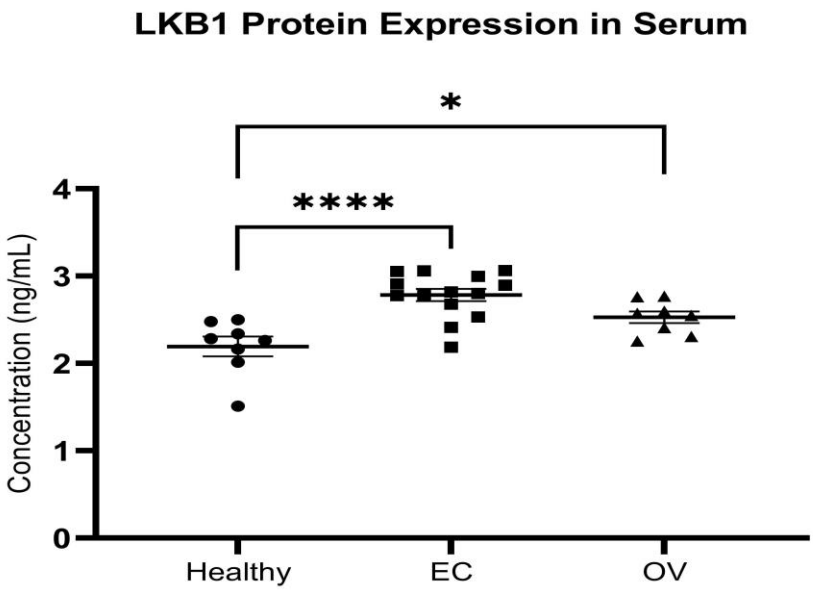

Figure 4.26. Determination of serum LKB1 protein levels of ovarian cancer, endometrium cancer and healthy group by ELISA method. Error bars of all patients show +SEM value. Statistical significance was calculated using One Way ANOVA - t test (non-parametric) Mann Whitney U test (*: $p <= 0.05$; **: $p <= 0.01$, ***: $p <= 0.001$).

4.5.3. Examination of LKB1 Protein Expression in Tissue Samples

Following protein isolation and the ELISA assay, the tissue of patients with gynecologic cancer was examined for LKB1 protein expression and compared with that of healthy tissue. The data obtained showed that Tissue LKB1 protein concentrations in patients with ovarian cancer ($p = 0.001$) were significantly increased compared to the control group. Additionally, it has been shown that LKB1 protein levels are significantly increased in tissue samples of endometrial cancer patients compared to tissues of healthy individuals. (Figure 4.27). Our results show that tissue LKB1 protein levels are interrelated between ovarian cancer and endometrial cancer patients and healthy individuals. Additionally, some of the samples with elevated LKB1 protein levels received chemotherapy while undergoing treatment.

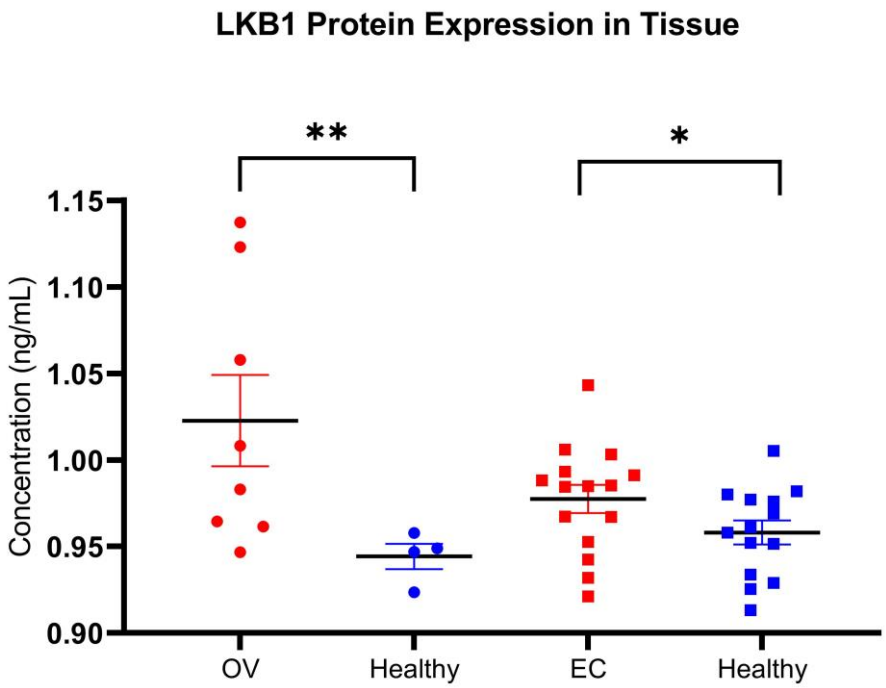

Figure 4.27. Determination of tissue LKB1 protein levels of ovarian cancer, endometrium cancer and their control group patients by ELISA method. Error bars of all patients show +SEM value. Statistical significance was calculated using One Way ANOVA - t test (non-parametric) Mann Whitney U test (*: $p <= 0.05$; **: $p <= 0.01$, ***: $p <= 0.001$).

5. DISCUSSION

Many organs, including the breast, colon, lung, skin, and cervix, have been significantly related to malignant transformation by the regulation of different epigenetic or posttranslational processes (Gibney et al., 2010). 17β-Estradiol, Vorinostat, and Decitabine were drugs used in this study which affect gene expression epigenetically. The sensitivity of the ovarian cancer cell lines A2780 and its chemoresistant clone A2780AD and endometrium cancer cell line RL95-2 to 17β-Estradiol, Vorinostat and Decitabine was investigated in the first part of this thesis study. According to MTT results, A2780AD was more sensitive to Vorinostat and Decitabine than A2780, and the most sensitive was RL95-2 with all cells. At the same time, 17β-Estradiol caused the cells to increase more than the control group. The cell line's viability toward drugs was not that sensitive to decrease the cell line's proliferation below 50%, and the IC50 concentration was not determined for any drug. Furthermore, the highest concentration of each drug was determined to be used in other procedures.

Many genes can be categorised into two major categories: tumour suppressor genes (TSGs) and oncogenes, commonly called cancer-promoting genes (CPGs). Three of the tumour suppressor genes (LKB1, STING, and IFI16) were used to analyse the effects of epigenetics on the genes. The drugs which work on genes epigenetically were used, 17β-Estradiol, which is present in the human body as a hormone that can increase gene expressions. Vorinostat inhibits histone deacetylase enzymes. Furthermore, Decitabine decreases DNA methylation. In our study, we consistently received outcomes in ovarian cancer cell lines A2780 and its chemoresistant clone A2780AD and endometrium cancer cell line RL95-2. We observed that 17β-Estradiol increased the LKB1 gene expression in A2780AD, while in A2780, the gene expression declined; however, the gene expression in RL95-2 did not change significantly according to the control group. 17β-Estradiol affected STING gene expression in RL95-2 and increased it. In A2780AD, the gene expression declined; however, the gene expression in A2780 did not change significantly according to the control group. The expression of the IFI16 gene was altered and elevated in RL95-2 by 17β-Estradiol. The control group reported that while the gene expression in A2780 decreased, it did not significantly change in A2780AD. So, the effect of 17β-Estradiol on each gene depends on the cell type and the presence of its promoter on that gene. The different expression of each gene in the cell lines may be due to the absence of a 17β-Estradiol promoter in the genes and cannot bind to the genes. Vorinostat raised the LKB1 gene expression in A2780AD, whereas the gene expression decreased in A2780; however, the control group found no significant change in

the gene expression of Rl95-2. Vorinostat declined STING gene expression in all cell lines, especially in A2780AD, which decreased significantly. Vorinostat dramatically reduced the IFI16 gene expression in RL95-2 and A2780. However, there was no significant change in A2780AD. Histone deacetylation generally inhibits gene expression; Vorinostat works by preventing histone deacetylase enzyme activity. It follows that Vorinostat had to boost the expression of the genes we used. However, this did not occur for most of the genes, as their expression fell; the lone exception was A2780AD, where the control group reported no change in the expression of LKB1 or IFI16. Perhaps more factors are at play than just deacetylation warrant lowering gene expression. In applying Decitabine to the cell lines, the expression of the LKB1 gene decreased in RL95-2 and A2780, while no significant change happened in LKB1 expression in A2780AD. STING gene expression under the effect of decitabine increased significantly in the RL95-2 cell line, while in ovarian cancer cell lines, STING expression decreased dramatically. In all cell lines, IFI16 gene expression declined significantly after applying Decitabine. Decitabine decreases DNA methylation and increases gene expressions, as we previously discussed. However, in the results, only the STING gene expression increased in the endometrial cancer cell line; the gene expressions in the other cell lines decreased. We can speculate that it might be because the impact of methylation on gene expression varies based on the kind of cell. These gene expressions were tested in blood and tissue samples from gynecologic cancer patients and compared with those from healthy persons. We observed that when all the genes in patients with gynaecological cancer were examined, the samples with higher levels of gene expression were identical across all genes. Most of these samples belonged to the group that received chemotherapy. Paclitaxel, Bevacizumab, and Carboplatin were the chemotherapies used.

In this study, we could also analyse the effect of the drugs on the protein level of LKB1 in all cell lines. As a result of ELISA, we contrasted each treated cell line with its control group. The RL95-2 cell line showed no change in LKB1 protein expression level when drugs were applied in comparison to the control group; the A2780AD cell line showed an increase in protein expression upon E2 treatment, while Decitabine and Vorinostat treatment led to a decrease in protein expression, and the A2780 cell line showed a decline in protein expression upon all drug treatments. So, the effect of the drugs on the LKB1 protein may depend on the cell type, drug dosage and time of drug exposure. LKB1 protein expression was also examined in blood and tissue samples from patients with gynecologic cancer and contrasted with that of healthy samples. We saw that while the protein expression in certain

samples was lower than in healthy samples, it was higher in others. A small number of the samples with elevated LKB1 protein received chemotherapy while undergoing treatment. Therefore, variations in protein expression could be caused by other treatments or chemotherapy.

6. CONCLUSION

This thesis study concludes by demonstrating that, depending on the gene types, organ types, and locations of mRNA and proteins in the nucleus and cytoplasm, epigenetics affects the mRNA and protein levels of the genes. Additionally, it demonstrates how medications that influence epigenetics affect cell survival and migration. Decitabine, Vorinostat, and 17β-Estradiol are the epigenetically active medications employed in this investigation. The expression of mRNA and proteins, as well as the survival and migration of the cells, were all impacted differently by each medication. 17β-Estradiol improved migration and vitality in all cell lines. However, its effects on mRNA expression varied depending on the cell type. Each cell line showed a loss in viability and a slowdown in migration when Vorinostat and Decitabine were administered. However, the effects on mRNA expression varied depending on the cell type.

This study tested the mRNA and protein expressions in the blood and tissue samples taken from gynecologic cancer patients and healthy persons. We concluded that in the patients who took chemotherapies as a treatment, their mRNA and protein expression of the LKB1, STING, and IFI16 increased.

Based on the study's findings, we can conclude that medications that increase the expression of tumour suppressor genes—particularly those we looked at, LKB1, STING, and IFI16—are important because those genes play a part in the body's immune system. The effects of these medications should be examined both in vivo and in vitro. Additionally, there are specific methods for studying each kind of epigenetics, such as methylation and acetylation, to determine how they affect gene expression levels.

7. REFERENCES

Akyuz, A., Dede, M., Cetinturk, A., Yavan, T., Yenen, M. C., Sarici, S. U., & Dilek, S. (2007). Self-application of complementary and alternative medicine by patients with gynecologic cancer. Gynecologic and obstetric investigation.

Alessi, D. R., Sakamoto, K., & Bayascas, J. R. (2006). LKB1-dependent signaling pathways. Annu. Rev. Biochem., 75, 137-163.

Ali, M. W., Cacan, E., Liu, Y., Pierce, J. Y., Creasman, W. T., Murph, M. M., Govindarajan, R., Eblen, S. T., Greer, S. F., & Hooks, S. B. (2013). Transcriptional suppression, DNA methylation, and histone deacetylation of the regulator of G-protein signaling 10 (RGS10) gene in ovarian cancer cells. PloS one, 8(3), e60185. https://doi.org/10.1371/journal.pone.0060185

Alimirah, F., Chen, J., Davis, F. J., & Choubey, D. (2007). IFI16 in human prostate cancer. Molecular cancer research, 5(3), 251-259.

Al-Janabi, A. S., Alheety, M. A., Osama'a, A. Y., Shaaban, S., Kibar, B., & Cacan, E. (2020). Anti-cancer and anti-fungal evaluation of novel palladium (II) 1-phenyl-1H-tetrazol-5-thiol complexes. Inorganic Chemistry Communications, 121, 108193.

Amant, F., Moerman, P., Neven, P., Timmerman, D., Van Limbergen, E., & Vergote, I. (2005). Endometrial cancer. Lancet (London, England), 366(9484), 491–505.

American Cancer Society, 2018. What is ovarian cancer? The American Cancer Society

Andrews, L., & Mutch, D. G. (2017). Hereditary ovarian cancer and risk reduction. Best practice & research Clinical obstetrics & gynaecology, 41, 31-48.

Assis, J., Pereira, D., Nogueira, A., & Medeiros, R. (2018). Ovarian cancer overview: molecular biology and its potential clinical application. Ovarian Cancer-From Pathogenesis to Treatment.

Babaier, A., & Ghatage, P. (2020). Mucinous cancer of the ovary: overview and current status. Diagnostics, 10(1), 52.

Baekelandt, M. M., & Castiglione, M. (2009). Endometrial carcinoma: ESMO clinical recommendations for diagnosis, treatment and follow-up. Annals of Oncology, 20, iv29-iv31.

Barber G. N. (2015). STING: infection, inflammation and cancer. Nature reviews. Immunology.

Bereshchenko, O. R., Gu, W., & Dalla-Favera, R. (2002). Acetylation inactivates the transcriptional repressor BCL6. Nature genetics, 32(4), 606-613.

Berkel, C., & Cacan, E. (2021). Involvement of ATMIN-DYNLL1-MRN axis in the progression and aggressiveness of serous ovarian cancer. Biochemical and biophysical research communications, 570, 74–81. https://doi.org/10.1016/j.bbrc.2021.07.004

Berkel, C., Kucuk, B., Merve, U. S. T. A., Yilmaz, E., & Cacan, E. (2020). The effect of Olaparib and Bortezomib combination treatment on ovarian Cancer cell lines. European Journal of Biology, 79(2), 115-123.

Bjornstrom, L., & Sjoberg, M. (2005). Mechanisms of estrogen receptor signaling: convergence of genomic and nongenomic actions on target genes. Molecular endocrinology, 19(4), 833-842.

Bokhman, J. V. (1983). Two pathogenetic types of endometrial carcinoma. Gynecologic oncology, 15(1), 10-17.

Bonanno, L., Zulato, E., Pavan, A., Attili, I., Pasello, G., Conte, P., & Indraccolo, S. (2019). LKB1 and tumor metabolism: the interplay of immune and angiogenic microenvironment in lung cancer. International journal of molecular sciences, 20(8), 1874.

Bouchekioua-Bouzaghou, K., Poulard, C., Rambaud, J., Lavergne, E., Hussein, N., Billaud, M., ... & Le Romancer, M. (2014). LKB1 when associated with methylatedERα is a

marker of bad prognosis in breast cancer. International journal of cancer, 135(6), 1307-1318.
Brown, K. A., McInnes, K. J., Takagi, K., Ono, K., Hunger, N. I., Wang, L., ... & Simpson, E. R. (2011). LKB1 expression is inhibited by estradiol-17β in MCF-7 cells. The Journal of steroid biochemistry and molecular biology, 127(3-5), 439-443.
Cacan, E., & Ozmen, Z. C. (2020). Regulation of Fas in response to bortezomib and epirubicin in colorectal cancer cells. Journal of chemotherapy (Florence, Italy), 32(4), 193–201. https://doi.org/10.1080/1120009X.2020.1740389
Cacan E. (2016). Histone Deacetylase-1-mediated Suppression of FAS in Chemoresistant Ovarian Cancer Cells. Anticancer research, 36(6), 2819–2826.
Caldiran, F. Y., & Cacan, E. (2022). RGS10 suppression by DNA methylation is associated with low survival rates in colorectal carcinoma. Pathology, research and practice, 236, 154007. https://doi.org/10.1016/j.prp.2022.154007
Cetin, I., Cozzi, V., & Antonazzo, P. (2008). Infertility as a cancer risk factor - a review. Placenta, 29 Suppl B, 169–177.
Chan, J. K., Loizzi, V., Magistris, A., Lin, F., Rutgers, J., Osann, K., ... & Berman, M. L. (2004). Differences in prognostic molecular markers between women over and under 45 years of age with advanced ovarian cancer. Clinical cancer research, 10(24), 8538-8543.
Chen, D. S., & Mellman, I. (2013). Oncology meets immunology: the cancer-immunity cycle. immunity, 39(1), 1-10.
Chen, G., Yan, Q., Liu, L., Wen, X., Zeng, H., & Yin, S. (2022). Histone Deacetylase 3 Governs β-Estradiol-ERα-Involved Endometrial Tumorigenesis via Inhibition of STING Transcription. Cancers, 14(19), 4718.
Chiva, L., Lapuente, F., González-Cortijo, L., Carballo, N., García, J. F., Rojo, A., & Gonzalez-Martín, A. (2008). Sparing fertility in young patients with endometrial cancer. Gynecologic oncology, 111(2), S101-S104.
Choubey, D., Deka, R., & Ho, S. M. (2008). Interferon-inducible IFI16 protein in human cancers and autoimmune diseases. Frontiers in Bioscience-Landmark, 13(2), 598-608.
Christopherson, W. M., Alberhasky, R. C., & Connelly, P. J. (1982). Carcinoma of the endometrium. II. Papillary adenocarcinoma: a clinical pathological study 46 cases. American Journal of Clinical Pathology, 77(5), 534-540.
Christopherson, W. M., Connelly, P. J., & Alberhasky, R. C. (1983). Carcinoma of the endometrium V. An analysis of prognosticators in patients with favorable subtypes and stage I disease. Cancer, 51(9), 1705-1709.
Cirisano Jr, F. D., Robboy, S. J., Dodge, R. K., Bentley, R. C., Krigman, H. R., Synan, I. S., ... & Clarke-Pearson, D. L. (1999). Epidemiologic and surgicopathologic findings of papillary serous and clear cell endometrial cancers when compared to endometrioid carcinoma. Gynecologic oncology, 74(3), 385-394.
Clark, T. J., Voit, D., Gupta, J. K., Hyde, C., Song, F., & Khan, K. S. (2002). Accuracy of hysteroscopy in the diagnosis of endometrial cancer and hyperplasia: a systematic quantitative review. Jama, 288(13), 1610-1621.
Clayton, R. D. (2006). Hysterectomy. Best practice & research Clinical obstetrics & gynaecology, 20(1), 73-87.
Co, N. N., Iglesias, D., Celestino, J., Kwan, S. Y., Mok, S. C., Schmandt, R., & Lu, K. H. (2014). Loss of LKB1 in high-grade endometrial carcinoma: LKB1 is a novel transcriptional target of p53. Cancer, 120(22), 3457-3468.
Cortez, A. J., Tudrej, P., Kujawa, K. A., & Lisowska, K. M. (2018). Advances in ovarian cancer therapy. Cancer chemotherapy and pharmacology, 81, 17-38.
Costanzo, E. S., Lutgendorf, S. K., Rothrock, N. E., & Anderson, B. (2006). Coping and quality of life among women extensively treated for gynecologic

cancer. Psycho-Oncology: Journal of the Psychological, Social and Behavioral Dimensions of Cancer.

Cridland, J. A., Curley, E. Z., Wykes, M. N., Schroder, K., Sweet, M. J., Roberts, T. L., ... & Stacey, K. J. (2012). The mammalian PYHIN gene family: phylogeny, evolution and expression. BMC evolutionary biology, 12, 1-17.

Critchley, H. O., Maybin, J. A., Armstrong, G. M., & Williams, A. R. (2020). Physiology of the endometrium and regulation of menstruation. Physiological reviews.

Dai, J., Huang, Y. J., He, X., Zhao, M., Wang, X., Liu, Z. S., ... & Li, T. (2019). Acetylation blocks cGAS activity and inhibits self-DNA-induced autoimmunity. Cell, 176(6), 1447–1460.

De Groot, J.M., Mah, K., Fyles, A.,Winton, S., Greenwood, S., Depetrillos, A.D., et al. (2005). The psychosocial impact of cervical cancer among affected women and their partners. International Journal of Gynecological Cancer, 15(5), 918–925.

Denschlag, D., Ulrich, U., & Emons, G. (2011). The diagnosis and treatment of endometrial cancer: progress and controversies. Deutsches Ärzteblatt International, 108(34-35), 571.

Der, S. D., Zhou, A., Williams, B. R., & Silverman, R. H. (1998). Identification of genes differentially regulated by interferon α, β, or γ using oligonucleotide arrays. Proceedings of the National Academy of Sciences, 95(26), 15623-15628.

Deroo, B. J., & Korach, K. S. (2006). Estrogen receptors and human disease. The Journal of clinical investigation, 116(3), 561-570.

Doll, A., Abal, M., Rigau, M., Monge, M., Gonzalez, M., Demajo, S., Colás, E., Llauradó, M., Alazzouzi, H., Planagumá, J., Lohmann, M. A., Garcia, J., Castellvi, S., Ramon y Cajal, J., Gil-Moreno, A., Xercavins, J., Alameda, F., & Reventós, J. (2008). Novel molecular profiles of endometrial cancer-new light through old windows. The Journal of steroid biochemistry and molecular biology, 108(3-5), 221–229. https://doi.org/10.1016/j.jsbmb.2007.09.020

Duska, L. R., & Kohn, E. C. (2017). The new classifications of ovarian, fallopian tube, and primary peritoneal cancer and their clinical implications. Annals of Oncology, 28, viii8-viii12.

Ekwall, E., Ternestedt, B. M., & Sorbe, B. (2003). Important aspects of health care for women with gynecologic cancer. Oncology nursing forum

Ekwall, E., Ternestedt, B.M., & Sorbe, B. (2003). Important aspects of health care for women with gynecological cancer. Oncology Nursing Forum, 30(2), 313–319.

Elsandabesee, D., & Greenwood, P. (2005). The performance of Pipelle endometrial sampling in a dedicated postmenopausal bleeding clinic. Journal of obstetrics and gynaecology, 25(1), 32-34.

Emons, G., & Kimmig, R. (2009). Interdisciplinary S2k guidelines on the diagnosis and treatment of endometrial carcinoma. Journal of cancer research and clinical oncology, 135, 1387-1391.

Engelhardt, J. J., Boldajipour, B., Beemiller, P., Pandurangi, P., Sorensen, C., Werb, Z., Egeblad, M., & Krummel, M. F. (2012). Marginating dendritic cells of the tumor microenvironment cross-present tumor antigens and stably engage tumor-specific T cells. Cancer cell, 21(3), 402–417. https://doi.org/10.1016/j.ccr.2012.01.008

Esteller, M., Avizienyte, E., Corn, P. G., Lothe, R. A., Baylin, S. B., Aaltonen, L. A., & Herman, J. G. (2000). Epigenetic inactivation of LKB1 in primary tumors associated with the Peutz-Jeghers syndrome. Oncogene, 19(1), 164-168.

Evans, E. C., Matteson, K. A., Orejuela, F. J., Alperin, M., Balk, E. M., El-Nashar, S., ... & Society of Gynecologic Surgeons Systematic Review Group. (2016). Salpingo-oophorectomy at the time of benign hysterectomy: a systematic review. Obstetrics & Gynecology, 128(3), 476-485.

Fader, A. N., Arriba, L. N., Frasure, H. E., & von Gruenigen, V. E. (2009). Endometrial cancer and obesity: epidemiology, biomarkers, prevention and survivorship. Gynecologic oncology, 114(1), 121–127.

Feinberg, A. P. (2018). The key role of epigenetics in human disease prevention and mitigation. New England Journal of Medicine, 378(14), 1323-1334.

Ferlay, J., Soerjomataram, I., Ervik, M., Dikshit, R., Eser, S., Mathers, C., ... & Bray, F. (2013). GLOBOCAN 2012 v1. 0, cancer incidence and mortality worldwide.

Finnin, M. S., Donigian, J. R., Cohen, A., Richon, V. M., Rifkind, R. A., Marks, P. A., ... & Pavletich, N. P. (1999). Structures of a histone deacetylase homologue bound to the TSA and SAHA inhibitors. Nature, 401(6749), 188-193.

Fraser, I. S., Critchley, H. O., Munro, M. G., & Broder, M. (2007). A process designed to lead to international agreement on terminologies and definitions used to describe abnormalities of menstrual bleeding∗. Fertility and sterility, 87(3), 466-476.

Fujiuchi, N., Aglipay, J. A., Ohtsuka, T., Maehara, N., Sahin, F., Su, G. H., ... & Ouchi, T. (2004). Requirement of IFI16 for the maximal activation of p53 induced by ionizing radiation. Journal of Biological Chemistry, 279(19), 20339-20344.

Fujiwara, K., Oda, K., Takano, M., & Matsumura, N. (2017). Clear cell carcinoma of the ovary. Textbook of Uncommon Cancer, 550-556.

Gasner, A. (2020). Physiology, Uterus.

Gibney, E. R., & Nolan, C. M. (2010). Epigenetics and gene expression. Heredity, 105(1), 4–13.

Gilbert, L., Basso, O., Sampalis, J., Karp, I., Martins, C., Feng, J., ... & Krishnamurthy, S. (2012). Assessment of symptomatic women for early diagnosis of ovarian cancer: results from the prospective DOvE pilot project. The lancet oncology, 13(3), 285-291.

Goodman, M. T., Wu, A. H., Tung, K. H., McDuffie, K., Kolonel, L. N., Nomura, A. M., ... & Hankin, J. H. (2002). Association of dairy products, lactose, and calcium with the risk of ovarian cancer. American journal of epidemiology, 156(2), 148-157.

Grant, S., Easley, C., & Kirkpatrick, P. (2007). Vorinostat. Nature reviews Drug discovery, 6(1).

Hauk, L. (2014). ACOG releases guidelines on management of abnormal uterine bleeding associated with ovulatory dysfunction. American Family Physician, 89(12), 987-988.

Hearle, N., Schumacher, V., Menko, F. H., Olschwang, S., Boardman, L. A., Gille, J. J., ... & Houlston, R. S. (2006). Frequency and spectrum of cancers in the Peutz-Jeghers syndrome. Clinical Cancer Research, 12(10), 3209-3215.

Hemminki, A., Markie, D., Tomlinson, I., Avizienyte, E., Roth, S., Loukola, A., ... & Aaltonen, L. A. (1998). A serine/threonine kinase gene defective in Peutz–Jeghers syndrome. Nature, 391(6663), 184-187.

Holzner, B., Kemmler, G., Meraner, V., Maislinger, A., Kopp, M., Bodner, T., et al. (2003). Fatigue in ovarian carcinoma patients.Aneglected issue? Cancer, 97(6), 1564–1572.

Hong, Z., Ma, T., Liu, X., & Wang, C. (2022). cGAS-STING pathway: post-translational modifications and functions in sterile inflammatory diseases. The FEBS Journal, 289(20), 6187-6208.

Ishikawa, H., & Barber, G. N. (2008). STING is an endoplasmic reticulum adaptor that facilitates innate immune signaling. Nature.

Ishikawa, H., Ma, Z., & Barber, G. N. (2009). STING regulates intracellular DNA-mediated, type I interferon-dependent innate immunity. Nature, 461(7265), 788-792.

Jabbour, E., Issa, J. P., Garcia-Manero, G., & Kantarjian, H. (2008). Evolution of decitabine development: accomplishments, ongoing investigations, and future strategies. Cancer: Interdisciplinary International Journal of the American Cancer Society, 112(11), 2341-2351.

Jakobsen, M. R., & Paludan, S. R. (2014). IFI16: at the interphase between innate DNA sensing and genome regulation. Cytokine & growth factor reviews, 25(6), 649-655.
Jemal, A., Bray, F., Center, M. M., Ferlay, J., Ward, E., & Forman, D. (2011). Global cancer statistics. CA: a cancer journal for clinicians.
Johnstone, R. W., & Trapani, J. A. (1999). Transcription and growth regulatory functions of the HIN-200 family of proteins. Molecular and cellular biology, 19(9), 5833-5838.
Jones, P. A., & Taylor, S. M. (1980). Cellular differentiation, cytidine analogs and DNA methylation. Cell, 20(1), 85-93.
Jordan, S. J., Siskind, V., C Green, A., Whiteman, D. C., & Webb, P. M. (2010). Breastfeeding and risk of epithelial ovarian cancer. Cancer Causes & Control, 21, 109-116
Ju, W., Yoo, B. C., Kim, I. J., Kim, J. W., Kim, S. C., & Lee, H. P. (2009). Identification of genes with differential expression in chemoresistant epithelial ovarian cancer using high-density oligonucleotide microarrays. Oncology Research Featuring Preclinical and Clinical Cancer Therapeutics, 18(2-3), 47–56.
Justice, J. L., Kennedy, M. A., Hutton, J. E., Liu, D., Song, B., Phelan, B., & Cristea, I. M. (2021). Systematic profiling of protein complex dynamics reveals DNA-PK phosphorylation of IFI16 en route to herpesvirus immunity. Science advances, 7(25), eabg6680.
Ka, N. L., Lim, G. Y., Kim, S. S., Hwang, S., Han, J., Lee, Y. H., & Lee, M. O. (2022). Type I IFN stimulates IFI16-mediated aromatase expression in adipocytes that promotes E2-dependent growth of ER-positive breast cancer. Cellular and Molecular Life Sciences, 79(6), 306
Kaaks, R., Lukanova, A., & Kurzer, M. S. (2002). Obesity, endogenous hormones, and endometrial cancer risk: a synthetic review. Cancer epidemiology, biomarkers & prevention : a publication of the American Association for Cancer Research, cosponsored by the American Society of Preventive Oncology, 11(12), 1531–1543.
Karatas, O., Yuce, H. B., Taskan, M. M., Gevrek, F., Yarkac, F. U., & Cacan, E. (2021). Detection of nuclear receptors in gingival samples of diabetic and nondiabetic periodontitis patients. Nigerian journal of clinical practice, 24(2), 269–276. https://doi.org/10.4103/njcp.njcp_216_20
Kazerouni, N., Greene, M. H., Lacey Jr, J. V., Mink, P. J., & Schairer, C. (2006). Family history of breast cancer as a risk factor for ovarian cancer in a prospective study. Cancer: Interdisciplinary International Journal of the American Cancer Society, 107(5), 1075-1083.
Kerur, N., Veettil, M. V., Sharma-Walia, N., Bottero, V., Sadagopan, S., Otageri, P., & Chandran, B. (2011). IFI16 acts as a nuclear pathogen sensor to induce the inflammasome in response to Kaposi Sarcoma-associated herpesvirus infection. Cell host & microbe, 9(5), 363–375.
Khan, M. I., Nur, S. M., & Abdulaal, W. H. (2022). A study on DNA methylation modifying natural compounds identified EGCG for induction of IFI16 gene expression related to the innate immune response in cancer cells. Oncology letters, 24(1), 218.
Kinkel, K., Lu, Y., Mehdizade, A., Pelte, M. F., & Hricak, H. (2005). Indeterminate ovarian mass at US: incremental value of second imaging test for characterization—meta-analysis and Bayesian analysis. Radiology, 236(1), 85-94.
Kitajima, S., Ivanova, E., Guo, S., Yoshida, R., Campisi, M., Sundararaman, S. K., ... & Barbie, D. A. (2019). Suppression of STING associated with LKB1 loss in KRAS-driven lung cancer. Cancer discovery, 9(1), 34-45.
Kitajima, S., Thummalapalli, R., & Barbie, D. A. (2016). Inflammation as a driver and vulnerability of KRAS mediated oncogenesis. Seminars in cell & developmental biology.

Konno, H., Konno, K., & Barber, G. N. (2013). Cyclic dinucleotides trigger ULK1 (ATG1) phosphorylation of STING to prevent sustained innate immune signaling. Cell, 155(3), 688-698.

Konno, H., Yamauchi, S., Berglund, A., Putney, R. M., Mulé, J. J., & Barber, G. N. (2018). Suppression of STING signalling through epigenetic silencing and missense mutation impedes DNA damage-mediated cytokine production. Oncogene, 37(15), 2037-2051.

Koshiyama, M., Matsumura, N., & Konishi, I. (2014). Recent concepts of ovarian carcinogenesis: type I and type II. BioMed research international, 2014.

Koshiyama, M., Matsumura, N., & Konishi, I. (2017). Subtypes of ovarian cancer and ovarian cancer screening. Diagnostics, 7(1), 12.

Kucuk, B., Kibar, B., & Cacan, E. (2021). A broad analysis in clinical and in vitro models on regulator of G-protein signalling 10 regulation that is associated with ovarian cancer progression and chemoresistance. Cell biochemistry and function, 39(3), 413–422. https://doi.org/10.1002/cbf.3607

Kurman, R. J., & Shih, I. M. (2008). Pathogenesis of ovarian cancer. Lessons from morphology and molecular biology and their clinical implications. International journal of gynecological pathology: official journal of the International Society of Gynecological Pathologists, 27(2), 151.

Kurman, R. J., & Shih, I. M. (2010). The origin and pathogenesis of epithelial ovarian cancer-a proposed unifying theory. The American journal of surgical pathology, 34(3), 433.

Kurman, R.J., Carcangiu, M.L., Herrington, C.S. ve Young, R.H., 2014. WHO Classification

Kvåle, G., Heuch, I., Nilssen, S., & Beral, V. (1988). Reproductive factors and risk of ovarian cancer: a prospective study. International Journal of cancer, 42(2), 246-251.

La Vecchia, C., Franceschi, S., Decarli, A., Gallus, G., & Tognoni, G. (1984). Risk factors for endometrial cancer at different ages. Journal of the National Cancer Institute, 73(3), 667–671.

Lacey Jr, J. V., Mutter, G. L., Nucci, M. R., Ronnett, B. M., Ioffe, O. B., Rush, B. B., ... & Sherman, M. E. (2008). Risk of subsequent endometrial carcinoma associated with endometrial intraepithelial neoplasia classification of endometrial biopsies. Cancer, 113(8), 2073-2081.

Lamminmaki, U., & Kankare, J. A. (2001). Crystal structure of a recombinant anti-estradiol Fab fragment in complex with 17β-estradiol. Journal of Biological Chemistry, 276(39), 36687-36694.

Lan, F., Cacicedo, J. M., Ruderman, N., & Ido, Y. (2008). SIRT1 modulation of the acetylation status, cytosolic localization, and activity of LKB1: possible role in AMP-activated protein kinase activation. Journal of Biological Chemistry, 283(41), 27628-27635.

Lattouf, H., Poulard, C., Treilleux, I., Hussein, N., Diab-Assaf, M., & Le Romancer, M. (2016). LKB1, A New Biomarker in Breast Cancer. Journal of Cancer Therapy, 7(10), 690-699.

Lax S. F. (2017). Pathology of Endometrial Carcinoma. Advances in experimental medicine and biology, 943, 75–96.

Lee, E. Y., & Muller, W. J. (2010). Oncogenes and tumor suppressor genes. Cold Spring Harbor perspectives in biology, 2(10), a003236.

Lengyel, E. (2010). Ovarian cancer development and metastasis. The American journal of pathology, 177(3), 1053-1064.

Li, S., Xu, H., Song, M., Shaw, B. I., Li, Q. J., & Kirk, A. D. (2022). IFI16-STING-NF-κB signaling controls exogenous mitochondrion-induced endothelial activation. American Journal of Transplantation, 22(6), 1578-1592.

Li, T., Diner, B. A., Chen, J., & Cristea, I. M. (2012). Acetylation modulates cellular distribution and DNA sensing ability of interferon-inducible protein

IFI16. Proceedings of the National Academy of Sciences of the United States of America, 109(26), 10558–10563.
Likes, W. M., Stegbauer, C., Tillmanns, T., & Pruett, J. (2007). Correlates of sexual function following vulvar excision. Gynecologic oncology.
Lin, E. Y., & Pollard, J. W. (2007). Tumor-associated macrophages press the angiogenic switch in breast cancer. Cancer research, 67(11), 5064-5066.
Lin, Z., Liu, Y., Lin, P., Li, J., & Gan, J. (2022). Clinical significance of STING expression and methylation in lung adenocarcinoma based on bioinformatics analysis. Scientific reports, 12(1), 13951. https://doi.org/10.1038/s41598-022-18278-6
Liu, S. Y., Sanchez, D. J., Aliyari, R., Lu, S., & Cheng, G. (2012). Systematic identification of type I and type II interferon-induced antiviral factors. Proceedings of the National Academy of Sciences, 109(11), 4239-4244.
Lobenhofer, E. K., Bennett, L., Cable, P. L., Li, L., Bushel, P. R., & Afshari, C. A. (2002). Regulation of DNA replication fork genes by 17β-estradiol. Molecular Endocrinology, 16(6), 1215-1229.
Ludlow, L. E., Johnstone, R. W., & Clarke, C. J. (2005). The HIN-200 family: more than interferon-inducible genes?. Experimental cell research, 308(1), 1-17.
Marks, P. A., & Breslow, R. (2007). Dimethyl sulfoxide to vorinostat: development of this histone deacetylase inhibitor as an anticancer drug. Nature biotechnology, 25(1), 84-90.
Marks, P. A., & Dokmanovic, M. (2005). Histone deacetylase inhibitors: discovery and development as anticancer agents. Expert opinion on investigational drugs, 14(12), 1497–1511.
McCann, S. E., Freudenheim, J. L., Marshall, J. R., & Graham, S. (2003). Risk of human ovarian cancer is related to dietary intake of selected nutrients, phytochemicals and food groups. The Journal of nutrition, 133(6), 1937-1942.
Michnovicz, J. J., Hershcopf, R. J., Naganuma, H., Bradlow, H. L., & Fishman, J. (1986). Increased 2-hydroxylation of estradiol as a possible mechanism for the anti-estrogenic effect of cigarette smoking. The New England journal of medicine, 315(21), 1305–1309.
Miyaki, M., Iijima, T., Hosono, K., Ishii, R., Yasuno, M., Mori, T., ... & Iwama, T. (2000). Somatic mutations of LKB1 and β-catenin genes in gastrointestinal polyps from patients with Peutz-Jeghers syndrome. Cancer research, 60(22), 6311-6313.
Modan, B., Ron, E., Lerner-Geva, L., Blumstein, T., Menczer, J., Rabinovici, J., Oelsner, G., Freedman, L., Mashiach, S., & Lunenfeld, B. (1998). Cancer incidence in a cohort of infertile women. American journal of epidemiology, 147(11), 1038–1042.
Mohammadian, M., Ghafari, M., Khosravi, B., Salehiniya, H., Aryaie, M., Bakeshei, F. A., & Mohammadian-Hafshejani, A. (2017). Variations in the incidence and mortality of ovarian cancer and their relationship with the human development index in European Countries in 2012. Biomedical Research and Therapy, 4(08), 1541-1557.
Momenimovahed, Z., Tiznobaik, A., Taheri, S., & Salehiniya, H. (2019). Ovarian cancer in the world: epidemiology and risk factors. International journal of women's health, 287-299.
Moorman, P. G., Calingaert, B., Palmieri, R. T., Iversen, E. S., Bentley, R. C., Halabi, S., ... & Schildkraut, J. M. (2008). Hormonal risk factors for ovarian cancer in premenopausal and postmenopausal women. American journal of epidemiology, 167(9), 1059-1069.
Morice, P., Gouy, S., & Leary, A. (2019). Mucinous ovarian carcinoma. New England Journal of Medicine, 380(13), 1256-1266.
Morgan, J. E., Shanderson, R. L., Boyd, N. H., Cacan, E., & Greer, S. F. (2015). The class II transactivator (CIITA) is regulated by post-translational modification cross-talk

between ERK1/2 phosphorylation, mono-ubiquitination and Lys63 ubiquitination. Bioscience reports, 35(4), e00233. https://doi.org/10.1042/BSR20150091

Moss, E. L., Moran, A., Reynolds, T. M., & Stokes-Lampard, H. (2013). Views of general practitioners on the role of CA125 in primary care to diagnose ovarian cancer. BMC Women's Health, 13(1), 1-6.

Mytton, J., Evison, F., Chilton, P. J., & Lilford, R. J. (2017). Removal of all ovarian tissue versus conserving ovarian tissue at time of hysterectomy in premenopausal patients with benign disease: study using routine data and data linkage. bmj, 356.

Nilsson, S., Makela, S., Treuter, E., Tujague, M., Thomsen, J., Andersson, G., ... & Gustafsson, J. Å. (2001). Mechanisms of estrogen action. Physiological reviews, 81(4), 1535-1565.

Olson, S. H., Mignone, L., Nakraseive, C., Caputo, T. A., Barakat, R. R., & Harlap, S. (2001). Symptoms of ovarian cancer. Obstetrics & Gynecology, 98(2), 212-217.

Oren, M. (1992). The involvement of oncogenes and tumor suppressor genes in the control of apoptosis. Cancer and Metastasis Reviews, 11, 141-148.

Pan, S. Y., Ugnat, A. M., Mao, Y., Wen, S. W., Johnson, K. C., & Canadian Cancer Registries Epidemiology Research Group. (2004). A case-control study of diet and the risk of ovarian cancer. Cancer Epidemiology Biomarkers & Prevention, 13(9), 1521-1527.

Pellerin, G. P., & Finan, M. A. (2005). Endometrial cancer in women 45 years of age or younger: a clinicopathological analysis. American journal of obstetrics and gynecology, 193(5), 1640-1644.

Peres, L. C., Risch, H., Terry, K. L., Webb, P. M., Goodman, M. T., Wu, A. H., ... & African American Cancer Epidemiology Study and the Ovarian Cancer Association Consortium. (2018). Racial/ethnic differences in the epidemiology of ovarian cancer: a pooled analysis of 12 case-control studies. International journal of epidemiology, 47(2), 460-472.

Pierson, W. E., Peters, P. N., Chang, M. T., Chen, L. M., Quigley, D. A., Ashworth, A., & Chapman, J. S. (2020). An integrated molecular profile of endometrioid ovarian cancer. Gynecologic Oncology, 157(1), 55-61.

Podrasky, A. E., Javitt, M. C., Glanc, P., Dubinsky, T., Harisinghani, M. G., Harris, R. D., ... & Zelop, C. M. (2013). ACR appropriateness Criteria® second and third trimester bleeding. Ultrasound quarterly, 29(4), 293-301.

Ratner, E. S., Tuck, D., Richter, C., Nallur, S., Patel, R. M., Schultz, V., ... & Weidhaas, J. B. (2010). MicroRNA signatures differentiate uterine cancer tumor subtypes. Gynecologic oncology, 118(3), 251-257.

Reid, B.M., Permuth, J.B. ve Sellers, T.A., 2017. Epidemiology of ovarian cancer: a review. Cancer Biol Med, 14 (1), 9-32.

Ries, L. A. G. (1993). Ovarian cancer: survival and treatment differences by age. Cancer, 71(S2), 524-529.

Risch, H. A., Marrett, L. D., Jain, M., & Howe, G. R. (1996). Differences in risk factors for epithelial ovarian cancer by histologic type: results of a case-control study. American journal of epidemiology, 144(4), 363-372.

Rojas, V., Hirshfield, K. M., Ganesan, S., & Rodriguez-Rodriguez, L. (2016). Molecular characterization of epithelial ovarian cancer: implications for diagnosis and treatment. International journal of molecular sciences, 17(12), 2113.

Romero, I., & Bast Jr, R. C. (2012). Minireview: human ovarian cancer: biology, current management, and paths to personalizing therapy. Endocrinology, 153(4), 1593-1602.

Rowan, A., Churchman, M., Jefferey, R., Hanby, A., Poulsom, R., & Tomlinson, I. (2000). In situ analysis of LKB1/STK11 mRNA expression in human normal tissues and

tumours. The Journal of Pathology: A Journal of the Pathological Society of Great Britain and Ireland, 192(2), 203-206.
Roy, R. N., Gerulath, A. H., Cecutti, A., & Bhavnani, B. R. (1999). Discordant expression of insulin-like growth factors and their receptor messenger ribonucleic acids in endometrial carcinomas relative to normal endometrium. Molecular and cellular endocrinology, 153(1-2), 19–27.
Russo, J., Lareef, M. H., Tahin, Q., Hu, Y. F., Slater, C., Ao, X., & Russo, I. H. (2002). 17β-Estradiol is carcinogenic in human breast epithelial cells. The Journal of steroid biochemistry and molecular biology, 80(2), 149-162.
Ryan, A. J., Susil, B., Jobling, T. W., & Oehler, M. K. (2005). Endometrial cancer. Cell and tissue research, 322, 53-61.
Sadikovic, B., Al-Romaih, K., Squire, J. A., & Zielenska, M. (2008). Cause and consequences of genetic and epigenetic alterations in human cancer. Current genomics, 9(6), 394-408.
Salani, R., Axtell, A., Gerardi, M., Holschneider, C., & Bristow, R. E. (2008). Limited utility of conventional criteria for predicting unresectable disease in patients with advanced stage epithelial ovarian cancer. Gynecologic oncology, 108(2), 271-275.
Sapkota, G. P., Boudeau, J., Deak, M., Kieloch, A., Morrice, N., & Alessi, D. R. (2002). Identification and characterization of four novel phosphorylation sites (Ser31, Ser325, Thr336 and Thr366) on LKB1/STK11, the protein kinase mutated in Peutz–Jeghers cancer syndrome. Biochemical journal, 362(2), 481-490.
Saso, S., Chatterjee, J., Georgiou, E., Ditri, A. M., Smith, J. R., & Ghaem-Maghami, S. (2011). Endometrial cancer. BMJ 343: d3954.
Saygi K.O., Cacan E. (2021). Antioxidant and cytotoxic activities of silver nanoparticles synthesized using tilia cordata flowers extract. Materials Today Communications, 27, Article 102316
Schiavoni, G., Mattei, F., & Gabriele, L. (2013). Type I interferons as stimulators of DC-mediated cross-priming: impact on anti-tumor response. Frontiers in immunology, 4, 483.
Secrist, J. P., Zhou, X., & Richon, V. M. (2003). HDAC inhibitors for the treatment of cancer. Current opinion in investigational drugs (London, England: 2000), 4(12), 1422-1427.
Seebacher, V., Schmid, M., Polterauer, S., Hefler-Frischmuth, K., Leipold, H., Concin, N., ... & Hefler, L. (2009). The presence of postmenopausal bleeding as prognostic parameter in patients with endometrial cancer: a retrospective multi-center study. BMC cancer, 9(1), 1-5.
Siegel, R. L., Miller, K. D., & Jemal, A. (2018). Cancer statistics, 2018. CA: a cancer journal for clinicians, 68(1), 7-30.
Siegel, R., Naishadham, D., & Jemal, A. (2012). Cancer statistics, 2012. CA: a cancer journal for clinicians.
Sorosky, J. I., & Joel, I. (2012). Cáncer endometrial. Obstet Gynecol, 120, 383-397.
Stempel, M., Chan, B., & Brinkmann, M. M. (2019). Coevolution pays off: Herpesviruses have the license to escape the DNA sensing pathway. Medical Microbiology and Immunology, 208(3-4), 495-512.
Sugawara, Y., Kakizaki, M., Nagai, M., Tomata, Y., Hoshi, R., Watanabe, I., Nishino, Y., Kuriyama, S., & Tsuji, I. (2013). Lactation pattern and the risk for hormone-related female cancer in Japan: the Ohsaki Cohort Study. European journal of cancer prevention : the official journal of the European Cancer Prevention Organisation (ECP), 22(2), 187–192.
Sundar, S., Neal, R. D., & Kehoe, S. (2015). Diagnosis of ovarian cancer. Bmj, 351.

Tanaka, Y., & Chen, Z. J. (2012). STING specifies IRF3 phosphorylation by TBK1 in the cytosolic DNA signaling pathway. Science signaling, 5(214), ra20-ra20.

Terada, K. Y., Ahn, H. J., & Kessel, B. (2016). Differences in risk for type 1 and type 2 ovarian cancer in a large cancer screening trial. Journal of Gynecologic Oncology, 27(3).

Torre, L. A., Islami, F., Siegel, R. L., Ward, E. M., & Jemal, A. (2017). Global cancer in women: burden and trends. Cancer epidemiology, biomarkers & prevention, 26(4), 444-457.

Trapani, J. A., Browne, K. A., Dawson, M. J., Ramsay, R. G., Eddy, R. L., Shows, T. B., ... & Dupont, B. (1992). A novel gene constitutively expressed in human lymphoid cells is inducible with interferon-γ in myeloid cells. Immunogenetics, 36, 369-376.

Trojan, J., Brieger, A., Raedle, J., Esteller, M., & Zeuzem, S. (2000). 5′-CpG island methylation of theLKB1/STK11 promoter and allelic loss at chromosome 19p13. 3 in sporadic colorectal cancer. Gut, 47(2), 272-276.

Tuesley, K. M., Protani, M. M., Webb, P. M., Dixon-Suen, S. C., Wilson, L. F., Stewart, L. M., & Jordan, S. J. (2020). Hysterectomy with and without oophorectomy and all-cause and cause-specific mortality. American journal of obstetrics and gynecology, 223(5), 723-e1.

Van Lier, M. G. F., Wagner, A., Mathus-Vliegen, E. M. H., Kuipers, E. J., Steyerberg, E. W., & van Leerdam, M. E. (2010). High cancer risk in Peutz–Jeghers syndrome: a systematic review and surveillance recommendations. Official journal of the American College of Gastroenterology| ACG, 105(6), 1258-1264.

Vasiyani, H., Shinde, A., Roy, M., Mane, M., Singh, K., Singh, J., ... & Singh, R. (2021). The analog of cGAMP, c-di-AMP, activates STING mediated cell death pathway in estrogen-receptor negative breast cancer cells. Apoptosis, 26, 293-306.

Veeranki, S., & Choubey, D. (2012). Interferon-inducible p200-family protein IFI16, an innate immune sensor for cytosolic and nuclear double-stranded DNA: regulation of subcellular localization. Molecular immunology, 49(4), 567-571.

Walsh, T., Casadei, S., Lee, M. K., Pennil, C. C., Nord, A. S., Thornton, A. M., ... & Swisher, E. M. (2011). Mutations in 12 genes for inherited ovarian, fallopian tube, and peritoneal carcinoma identified by massively parallel sequencing. Proceedings of the National Academy of Sciences, 108(44), 18032-18037.

Waterland, R. A. (2006). Epigenetic mechanisms and gastrointestinal development. The Journal of pediatrics, 149(5), S137-S142.

Wei, W., Clarke, C. J., Somers, G. R., Cresswell, K. S., Loveland, K. A., Trapani, J. A., & Johnstone, R. W. (2003). Expression of IFI 16 in epithelial cells and lymphoid tissues. Histochemistry and cell biology, 119, 45-54.

Woo, S. R., Corrales, L., & Gajewski, T. F. (2015). The STING pathway and the T cell-inflamed tumor microenvironment. Trends in immunology.

Xin, H., Curry, J., Johnstone, R. W., Nickoloff, B. J., & Choubey, D. (2003). Role of IFI 16, a member of the interferon-inducible p200-protein family, in prostate epithelial cellular senescence. Oncogene, 22(31), 4831-4840.

Yap, O. W., & Matthews, R. P. (2006). Racial and ethnic disparities in cancers of the uterine corpus. Journal of the National Medical Association, 98(12), 1930–1933.

Yi, X., & Zheng, W. (2008). Endometrial glandular dysplasia and endometrial intraepithelial neoplasia. Current Opinion in Obstetrics and Gynecology, 20(1), 20-25.

Zeqiraj, E., Filippi, B. M., Deak, M., Alessi, D. R., & Van Aalten, D. M. (2009). Structure of the LKB1-STRAD-MO25 complex reveals an allosteric mechanism of kinase activation. Science, 326(5960), 1707-1711.

Zhang, F., Yuan, Y., & Ma, F. (2021). Function and regulation of nuclear DNA sensors during viral infection and tumorigenesis. Frontiers in immunology, 11, 624556.

Zhang, Y., Staley, S. A., Tucker, K., & Clark, L. H. (2019). Malignant Brenner tumor of the ovary: Case series and review of treatment strategies. Gynecologic Oncology Reports, 28, 29-32.

Zhao, Y., Tan, J., Zhuang, L., Jiang, X., Liu, E. T., & Yu, Q. (2005). Inhibitors of histone deacetylases target the Rb-E2F1 pathway for apoptosis induction through activation of proapoptotic protein Bim. Proceedings of the National Academy of Sciences, 102(44), 16090-16095.

Zheng, R., & Heller, D. S. (2019). Borderline Brenner tumor: a review of the literature. Archives of pathology & laboratory medicine, 143(10), 1278-1280.

Zhu, H., Moriasi, C. M., Zhang, M., Zhao, Y., & Zou, M. H. (2013). Phosphorylation of serine 399 in LKB1 protein short form by protein kinase Cζ is required for its nucleocytoplasmic transport and consequent AMP-activated protein kinase (AMPK) activation. Journal of Biological Chemistry, 288(23), 16495-16505.

Koivunen, J. P., Kim, J., Lee, J., Rogers, A. M., Park, J. O., Zhao, X., ... & Jänne, P. A. (2008). Mutations in the LKB1 tumour suppressor are frequently detected in tumours from Caucasian but not Asian lung cancer patients. British journal of cancer, 99(2), 245-252.

Balagunaseelan, N. (2014). Evaluation of the gene expression of STING, IFN-β and osteopontin in tissue obtained from pigs treated with Matrix-M.

Baggetta, R., De Andrea, M., Gariano, G. R., Mondini, M., Rittà, M., Caposio, P., ... & Landolfo, S. (2010). The interferon-inducible gene IFI16 secretome of endothelial cells drives the early steps of the inflammatory response. European journal of immunology, 40(8), 2182-2189.

Jønsson, K. L., Laustsen, A., Krapp, C., Skipper, K. A., Thavachelvam, K., Hotter, D., ... & Jakobsen, M. R. (2017). IFI16 is required for DNA sensing in human macrophages by promoting production and function of cGAMP. Nature communications, 8(1), 14391.

8. ETHICAL APPROVAL

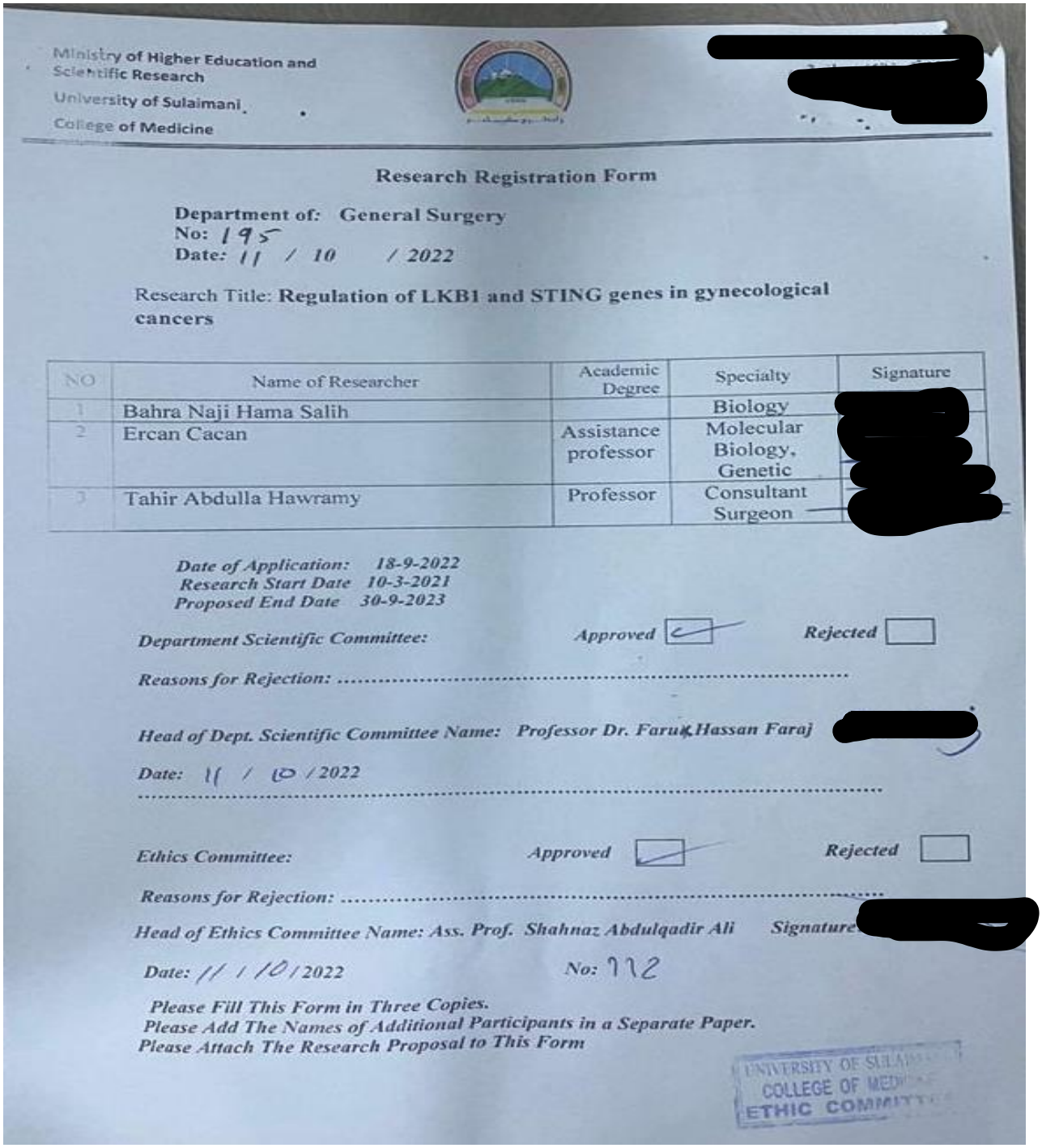

Ministry of Higher Education and Scientific Research
University of Sulaimani
College of Medicine

[redacted]

Research Registration Form

Department of: General Surgery
No: 195
Date: 11 / 10 / 2022

Research Title: **Regulation of LKB1 and STING genes in gynecological cancers**

NO	Name of Researcher	Academic Degree	Specialty	Signature
1	Bahra Naji Hama Salih		Biology	[redacted]
2	Ercan Cacan	Assistance professor	Molecular Biology, Genetic	[redacted]
3	Tahir Abdulla Hawramy	Professor	Consultant Surgeon	[redacted]

Date of Application: 18-9-2022
Research Start Date 10-3-2021
Proposed End Date 30-9-2023

Department Scientific Committee: *Approved* ✓ *Rejected* ☐

Reasons for Rejection: .....

Head of Dept. Scientific Committee Name: *Professor Dr. Faruk Hassan Faraj* [redacted]

Date: 11 / 10 / 2022

.....

Ethics Committee: *Approved* ✓ *Rejected* ☐

Reasons for Rejection: .....

Head of Ethics Committee Name: *Ass. Prof. Shahnaz Abdulqadir Ali* *Signature* [redacted]

Date: 11 / 10 / 2022 *No:* 112

Please Fill This Form in Three Copies.
Please Add The Names of Additional Participants in a Separate Paper.
Please Attach The Research Proposal to This Form

UNIVERSITY OF SULAIMANI
COLLEGE OF MEDICINE
ETHIC COMMITTEE

Ministry of Higher Education and Scientific Research

University of Sulaimani

College of Medicine

Ethics committee

[redacted]

Number: 112
Date: 11/10/2022

The Ethics Committee of the College of Medicine

We the members of the ethical committee approved the research project below in the meeting (No: 3) on the date (11 /10 /2022).

Title of the research project:

Regulation of LKB1 and STING genes in gynecological cancers

Name and title of the participants:
1-Bahra Naji Hama Salih, Tokat Gaziosmsnpasa university, Institute of. Graduate Study, department of biology, Turkey

2- Assistance Professor Dr. Ercan Cacan, Tokat Gaziosmsnpasa university, department of Molecular Biology and Genetics, Turkey
3- Professor Dr. Tahir Abulla Hawramy , Consultant General, digestive and oncologic surgeon, University of Slemani ,College of Medicine

Place of research study Tokat Gaziosmsnpasa university,

Members of Ethical committee of the College of Medicine

UNIVERSITY OF SULAIMANI COLLEGE OF MEDICINE ETHICS COMMITTEE

[redacted]
Ass. Prof. Dr Shahnaz Abdulqadir Ali
Head of the committee

[redacted]
L .Dr. Kazhan Ali Towfiq
Member

[redacted]
L. Dr. Ali Mohammed Karim

[redacted]
Ass.Prof.Dr.Anwer Aboubaker kareem Jaff
Member

[redacted]
Ass.Prof. Dr.Nawzad Rashid Abdulrahman

[redacted]
Dr. Karim Mohammed Hassan
Member

[redacted]
Dr. [redacted] Qadir
Member